Title

Infant onset spinocerebellar ataxia type 13 mutation leads to developmental and rapid degenerative phenotypes related to hyperexcitability in Purkinje cells

Author

Ulrich, Brittany Nicole

Publication Date

2017

Peer reviewed|Thesis/dissertation

UNIVERSITY OF CALIFORNIA

Los Angeles

Infant onset spinocerebellar ataxia type 13 mutation leads to developmental and rapid degenerative phenotypes related to hyperexcitability in Purkinje cells

A dissertation submitted in partial satisfaction of the requirements for the degree Doctor of Philosophy in Molecular, Cellular and Integrative Physiology

by

Brittany Nicole Ulrich

2017

ABSTRACT OF THE DISSERTATION

Infant onset spinocerebellar ataxia type 13 mutation leads to developmental and rapid degenerative phenotypes related to hyperexcitability in Purkinje cells

by

Brittany Nicole Ulrich

Doctor of Philosophy in Molecular, Cellular and Integrative Physiology

University of California, Los Angeles 2017

Professor Diane M. Papazian, Chair

Spinocerebellar ataxia type 13 (SCA13) is an autosomal dominant neurodegenerative disease that leads to cerebellar ataxia and atrophy. It can exist in both adult and infant onset forms, caused by different mutations in voltage-gated K^+ channel 3.3 (Kv3.3). The three causative mutations are adult onset R3H, infant onset R4H, and infant onset FL. The adult onset R3H and infant onset R4H mutations are located in the voltage sensor and lead to differential defects in channel function, which then lead to differential changes in Purkinje cell excitability. The adult onset mutation leads to latent hypoexcitability, whereas the infant onset mutation leads to rapid hyperexcitability followed by silence. We hypothesized that differential changes in Purkinje cell excitability caused by each mutation lead to differential changes in Purkinje cell development and survival and that reducing the hyperexcitability in Purkinje cells expressing the infant onset mutation would rescue the degenerative phenotype. We first confirmed the expression of Nav1.6 and Kv3.3 channels, both involved in mediating spontaneous tonic firing in

mammalian Purkinje cells. It was necessary to confirm that this regulation was conserved in zebrafish, and that endogenous Kv3.3 was expressed in order to use zebrafish as a model for SCA13. The infant onset mutation leads to developmental abnormalities in Purkinje cells, as well as rapid degeneration and cell loss due to apoptotic cell death, typically by 6 dpf. The adult onset mutation did not alter Purkinje cell development or survival. When zebrafish expressing the infant onset mutation were treated with the SK2 channel agonist NS13001 to reduce hyperexcitability, the frequency of mutant cells significantly increased compared to DMSO controls, however, the degenerative phenotype was not rescued. This suggests a possible effect on Purkinje cell viability. We cannot rule out the role of hyperexcitability in degeneration because the efficacy of the drug was unclear. Previously, increased intracellular Ca^{2+} was observed in Purkinje cells expressing the infant onset mutation and may be implicated in a variety of cellular stress responses, such as mitochondrial dysfunction and/or ER stress, that could lead to apoptosis. Altered neuronal excitability and increased Ca^{2+} concentration have been observed in several neurodegenerative diseases and further investigating SCA13 will provide invaluable insight to our understanding of the mechanisms behind neurodegeneration.

The dissertation of Brittany Nicole Ulrich is approved.

Baljit S. Khakh

Riccardo Olcese

Alvaro Sagasti

Diane M. Papazian, Committee Chair

University of California, Los Angeles

2017

Table of Contents

List of Figures

Acknowledgements

I would like to take this opportunity to thank Dr. Diane Papazian for the opportunity to perform my thesis research in her laboratory and for her support and mentorship throughout my doctoral training. I would also like to thank my committee: Dr. Baljit Khakh, Dr. Riccardo Olcese, and Dr. Alvaro Sagasti, who provided valuable insight that challenged me and allowed me to grow as a student and scientist. Furthermore, I would like to thank Dr. Mark Frye and the Molecular, Cellular and Integrative Physiology program, who helped me navigate my years at University of California, Los Angeles.

The content in Chapter 3 of this thesis was previously published in Hsieh et al., 2014. Dr. Jui-Yi Hsieh, Dr. Diane Papazian, Dr. Fadi Issa, and Dr. Ji-Jun Wan co-authored this study. Dr. Diane Papazian was the principle investigator, Dr. Fadi Issa helped conduct the confocal imaging, and Dr. Ji-Jun Wan provided electrophysiological support. I included data from Dr. Jui-Yi Hsieh who performed the electrophysiological recordings through this thesis. I greatly appreciate him letting me include his data. I would like to thank Dr. Meng-Chin Lin and Brandon Brown for their insight and support in the laboratory.

Figure 1.2 in this thesis is a reprint from: Waters, M., Minassian, N., Stevanin, G., Figueroa, K., Bannister, J., Nolte, D., Mock, A., Evidente, V., Fee, D., Muller, U., Durr, A., Brice, A., Papazian, D., Pulst, S. (2006) Mutations in voltage-gated potassium channel KCNC3 cause degenerative and developmental central nervous system phenotypes. *Nature Genetics.* **38(4)**: 447-451. It was kind of Nature Publishing Group to grant the permission of using this figure in this thesis. Figure 1.3 is a reprint from: Hashimoto and Hibi (2012), Development and evolution of cerebellar neural circuits. *Development, Growth & Differentiation*, **54**: 373–389.

doi: 10.1111/j.1440-169X.2012.01348.x. It is very kind of John Wiley and Son publisher to grant the permission of using this figure in my thesis.

I would like to thank my parents for supporting my academic endeavors and dreams. They never once allowed me to worry about the next step, always ensuring that I never had to compromise. Without the upbringing they provided me, I would not have made it this far or have confidence in my abilities to climb farther. I will never repay their love and sacrifice. I would also like to thank Derek, my partner, for providing me strength when the challenges were at their peak, providing me peace of mind through anxiety, and never doubting that I could succeed in my doctoral program. His love, and the support of my friends who were going through this experience alongside me, made every moment of the last five years feel possible.

Brittany Nicole Ulrich

EDUCATION

University of California, Los Angeles *2013-2017*
Doctoral Candidate in Molecular, Cellular and Integrative Physiology
Skidmore College *2008-2012*
Bachelor of Arts in Molecular Biology and Genetics

RESEARCH EXPERIENCE

Department of Physiology, University of California, Los Angeles *2013-2017*
Graduate Student Researcher for Dr. Diane Papazian
Focus: Investigating the mechanism behind the differential Purkinje cell defects caused by the spinocerebellar ataxia type 13 (SCA13) adult and infant onset Kv3.3 mutations

- Determined the expression of Nav1.6 and Kv3.3 channels in zebrafish Purkinje cells
- *In vivo c*onfocal imaging of single Purkinje cells expressing the SCA13 adult or infant onset mutations over developmental time
- Acridine orange staining to monitor apoptotic cell death in Purkinje cells expressing the SCA13 infant onset mutation
- Chronic treatment of zebrafish with SK2 channel agonist to reduce hyperexcitability in Purkinje cells expressing the infant onset mutation and *in vivo* confocal imaging to monitor its effect on mutant phenotypes

Department of Chemistry, Skidmore College *2011-2012*
Summer Research Fellow for Dr. Kelly Sheppard
Focus: Investigating the ability of *Bdellovibrio bacteriovorus* aspartyl-tRNA synthetase to recognize $tRNA^{Asn}$ as a substrate
Department of Biology, Skidmore College *2011-2012*
Independent Study Researcher for Dr. Bernard Possidente
Focus: Investigating how different light-dark conditions alter *Drosophila melanogaster* circadian rhythms

TECHNIQUES AND SKILLS

- ***In situ* hybridization**
  - Designed probes for the *aldoca* and *scn8aa* genes in zebrafish
- **Confocal imaging**
  - *In vivo* imaging of single Purkinje cells in zebrafish
- **Vital dye staining** and **pharmacology** in zebrafish
- **Microinjections** of zebrafish embryos
- **Standard molecular biology** and **biochemistry techniques**
- **Analysis computer software:** Imaris, GraphPad Prism, SPSS

FELLOWSHIPS AND AWARDS

- **Jennifer S. Buchwald Graduate Fellowship in Physiology** *2013-2014*
- **Certificates of Distinction in Teaching** *2015, 2016*
  - Introduction to Molecular Biology
- **Graduate Student Travel Award** *2016*
  - Brain Research Institute and Semel Institute for Neuroscience & Human Behavior.

PUBLICATIONS

Do, TD., LaPointe, NE., Nelson, R., Krotee, P., Hayden EY., **Ulrich, B.**, Quan, D., Feinstein, SC., Teplow, DB., Eisenberg, D., Shea, JE., and Bowers., MT. (2016) Amyloid B-protein C-terminal fragments: Formation of cylindrins and B-barrels. J Am Chem Soc. **138(2)**: 549-57.

Hsieh, JY., **Ulrich, B.**, Issa, FA., Wan, J., and Papazian, D. (2014) Rapid development of Purkinje cell excitability, functional cerebellar circuit, and afferent sensory input to cerebellum in zebrafish. Front Neural Circuits. **8**: 147.

Alperstein, A., **Ulrich, B.**, Garofalo, DM., Dreisbach, R., Raff, H., and Sheppard, K. (2014) The predatory bacterium Bdellovibrio bacteriovorus aspartyl-tRNA synthetase recognizes tRNAAsn as a substrate. PLoS One. **9(10)**: e110842.

ABSTRACTS AND PRESENTATIONS

Ulrich, B. Rapid atrophy and degeneration of neuronal cells expressing infant onset spinocerebellar ataxia type 13 (SCA13) Kv3.3 mutation. Physiology Department Seminar. UCLA. 2015. (Oral Presentation)

Papazian, D., **Ulrich, B.,** Hsieh, J-Y., Issa, F., Brown, B. & Lin, M-C. Rapid atrophy and hyperexcitability in cerebellar Purkinje cells expressing infant-onset spinocerebellar ataxia type 13 Kv3.3 mutation. SfN Meeting. San Diego. 2016. (Abstract and Poster Presentation)

Papazian, D., **Ulrich, B.,** Hsieh, J-Y., Issa, F., Brown, B. & Lin, M-C. Lin. Rapid atrophy and hyperexcitability in cerebellar Purkinje cells expressing infant-onset spinocerebellar ataxia type 13 Kv3.3 mutation. 28th Annual Brain Research Institute's Neuroscience Poster Session. UCLA. 2016. (Poster Presentation)

Ulrich, B. Rapid atrophy and hyperexcitability in cerebellar Purkinje cells expressing infant-onset spinocerebellar ataxia type 13 Kv3.3 mutation. Molecular, Cellular, and Integrative Physiology Program Retreat. UCLA. 2017. (Oral Presentation)

Chapter 1

Introduction

Aims of this thesis

The aims of this thesis are to determine the expression in zebrafish Purkinje cells of the ion channels thought to control their characteristic pattern of excitability, elucidate the differential effects of mutations causing adult and infant onset spinocerebellar ataxia 13 (SCA13) on Purkinje cell development and survival, and begin to understand the mechanism that leads to these differential effects. In the first chapter, I will briefly describe the background and current information relevant to the work in this thesis, including the clinical phenotypes of SCA13, the genetic mutations in voltage-gated K^+ channel 3.3 (Kv3.3) that cause SCA13, the usefulness of zebrafish as a model organism for cerebellar research, and the relationship between altered neuronal excitability and neurodegenerative disease.

Using zebrafish as our model organism, we investigated 1) the expression of voltage-gated Na^+ channel 1.6 (Nav1.6) and Kv3.3 in zebrafish Purkinje cells, both thought to control spontaneous tonic firing and the latter mutated in SCA13, 2) the developmental and/or degenerative consequences of specifically expressing the adult and infant onset SCA13 mutations in zebrafish Purkinje cells *in vivo*, over developmental time, and 3) whether apoptotic cell death occurs in hyperexcitable zebrafish Purkinje cells expressing the infant onset SCA13 mutation and if suppressing hyperexcitability can rescue the degenerative phenotype and reduced cell survival.

Spinocerebellar Ataxia Type 13

Autosomal dominant spinocerebellar ataxias are progressive neurodegenerative diseases exhibiting a wide array of phenotypes including cerebellar ataxia, cerebellar atrophy,

extrapyramidal signs, dysarthria, oculomotor abnormalities, motor neuron signs, and cognitive decline (Pulst, 2003; Schols et al., 2004). Spinocerebellar ataxia type 13 (SCA13) is a member of this family of diseases, with unique characteristics that set it apart from the other types. SCA13 exists as two distinct forms, adult onset and infant onset (Herman-Bert et al., 2000; Waters et al., 2006; Figueroa et al., 2010). The age of onset in adult onset SCA13 is 20-30 years old, whereas the age of onset in infant onset SCA13 can be as early as the first year of life (Herman-Bert et al., 2000; Waters et al., 2006). Both the adult and infant onset forms of SCA13 display several of the hallmark clinical phenotypes including cerebellar ataxia and atrophy (Figure 1.1), however, only the infant onset form leads to cognitive delay with some evidence of patients experiencing epilepsy (Herman-Bert et al., 2000).

The locus for SCA13 was first discovered at 19q13 in a French pedigree (Herman-Bert et al., 2000). It was then determined to be caused by mutations in the *KCNC3* gene, which encodes voltage-gated K^+ channel 3.3 (Kv3.3) (Waters et al., 2006; Figueroa et al., 2010; Figueroa et al., 2011). Members of the Kv3 family have unique gating properties that set them apart from other K^+ channels, and SCA13 is the only known neurodegenerative disease caused by a mutation in the gene. The mutations that cause SCA13 include Arg420His (R420H), Arg423H (R423H), and Phe448Leu (F448L) (Figure 1.2). The R420H mutation causes the adult onset form and R423H and F448L mutations cause the infant onset form (Waters et al., 2006; Figueroa et al., 2010).

Kv3.3 and causative SCA13 mutations

Members of the Kv3 family of voltage-gated K^+ channels, encoded by *KCNC1-4*, have unique properties that set them apart from other K^+ channels. Kv3 currents are apparent at

membrane potentials more positive than -10 mV with a fast rate of rise, and the probability of opening increases with voltage. This is considered a more depolarized activation range than other K^+ channels. Deactivation is 10X faster in Kv3 channels upon repolarization of the membrane (Rudy et al., 1999). Kv3 channels have been implicated in repetitive, high frequency firing. Blocking Kv3 channels in fast-spiking neocortical neurons produces near complete elimination of the afterhyperpolarization and decreased steady state firing rate, particularly reducing the frequency of the spike train (Erisir et al., 1999). Furthermore, blocking Kv3 channels in cerebellar Purkinje cells reduced the number of Na^+ spikes during Ca-Na bursts and slowed the rate of Na^+ spikes, specifically reducing the ability of spikes to discharge repetitively during the burst (McKay & Turner, 2004). These effects are attributable to the role of Kv3 in limiting the accumulation of Na^+ channel inactivation and repolarization of the cell during repetitive firing (Erisir et al., 1999; McKay & Turner, 2004).

Mutations in *KCNC3*, which encodes Kv3.3, cause both adult and infant onset SCA13. Interestingly, two of these mutations are located in the S4 transmembrane segment, which plays an essential role in voltage gating (Figure 1.2) (Waters et al., 2006; Figueroa et al., 2010). The S1-S4 transmembrane segments make up the voltage sensor, and four positively-charged arginine residues in S4 are responsible for initiating movement of the domain. Upon depolarization, the voltage sensor moves toward the extracellular side of the membrane through charge interactions with these residues, which increases the probability of channel opening. Electrostatic interactions are required to stabilize this conformational change (Papazian et al., 1995; Seoh et al., 1996; Tiwari-Woodruff et al., 1997; Tiwari-Woodruff et al., 2000; Laine et al., 2003; Silverman et al., 2003; Borjesson & Elinder, 2008; Jensen et al., 2012). The adult onset mutation in the voltage

sensor is R420H, which changes the third arginine of the S4 transmembrane segment, and the infant onset mutation is R423H, which changes the fourth arginine (Figure 1.2) (Waters et al., 2006; Figueroa et al., 2010).

The arginine residues of the S4 transmembrane segment facilitate an increase in the open probability of Kv3.3 channels, and it was first hypothesized that the adult onset R420H mutation and infant onset R423H mutation would affect channel function. Despite their proximity in the primary sequence, only three residues apart, and functional similarities, these mutations lead to differential changes. SCA13 patients have one WT *KCNC3* allele and one mutant allele. Kv3 channels exist as tetramers, suggesting that mutant and WT Kv3.3 subunits can co-assemble (MacKinnon, 1991; Waters et al., 2006). Subunits containing the adult onset R420H mutation cannot form functional channels on their own, however, lead to a dominant negative suppression of current amplitude when co-assembled with WT subunits (Waters et al., 2006; Figueroa et al., 2010). In *Xenopus* oocytes, residual current amplitudes when expressed at ratios of 1:0.25 to 1:4 (WT:R420H) suggest that one mutant subunit can incorporate into a functional channel, however, remaining amplitudes are less than if more than one subunit can incorporate into a functional channel. Since it has no effect on channel gating, this mutation is considered purely dominant negative (Minassian, Lin & Papazian, 2012). Subunits containing the infant onset R423H mutation suppress current amplitude in a dose-dependent manner as well, however, current amplitudes at higher doses of R423H matched well with more than one mutant subunit incorporating into a functional channel. The infant onset mutation causes a modest change in channel gating that the adult onset does not, including a moderate shift of the half-maximal activation voltage ($V_{1/2}$), slowed activation between +10 and +50 mV, and slowed deactivation

(Minassian, Lin & Papazian, 2012). Notably, the infant onset F448L mutation causes the same gating defects as R423H, however, does not cause a dominant negative suppression of current amplitude (Minassian, Lin & Papazian, 2012).

Cerebellar function and circuitry are conserved in the zebrafish cerebellum

Considering the unique properties of Kv3.3 channels and their role in repetitive firing, we hypothesized that the differential effects on channel function caused by the adult onset R420H mutation and infant onset R423H mutation lead to differential changes in cerebellar Purkinje cell excitability. We chose to investigate this question in the zebrafish cerebellum. Zebrafish are a strong model due to the high level of structural and functional conservation between the teleost cerebellum and mammalian cerebellum and the unique experimental tools they provide.

The cerebellum is responsible for smooth and skillful movements, precise motor control, and motor learning through the integration of sensory and predictive inputs, as well as implicated in certain cognitive and emotional functions (Bell, 2002; Ito, 2002; Rodriguez et al., 2005; Ito, 2006; Bell et al., 2008; Ito, 2008). It contains a highly organized network of excitatory and inhibitory neurons that connect to one another and to other regions of the brain. The excitatory neurons use the neurotransmitter glutamate, and include granule cells and deep cerebellar nuclei (DCN) and the inhibitory neurons use gamma-aminobutyric acid (GABA), and include Purkinje cells and interneurons (Hibi & Shimizu, 2011; Hashimoto & Hibi, 2012). Cerebellar neurons are organized into three layers, the granule cell layer (GCL), the Purkinje cell layer (PCL), and the molecular layer (ML). These three layers are located over an inner core composed of white matter and the large and small cells of the DCN. The GCL contains granule cell bodies, the PCL

contains Purkinje cell bodies, and the ML contains granule cell axons, or parallel fibers, and Purkinje cell dendrites. Interneurons are found in all three layers. (Figure 1.3A) (Hibi & Shimizu, 2011; Hashimoto & Hibi, 2012).

Purkinje cells are particularly vital to cerebellar function, as they are the sole output neurons of the cerebellum. They have stereotyped morphological characteristics that include a large, spherical cell body and extensively branched dendrites with spines (Armengol & Sotelo, 1991; Kapfhammer, 2004). Purkinje cells receive inputs from climbing fibers that originate from the inferior olive (IO) and mossy fibers that originate from pre-cerebellar nuclei. Granule cells are the intermediate between mossy fibers and Purkinje cells, receiving inputs from mossy fibers and sending parallel fibers to Purkinje cell dendrites. Purkinje cells send their axons to adjacent Purkinje cells or to DCN, which send axons to other regions of the brain (Figure 1.3A) (Hibi & Shimizu, 2011; Hashimoto & Hibi 2012).

In the zebrafish cerebellum, many cell types are conserved with the exception of certain interneurons. Eurydendroid cells innervate analogous brain structures to the DCN, however, they differ both structurally and geographically (Figure 1.3B). The mammalian cerebellum is organized into 10 lobules (I-X) and each lobule contains the three-layered structure, whereas the zebrafish cerebellum is organized into three major lobes, the valvula cerebelli (Va, anterior lobe), the corpus cerebelli (Cce, main lobe), and the vestibulo-lateral lobe (caudo-lateral lobe). The zebrafish cerebellum is located in the hindbrain, and these lobes are organized into two hemispheres (Figure 1.3C). There is conservation between the orientation of the three-layered structure in the mammalian cerebellum and in the Cce lobe of the zebrafish cerebellum (Bae et al., 2009; Hashimoto & Hibi, 2012).

In zebrafish, Purkinje cells are born ~3 days post-fertilization (dpf) and begin to extend an array of thin neurites. By 4 dpf, a primary dendrite and axons extend from the cell body . Over subsequent days dendritic complexity and dendritic spines develop (Tanabe et al., 2010). The morphological characteristics of mammalian and zebrafish Purkinje cells are highly conserved, however, dendritic areas differ substantially. The mature dendritic area of mammalian Purkinje cells is about 5,480 μm^2 (McKay & Turner, 2005), whereas the mature dendritic area of zebrafish Purkinje cells is 143.5 μm^2 (Tanabe et al., 2010). The stereotypical morphology of these cells lends itself well to studies which focus on neuronal development or degeneration.

Electrophysiological experiments performed previously in our laboratory confirmed that along with morphology, Purkinje cell excitability is conserved in zebrafish (Hsieh et al., 2014). Zebrafish Purkinje cells are electrically excitable by 4 dpf, and develop a mature pattern of spontaneous firing with interspersed complex spiking over the next 48 hours (Figure 1.4A). Firing frequency significantly increases from ~5 Hz at 4 dpf to ~9 Hz at 5 dpf and remains stable thereafter [compared to 12 Hz in mammalian Purkinje cells at room temperature (Wulff et al., 2009)] (Figure 1.4B). Firing regularity significantly increases between 4 dpf and 6 dpf (Figure 1.4C). Complex spiking emerges around 5 dpf (Figure 1.4A), with the highest complex spike frequency occurring upon first emergence (Hsieh et al., 2014). Complex spiking is reflective of climbing fiber input, whereas mossy fibers modulate spontaneous tonic firing (D'Angelo et al., 2011).

The zebrafish cerebellum is simpler and develops more rapidly than the mammalian cerebellum, however, cerebellar structure and neuronal excitability are highly conserved. This conservation makes zebrafish a useful model organism for studying the cerebellum and

neurodegenerative diseases that specifically target the cerebellum. We chose to investigate the effects and mechanisms of SCA13 mutations in zebrafish for these reasons, and for the unique experimental advantages they provide. The tupfel longfin nacre (TLN) mutant line of zebrafish are unpigmented, allowing for *in vivo* imaging of the brain over developmental time. Transient transgenic zebrafish, in which a target gene is integrated into the genome of somatic cells rather than germ line cells, can be developed through microinjections of plasmid DNA containing the minimal sequences for Tol2 transposition, and exhibit a mosaic pattern of expression. Furthermore, pharmacological agents can be easily applied to zebrafish through chronic treatment in the water, depending on solubility and permeability.

Differential effects of SCA13 adult and infant onset mutations on Purkinje cell excitability

Electrophysiological studies previously performed in the laboratory investigated the hypothesis that differential effects on Kv3.3 channel function caused by the SCA13 adult onset R420H mutation and infant onset R423H mutation lead to differential changes in Purkinje cell excitability. This was accomplished through expression of the mutated zebrafish homolog of Kv3.3 (zKv3.3). The adult onset mutation in zKv3.3 is R335H, or R3H, referring to the third arginine of the voltage sensor, and the infant onset mutation in zKv3.3 is R338H, or R4H, referring to the fourth arginine of the voltage sensor. The mutated genes were expressed through transient transgenesis. Loose patch recordings from Purkinje cells expressing either the adult or infant onset mutations confirmed that expression of these mutations in zebrafish Purkinje cells leads to differential changes in neuronal excitability.

Expression of the adult onset R3H mutation causes latent hypoexcitability in Purkinje cells. During spontaneous tonic firing, Purkinje cell excitability is unaltered (Figure 1.5). The effect of the mutation was then investigated after stimulation. Retinal photoreceptors are connected to Purkinje cells. In order to drive mutant cells, zebrafish were normalized to light conditions then exposed to sudden darkness. During this protocol, Purkinje cell hypoexcitability becomes apparent. Complex spiking is still observed (Hsieh & Papazian, unpublished).

Expression of the infant onset mutation caused obvious and dramatic hyperexcitability in spontaneously firing Purkinje cells, without stimulation. Excitability emerges similarly to uninjected Purkinje cells, around 3.75 dpf with a frequency of 1-2 Hz. Rapidly, hyperexcitability emerges with a bursting phenotype that exhibits a frequency of up to 50 Hz (Figure 1.6). The properties of cell excitability were followed over developmental time. The majority of mutant Purkinje cells are typically silent by 5 dpf (Hsieh & Papazian, unpublished).

Altered neuronal excitability in neurodegenerative disease

Altered neuronal excitability is observed in other spinocerebellar ataxias, particularly those caused by polyQ expansions (reviewed in Chopra & Shakkottai, 2014). In spinocerebellar ataxia type 2 (SCA2), a loss of molecular layer thickness in mouse models is observed beginning at 12 weeks and a complete loss of Purkinje cells is observed beginning at 40 weeks (Hansen et al., 2012). Conflicting reports of altered Purkinje cell excitability have been made. Kasumu et al. reported a significant bursting phenotype with periods of reduced firing or silence in between bursts (Kasumu et al., 2012). Hansen et al. only observed this bursting phenotype rarely, and reported that Purkinje cell firing progressed towards slower firing frequencies over time (Hansen

et al., 2012). When mice were fed NS13001, a small conductance Ca^{2+}-activated K^+ channel 2 (SK2) agonist, which regulates Purkinje cell pacemaking, degeneration was rescued and motor performance on the beamwalk improved (Kasumu et al., 2012). In spinocerebellar ataxia type 3 (SCA3), the motor phenotype preceded cerebellar degeneration in mouse models. Less than half of Purkinje cells exhibited spontaneous tonic firing. The majority of cells were silent with a depolarized membrane potential, indicative of depolarization block. Similarly to the results observed in the SCA2 model, when mice were fed with the SK channel agonist SKA-31, excitability in Purkinje cells was converted back to characteristic tonic firing and beamwalk performance was improved (Shakkottai et al., 2011). Rescue of degeneration and motor phenotypes by restoring normal firing in Purkinje cells suggests that altered excitability likely contributes to the phenotypes observed in the SCA2 and SCA3 models.

Another polyQ expansion disease, Huntington's Disease (HD), displays altered neuronal excitability as well. In medium spiny neurons (MSNs) from mouse models, a progressive reduction of excitatory post-synaptic current (EPSC) frequency was observed beginning at 5-7 weeks and was more pronounced at later time points. High frequency bursts began around this time point, peaking when the behavioral symptoms became apparent and the frequency of small amplitude events decreased. Presynaptic changes appear to precede post-synaptic changes, leading to denervation and susceptibility to glutamate excitotoxicity (Cepeda et al., 2003). This provided confirmation of an earlier study, where MSNs were found to be more excitable, particularly in older mice (Klapstein et al., 2001). Similar alterations in excitability were observed in pyramidal neurons (Cummings et al., 2009). K^+ currents were specifically altered in MSNs, reduced beginning at 11-15 weeks. The characteristic increase in K^+ channel expression

was not observed (Ariano et al., 2005). Interestingly, Purkinje cell dysfunction is observed in HD models, including a reduction in cell density and decrease in spike frequency (Dougherty et al., 2012; Dougherty et al., 2013). It is thought that neuronal dysfunction precedes the behavioral phenotypes as altered excitability is most apparent as mice become symptomatic (Cepeda et al., 2003).

Hyperexcitability in the hippocampus is a common observation in Alzheimer's Disease (AD). In CA1 pyramidal neurons from AD mouse models, action potential firing frequency is increased and is predominantly observed as bursts (Siskova et al., 2014). It was determined that hyperexcitability was localized to the dendrites and that epileptiform activity in CA1 and the dentate gyrus could lead to depletion of voltage-gated K^+ channel 4.2 (Kv4.2), a rapidly inactivating A-type channel. This depletion could be rescued by reducing the level of Tau expression, suggesting that protein aggregation may cause or exacerbate altered neuronal excitability (Hall et al., 2015).

Amyotrophic lateral sclerosis (ALS) displayed neuronal hyperexcitability as well, however, altered excitability is specifically observed in motor neurons. The popular hypothesis (reviewed in Bae et al., 2013) is that hyperexcitability is involved in a "dying forward" phenomenon, suggesting that neuronal death is caused by increased impulse burden on lower motor neurons (LMNs) from hyperexcitable upper motor neurons (UMNs) (Eisen, Kim & Pant, 1992). In ALS patient-derived MNs with SOD1 mutations, a significantly higher firing rate was observed, which was determined to specifically be an alteration in the intrinsic firing properties. A decrease in the ratio of the delayed rectifyer K^+ current to Na^+ current was observed. When the SOD1 mutation was corrected, the firing rate was lowered, and when firing rate was reduced,

MN survival increased (Wainger et al., 2014). It is thought that hyperexcitability contributes to apoptotic cell death in MNs, possibly through endoplasmic reticulum (ER) stress and the unfolded protein response (UPR). When hyperexcitability is reduced, the ER stress response is reduced. Interestingly, the inverse is true as well, suggesting that hyperexcitability and ER stress are highly interconnected (Kiskinis et al., 2014).

Variability is apparent between each of these neurodegenerative diseases and their relationship to altered excitability, however, it does appear to be a common link between them. Both hypoexcitability and hyperexcitability have been observed, possibly a product of the causative mutations or related to ion channel expression, protein aggregation, and/or synaptic and morphological degeneration. Notably, altered excitability appears to be cell-type specific and likely plays a role in their unique pathologies. Previous experiments determined that differential changes in Kv3.3 channel function caused by expression of the adult and infant onset SCA13 mutations translates into differential effects on Purkinje cell excitability. Based on the results of these experiments, and our current understanding of the relationship between neurodegeneration and neuronal excitability, we hypothesized that differential changes in Purkinje cell excitability due to expression of the adult and infant onset SCA13 mutations leads to differential consequences on Purkinje cell development and cell survival, and that the defects caused by the infant onset mutation will be rescued through reduction of hyperexcitability. Investigation of the mechanisms behind neurodegeneration in rare diseases can provide insight into all neurodegenerative diseases, particularly between those in which common phenotypes are observed, such as altered neuronal excitability.

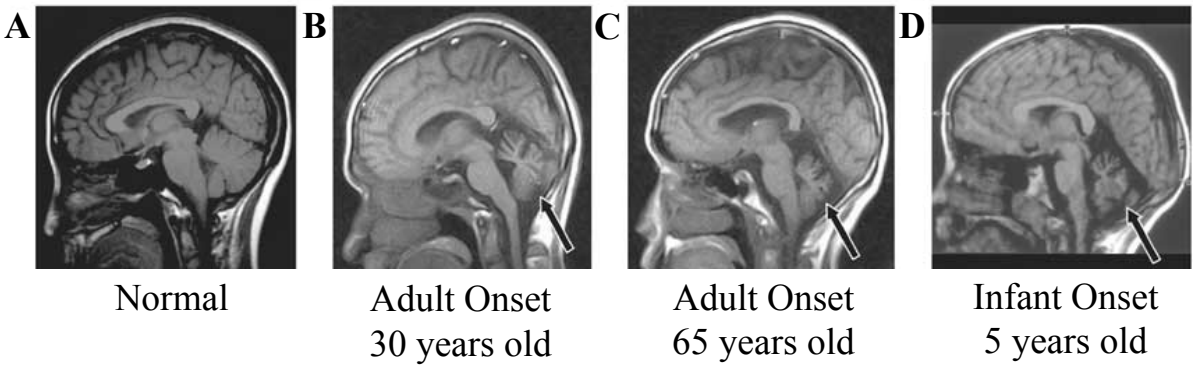

Figure 1.1 Cerebellar atrophy in spinocerebellar ataxia type 13 (SCA13).
Magnetic resonance images of cerebellar anatomy in (A) a normal individual, (B) an adult onset SCA13 patient at 30 years of age, an (C) adult onset SCA13 patient at 65 years of age, and (D) an infant onset SCA13 patient at 5 years of age. The 30 year old and 65 year old patients had a disease duration of 4 years and 43 years, respectively.

Figure reprinted and modifed from:
Waters, M., Minassian, N., Stevanin, G., Figueroa, K., Bannister, J., Nolte, D., Mock, A., Evidente, V., Fee, D., Müller, U., Dürr, A., Brice, A., Papazian, D., Pulst, S. (2006) Mutations in voltage-gated potassium channel KCNC3 cause degenerative and developmental central nervous system phenotypes. *Nature Genetics*. **38(4)**: 447-451.

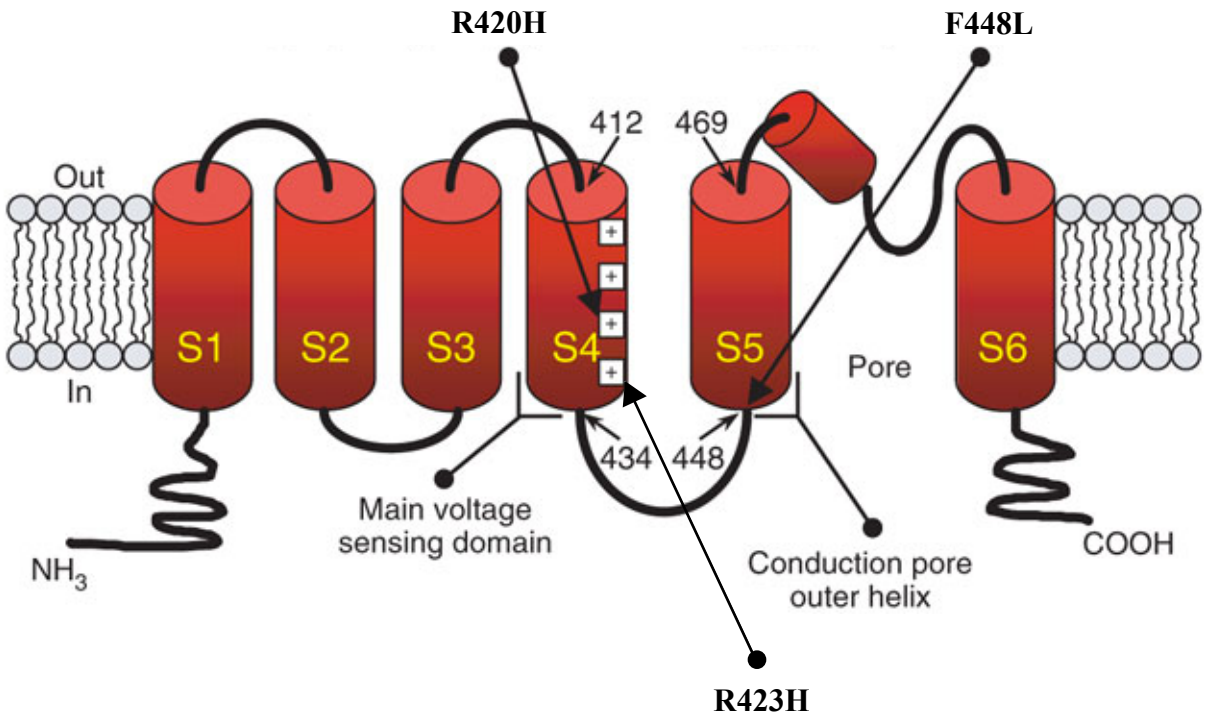

Figure 1.2 Kv3.3 topography and location of adult and infant onset SCA13 mutations. Schematic of human Kv3.3 subunit illustrating each of six transmembrane segments (S1-6). Functional Kv3.3 channels exist as tetramers, either as homotetramers with other Kv3.3 subunits or heterotetramers with other members of the Kv3 family. Mutations are labeled with arrows and include the infant onset F448L mutation in S5, part of the pore region, and the adult onset R420H and infant onset R423H mutations in S4, part of the voltage sensor. These mutations have differential effects on channel function.

Figure reprinted and modified from:
Waters, M., Minassian, N., Stevanin, G., Figueroa, K., Bannister, J., Nolte, D., Mock, A., Evidente, V., Fee, D., Müller, U., Dürr, A., Brice, A., Papazian, D., Pulst, S. (2006) Mutations in voltage-gated potassium channel KCNC3 cause degenerative and developmental central nervous system phenotypes. *Nature Genetics*. **38(4)**: 447-451.

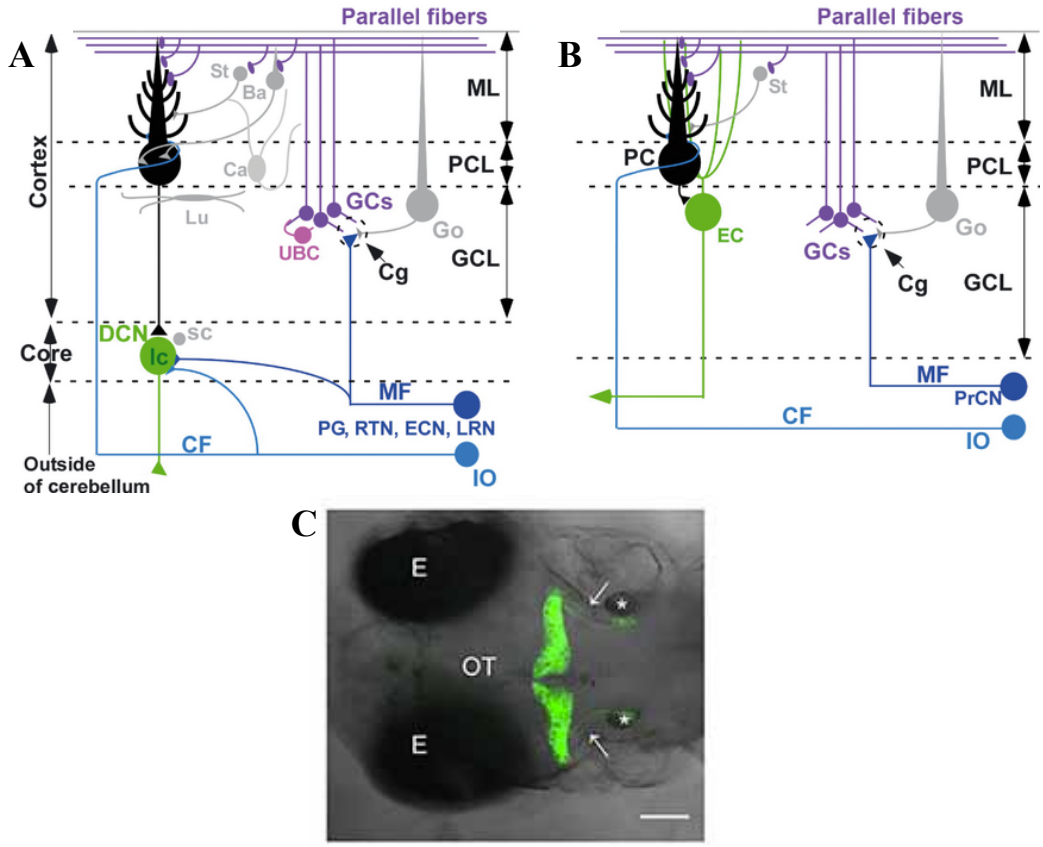

Figure 1.3 Conservation between mammalian and zebrafish cerebellar circuitry and anatomy of zebrafish cerebellum.
Schematic of cerebellar circuitry of the (A) mouse cerebellum and (B) zebrafish cerebellum. Ba, basket cell; Ca, candelabrum cell; CF, climbing fiber; Cg, cerebellar glomeruli; DCN, deep cerebellar nuclei (lc, large cell; sc, small cell); EC, eurydendroid cell; ECN, external cuneate nuclei; GCs, granule cells; GCL, granule cell layer; Go, Golgi cell; IO, inferior olive nuclei; Lu, Lugaro cell; LRN, lateral reticular nuclei; MF, mossy fiber; ML, molecular layer; PC, Purkinje cell; PCL, Purkinje cell layer; PG, pontine gray nuclei; PrCN, precerebellar nuclei (except IO); RTN, reticulotegmental nuclei; St, stellate cells; UBC, unipolar brush cell. (C) Confocal image z-projection of 168 1 µm slices from *Tg(aldoca:gap43-Venus)* at 5 dpf displaying Venus fluorescent protein specifically expressed in Purkinje cells. Anterior is to the left. E, eye; OT, optic tectum; *, otic vesicle; arrows, cerebellovestibular axon tracts. Scale bar, 100 µm.

(A) and (B) reprinted from: Hashimoto, M. and Hibi, M. (2012), Development and evolution of cerebellar neural circuits. *Development, Growth & Differentiation*, **54**: 373–389. doi: 10.1111/j.1440-169X.2012.01348.x
Permission has been granted by John Wiley and Son through Copyright clearance center (RightsLink) website.

(C) reprinted from: Hsieh J-Y, Ulrich B, Issa FA, Wan J and Papazian DM (2014) Rapid development of Purkinje cell excitability, functional cerebellar circuit, and afferent sensory input to cerebellum in zebrafish. *Front. Neural Circuits* **8**:147. doi: 10.3389/fncir.2014.00147

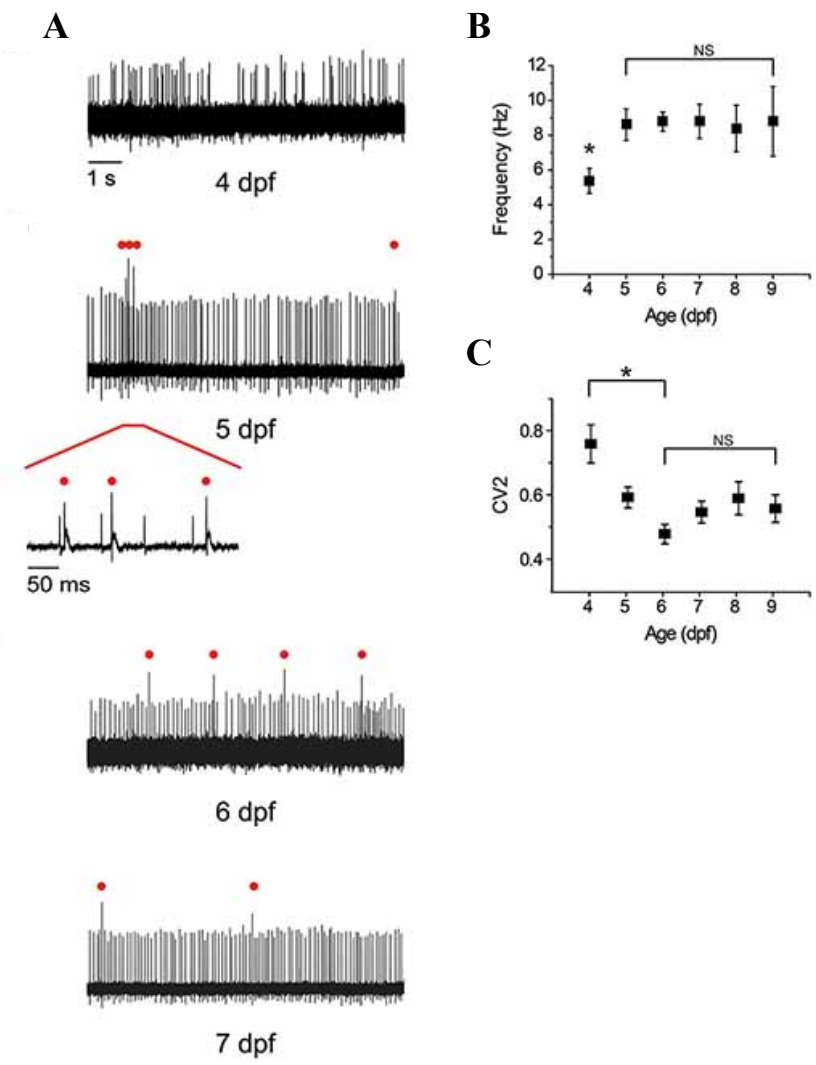

Figure 1.4 Rapid emergence and development of zebrafish Purkinje cell excitability. (A) Representative loose patch recordings of zebrafish Purkinje cells over developmental time, on 4 dpf, 5 dpf, 6 dpf, and 7 dpf. Red dots indicate complex spikes, shown on an expanded time scale at 5 dpf. (B) Average simple spike frequency on 4 dpf through 9 dpf. Simple spike frequency significantly increased on 5 dpf compared to 4 dpf, but not on subsequent days (ANOVA, followed by Holm-Bonferroni post-hoc test, $p < 0.05$). (C) Coefficient of variation of adjacent intervals (CV2), of which a decreasing value indicates increasing firing regularity, significantly decreased between 4 dpf and 6 dpf, but not on subsequent days (ANOVA, followed by Holm-Bonferroni post-hoc test, $p < 0.05$).

Figure reprinted from:
Hsieh J-Y, Ulrich B, Issa FA, Wan J and Papazian DM (2014) Rapid development of Purkinje cell excitability, functional cerebellar circuit, and afferent sensory input to cerebellum in zebrafish. *Front. Neural Circuits* **8**:147. doi: 10.3389/fncir.2014.00147

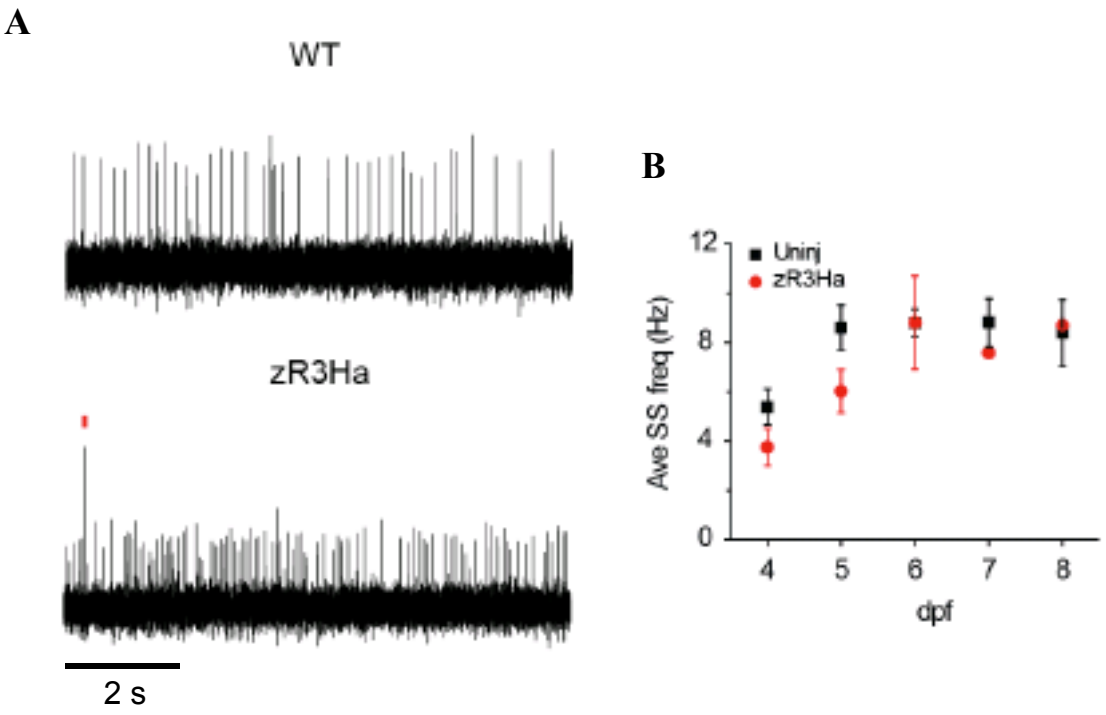

Figure 1.5 The adult onset R3H mutation in zKv3.3 has no significant effect on spontaneous tonic firing in zebrafish Purkinje cells.
(A) Representative loose patch recordings of zebrafish Purkinje cells expressing exogenous WT zKv3.3 or adult onset R3H mutant zKv3.3 at 5 dpf. The stereotypical spontaneous tonic firing pattern was observed in both cells at this time point. (B) Average simple spike frequency in uninjected (black) and R3H (red) expressing Purkinje cells on 4 dpf through 8 dpf. There was no significant difference between these expression conditions at any time point (ANOVA, followed by Holm-Bonferroni post-hoc test, $p < 0.05$)

Credit: Dr. Jui-Yi Hsieh

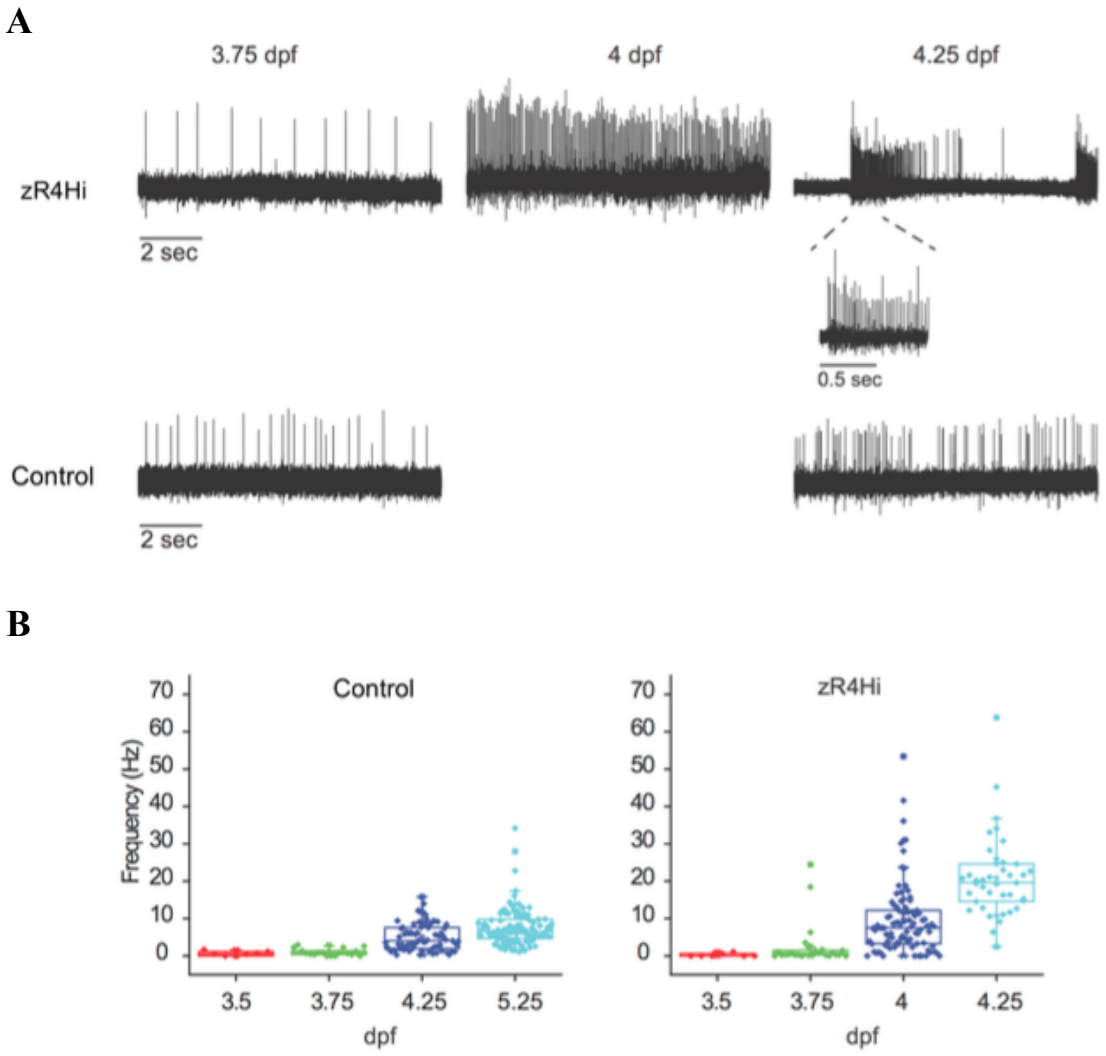

Figure 1.6 The infant onset R4H mutation in zKv3.3 leads to hyperexcitability in zebrafish Purkinje cells.
(A) Representative loose patch recordings of control, uninjected, zebrafish Purkinje cells and zebrafish Purkinje cells expressing exogenous infant onset R4H mutant zKv3.3 at 3.75 dpf, 4 dpf, and 5 dpf. Spontaneous tonic firing emerges in both cases, however, infant onset mutant Purkinje cells rapidly become hyperexcitable with a bursting phenotype (show on an expanded time scale at 4.25 dpf). (B) Average simple spike frequency in control Purkinje cells and infant onset mutant Purkinje cells. A significant increase in firing frequency occurs in control cells between 3.5 and 3.75 dpf, and a significantly higher increase in firing frequency occurs in mutant Purkinje cells between 3.5 and 4.25 dpf (ANOVA, $p < 0.05$). The onset of hyperexcitability occurs at ~3.75 dpf, when mutant Purkinje cells first significantly diverged from control cells (Student's t-test).

Credit: Dr. Jui-Yi Hsieh

Chapter 2

Materials and Methods

Animal maintenance

Zebrafish were housed at the University of California, Los Angeles (UCLA) Zebrafish Core facility at 28°C in a 14 hour/10 hour light-dark cycle. Adult zebrafish were bred to produce embryos for microinjections. Injected zebrafish were raised until 8 dpf in a 28°C incubator in the same light-dark cycle as mentioned previously. Zebrafish were euthanized using 0.2% MS-222 followed by decapitation. Beginning at 5 dpf, larvae were fed brine shrimp powder twice daily. Animal procedures were approved by the Chancellor's Animal Research Committee at UCLA.

RNA ***in situ*** **hybridization**

The protocol for RNA *in situ* hybridization was published previously and is presented here in modified format: Hsieh J-Y, Ulrich B, Issa FA, Wan J and Papazian DM (2014) Rapid development of Purkinje cell excitability, functional cerebellar circuit, and afferent sensory input to cerebellum in zebrafish. *Front. Neural Circuits*. **8**:147. doi: 10.3389/fncir.2014.00147.

Probes derived from the zebrafish *kcnc3a* (Kv3.3a) or *scn8aa* (Nav1.6a) genes were separately mixed with an *aldoca* (Zebrin-II) probe, which was used to identify differentiated Purkinje cells (Tsai et al., 2001; Bae et al., 2009; Mock et al., 2010; Tanabe et al., 2010). Whole mount, double fluorescent *in situ* hybridization was performed as described by Brend and Holley (2009) at 3 dpf, 4 dpf, 5 dpf, and 6 dpf using TLN zebrafish. Animals were euthanized by immersion in 0.2% MS-222, then fixed overnight in 4% paraformaldehyde (PFA) at 4°C. Yolk sacs were removed by dissection. Larvae were permeabilized by digesting with 200 µg/mL proteinase K for 25 min at room temperature. Zebrafish were incubated overnight at 68°C in 50 µL prehybridization buffer containing 1 µL *aldoca* probe and 1 µL *kcnc3a* or 1µL *scn8aa* probe.

Fluorescein-labeled *kcnc3a* and *scn8aa* probes were visualized using the TSA Plus Fluorescein Kit (PerkinElmer) with an incubation time of 45 min at room temperature. Digoxigenin-labeled *aldoca* probes were visualized using the TSA Plus Cy5 Solution (PerkinElmer) with an incubation time of 30 min at room temperature. Specimens were mounted dorsal side up in 75% glycerol.

Gene-specific probes for *aldoca* and *scn8aa* were made using primers from the last coding exon and the 3' untranslated region of each gene (Thisse & Thisse, 2008). To generate the 698 bp antisense and sense probes for the zebrafish *aldoca* gene (NM_001029952), zebrafish genomic DNA was amplified by PCR using the forward primer 5'-ATTTAGGTGACACTATAG AAGGGAAGTACACGGTTTGTGGTGA-3' and the reverse primer 5'-TAATACGACTCACTA TAGGGCACATCTCACAGTTTTATTGCAGCAC-3'. To generate the 703 bp probes for *scn8aa* (NM_131628) genomic DNA was amplified using the forward primer 5'-ATTTAGGTGACACT ATAGAAGACAGTAAGGGCAAAAAGGGCAA-3' and the reverse primer 5'-TAATACGACT CACTATAGGGAATGGGCTGAACGTTTTCCCC-3'. The *aldoca* probe and *scn8aa* probe were transcribed using the RNA Labeling Kit with Digoxigenin or Fluorescein NTP Labeling Mix (Roche Diagnostics), respectively, by T7 RNA polymerase to make the antisense probe and SP6 polymerase to make the sense probe. Probes for *kcnc3a* (NM_001195240.1) were made using a clone containing the first 1363 bp of the cDNA sequence in the pCRII vector (Mock et al., 2010). To generate the antisense probe, the clone was linearized by digestion with HindIII (New England BioLabs), and to generate the sense probe, the clone was linearized by digestion with XhoI (New England BioLabs). Probes were transcribed using the same protocol as mentioned previously for *scn8aa*.

Cloning

All cDNAs/ORFs to be expressed specifically in zebrafish Purkinje cells were cloned into the pminiTol2 plasmid backbone, which contains the minimal sequences necessary for Tol2 transposition (Balciunas et al., 2006). The pminiTol2 plasmid was digested with BglII and HindIII (New England Biolabs) for gene insertion between the 5'- and 3'-miniTol2 sequences. The *aldoca* (Zebrin-II) gene promotor was used to drive Purkinje cell-specific expression in zebrafish (Tanabe et al., 2010). The *aldoca* promoter, the *gap43* palmitoylation sequence, and EGFP were amplified separately and inserted into the pminiTol2 plasmid using In Fusion cloning (Clontech) to generate the pminiTol2-aldoca-gap43-EGFP control clone. The gap43 palmitoylation sequence generates membrane-bound EGFP (mEGFP). A nucleotide was mutagenized using the Quickchange XL Mutagenesis Kit (Agilent Technologies) to create a SalI (New England BioLabs) restriction site. Amplified WT and mutant zKv3.3 and the viral P2A sequence were inserted between the *aldoca* promoter and *gap43* palmitoylation sequence using In Fusion cloning (Clontech) to generate pminiTol2-aldoca-zKv3.3-P2A-gap43-EGFP. The P2A sequence is used to create two separate proteins from one mRNA, in this case to separate zKv3.3 from mEGFP (Ryan & Drew, 1991; reviewed by Szymczak & Vignali, 2005; de Felipe et al., 2006; Kim et al., 2011). This design was used to label the cell morphology independently from the distribution of zKv3.3 expression.

Zebrafish Embryo Microinjections

For overexpression experiments, approximately 200 pg of plasmid DNA was injected into zebrafish embryos at the 1-2 cell stage using a Picospritzer II (Parker Instruments). Injected

embryos were raised in a 28°C incubator in a 14 hour/10 hour light-dark cycle, and every 12 hours after injection, eggs that did not survive were removed and the fish water was replaced. At 48 hpf, embryos were manually dechorionated with forceps. Zebrafish were screened beginning at 3 dpf, when Purkinje cells are first born, using a Zeiss Discovery V12 epifluorescence microscope (Zeiss) or Olympus Fluoview FV300 laser scanning confocal microscope (Olympus).

Acridine Orange Staining

Acridine orange fluoresces green in apoptotic cells, therefore experiments investigating cell death due to mutant zKv3.3 required that mEGFP be replaced with membrane-bound tdTomato (mtdTomato). A previously created clone, pminiTol2-aldoca-Kir2.1-P2A-tdTomato, was digested with AgeI and BamHI (New England BioLabs) to remove the Kir2.1 and P2A sequences. The *gap43* palmitoylation sequence was amplified and inserted using In Fusion cloning (Clontech) to generate the pminiTol2-aldoca-gap43-tdTomato control clone. Mutant zKv3.3, the P2A sequence, and the *gap43* palmitoylation sequence were amplified and inserted between the same restriction site using In Fusion cloning (Clontech) to generate pminiTol2-aldoca-zKv3.3-P2A-gap43-tdTomato.

Zebrafish expressing mutant zKv3.3 and mtdTomato were closely monitored to determine when Purkinje cells began to degenerate with an Olympus Fluoview FV300 laser scanning confocal microscope (Olympus). At this point, typically ~5 dpf, zebrafish were incubated in 1.5 uL/mL acridine orange (Invitrogen) for 1 hour at 28°C then washed 3X in fish water for 5 min each. The staining protocol was done with minimal exposure to light, as acridine

orange bleaches rapidly. Fish were imaged within 15 minutes of the final wash. Acridine orange experiments were repeated in zebrafish expressing mtdTomato alone as a control.

Chronic NS13001 Treatment

Zebrafish expressing mutant zKv3.3 and mEGFP were chronically treated with 20 μM NS13001 (ChemShuttle) to dampen Purkinje cell excitability (Kasumu et al., 2014), beginning at 3.25 dpf through 7 dpf. NS13001 solution was changed every 24 hours, as it precipitates out of solution if left longer. Zebrafish were screened at 4 dpf with an Olympus Fluoview FV300 laser scanning confocal microscope (Olympus), 12 hours after treatment began. NS13001 experiments were repeated in zebrafish expressing mEGFP alone as a control.

Confocal Imaging

Zebrafish were embedded in 1% w/v agarose dorsal side up for imaging. Slices, 1 μm in thickness were taken using an Olympus Fluoview FV300 laser scanning confocal microscope (Olympus). Zebrafish were carefully removed from the agarose between time points and re-embedded for subsequent imaging. For experiments following the development and survival of Purkinje cells, zebrafish expressing mEGFP alone or with WT or mutant zKv3.3 were imaged beginning at 3.25 dpf or 3.75 dpf, depending on the time of birth, through 8 dpf or until cells were no longer visible. For acridine orange experiments, zebrafish expressing mtdTomato alone or with mutant zKv3.3 were imaged before staining at 4 dpf and 5 dpf, and after staining ~5 dpf, or when cells began to degenerate. For NS13001 experiments, zebrafish expressing mEGFP

alone or with mutant zKv3.3 chronically treated with NS13001 or DMSO were imaged beginning at 4 dpf through 7 dpf or until cells were no longer visible.

Data Analysis and Statistics

Morphological images of single Purkinje cells expressing mEGFP alone or with WT or mutant zKv3.3 were traced using Imaris 8.0 (Bitplane) and the quantitative values, including total process length and number of branches, were obtained from these traces. Spines were quantified manually in ImageJ (NIH). To assess the reproducibility of spine quantification, spine counts from three trials were averaged, and differed by less than 10% of the total number in each trial. For the NS13001 experiments, the number of fluorescent Purkinje cells expressing mEGFP alone or with mutant zKv3.3 treated with NS13001 or DMSO were counted manually using ImageJ (NIH). Quantitative values were plotted using GraphPad Prism 7.0 (GraphPad). Statistical analyses were performed using SPSS (IBM). Values were $\log_{10}$-transformed, because individual data points were right-skewed rather than normally distributed within each condition. Comparisons were made using a Linear Mixed Model with Bonferroni post-hoc tests. Statistical significance was assessed as $p < 0.05$. Figures were prepared using Adobe Illustrator (Adobe).

Chapter 3

Expression of Nav1.6 and Kv3.3 in zebrafish Purkinje cells

Introduction

The *KCNC3* gene, which encodes voltage-gated K^+ channel 3.3 (Kv3.3), is mutated in spinocerebellar ataxia type 13 (SCA13). Two mutations, the adult onset R420H mutation and the infant onset R423H mutation are located in the S4 transmembrane segment, an integral part of the voltage sensor (Figure 1.2) (Waters et al., 2006; Figueroa et al., 2010). Notably, Kv3.3 has been implicated in the regulation of spontaneous pacemaking activity in Purkinje cells, along with the resurgent voltage-gated Na^+ channel 1.6 (Nav1.6). In order to investigate SCA13 in zebrafish, it is necessary for us to determine the level of conservation between Purkinje cells in the zebrafish and mammalian cerebellum and determine the presence of Kv3.3 expression.

The mammalian cerebellum consists of 10 lobules (I-X), each containing three layers including the granule cell layer (GCL), the Purkinje cell layer (PCL), and the molecular layer (ML) (Figure 1.3A). Purkinje cell somas reside in the PL, whereas their dendritic arbors reside in the ML. The zebrafish cerebellum consists of three lobes, the valvula cerebelli (Va, anterior lobe), the corpus cerebelli (Cce, main lobe), and vestibulo-lateral lobe (caudo-lateral lobe) located in the hindbrain and organized into two hemispheres (Figure 1.3C). The Va and Cce lobes contain the same three-layered structure as the mammalian cerebellum, however, layers are in the opposite orientation in the Va lobe (Figure 1.3B) (Bae et al., 2009; Hibi & Shimizu, 2011; Hashimoto & Hibi, 2012). The level of conservation is highest between the mammalian and zebrafish cerebellum in the Cce lobe.

The stereotypical morphological features of mammalian Purkinje cells are well characterized. Immediately after birth, small neurites extend from the soma. Obvious polarity emerges with the development of a primary dendrite and axonal processes. The dendrites

massively expand over the first 1-3 months both horizontally and vertically, with a dendritic area of over 5,000 μm^2. Dendritic spines develop over this time period as well (Berry & Bradley, 1976; Hendelman & Aggerwal, 1980; McKay & Turner, 2005). In zebrafish, Purkinje cells are born at ~3 dpf, and extend small neurites similar to those seen in mammalian Purkinje cells. Within 24 hours, a primary dendrite and axonal processes develop. Over successive days, an expansion of the dendrites occurs and dendritic spines develop. Although the dendritic area is much smaller in zebrafish Purkinje cells, 143.5 μm^2, this expansion resembles that observed in mammalian cells (Tanabe et al., 2010).

Purkinje cells fire spontaneous, repetitive action potentials, which do not require excitatory input. The simple spike frequency in Purkinje cells ranges from 1-148 Hz, with a mean frequency of ~40 Hz. (Hausser & Clark, 1997). The pacemaking activity of Purkinje cells can be modulated through parallel fiber input from granule cells, which receive inputs from mossy fibers that originate in the pre-cerebellar nuclei (D'Angelo et al., 2011). This is demonstrated by an increase in firing frequency due to tactile stimulation in mice (Shin et al., 2007). Electrophysiological experiments in our laboratory were the first to describe the electrical activity of zebrafish Purkinje cells using loose patch recordings at room temperature. Zebrafish Purkinje cell excitability emerges at ~4 dpf with a simple spike frequency of 5 Hz (Figure 1.4A). The frequency significantly increases to 9 Hz over the next 24 hours, which is comparable to ~12 Hz in mammalian Purkinje cells at room temperature (Figure 1.4B). The regularity of firing significantly increases over 48 hours after excitability emerges (Figure 1.4C). Exposure to sudden darkness after normalization to light conditions lead to an increase in simple spike

frequency, suggesting that tonic firing can be modulated through stimuli similar to that observed in mammalian Purkinje cells (Hsieh et al., 2014).

Climbing fibers from the inferior olive (IO) trigger distinctive high frequency bursts of spikes, called complex spikes. These complex waveforms consist of a large initial spike followed by several lower amplitude spikelets (Davie, Clark & Hausser, 2008). In zebrafish Purkinje cells, complex spikes emerge at ~ 5 dpf at a maximal frequency (Figure 1.4A), and then subside to a lower frequency that remains stable beginning at 6 dpf (Hsieh et al., 2014). Electrophysiological evidence confirms that the pattern of Purkinje cell excitability and modulation through excitatory input from parallel and climbing fibers is conserved between mammals and zebrafish.

Two currents are thought to regulate spontaneous tonic firing in mammalian Purkinje cells, and we hypothesized that the channels through which these currents pass are expressed in zebrafish Purkinje cells. The Na^+ current implicated in regulation of repetitive firing in zebrafish activates and deactivates slightly faster than typical Na^+ currents. Interestingly, during a protocol designed to produce maximal inactivation, an inward current was observed. The mechanism behind the "resurgent" sodium current is inactivation that behaves like "open channel block," much like in the Shaker potassium channel. Resurgent sodium channels recover from inactivation by passing through open states. (Raman & Bean, 1997). Knockout of the resurgent Nav1.6 channel in mice slowed spontaneous tonic firing in Purkinje cells, suggesting that this channel is particularly important in mediating the current (Khaliq, Gouwens & Raman, 2003). The K^+ current implicated has a depolarized activation range, and compared to other K^+ currents activates and deactivates rapidly. Blocking these currents through Kv3 channels slowed the rate of repolarization of Na^+ spikes in Purkinje cells and attenuated the afterhyperpolarization, as well

as reduced the ability of spikes to discharge repetitively (McKay & Turner, 2004). Kv3.3 channels are highly expressed in the soma and proximal dendrites of Purkinje cells and are likely to be activated by somatic action potentials, suggesting their particular importance in the regulation of firing (Martina, Yao & Bean, 2003).

The interplay between Nav1.6 and Kv3.3 channels in Purkinje cells was reported in Kv3.3 KO mice. Action potentials fire at half the frequency with broader and lower amplitude action potentials in Kv3.3 KO, and restoring a Kv3-like current increased the firing rate by ~50% and the shape of the spikes. The Kv3-like current enhanced the current flow through Nav1.6, and when open channel block in Nav1.6 was decreased, the efficacy of the Kv3-like current on firing rate was reduced (Akemann & Knopfel, 2006). Together the currents from these channels drive depolarization for repetitive neuronal firing through Na^+ currents and rapidly repolarize Na^+ spikes and maintain the duration of action potentials.

We performed whole mount double fluorescent *in situ* hybridization to confirm the expression of these channels in zebrafish Purkinje cells and to characterize the pattern of emergence. We used antisense probes for the *aldoca* gene, which is specifically expressed in Purkinje cells, and for the *scn8aa* and *kcnc3a* genes, which encode Nav1.6 and Kv3.3, respectively. Expression of Nav1.6 and Kv3.3 emerged in zebrafish Purkinje cells at ~4 dpf and presisted through 6 dpf. This pattern of emergence parallels the emergence of excitability. Confirmation of Kv3.3 expression, the gene mutated in SCA13, in zebrafish Purkinje cells is essential before using zebrafish as a model for the disease.

Results

In order to determine whether Nav1.6 and Kv3.3 are expressed in zebrafish Purkinje cells, we performed whole mount double fluorescent *in situ* hybridization as described by Brend and Holley (2009). Antisense and sense probes were designed against the *aldoca* gene, which encodes Zebrin-II, and is specifically expressed in zebrafish Purkinje cells (Tsai et al., 2001; Bae et al., 2009; Mock et al., 2010; Tanabe et al., 2010), and against *scn8aa* and *kcnc3a*, which encode Nav1.6 and Kv3.3, respectively. Probes against *aldoca* and *scn8aa* were designed from sequences spanning the last coding exon and 3' untranslated region (Figure 3.1A) (Thisse & Thisse, 2008) and the probe against *kcnc3a* was designed from the cDNA sequence (Mock et al., 2010) (Figure 3.1B). Zebrafish Purkinje cells are born beginning at ~3 dpf, therefore, zebrafish were fixed and processed at 3 dpf, 4 dpf, 5 dpf, and 6 dpf to determine the emergence and pattern of expression over developmental time. The *aldoca* probe was labeled with digoxigenin, antibodies against which were labeled with Cy5 that fluoresces red, and the *scn8aa* and *kcnc3a* probes were labeled with fluorescein, antibodies against which were labeled with an amplified fluorescein signal that fluoresces green. The expression patterns of *scn8aa* and *kcnc3a* were determined separately.

Expression of *aldoca* was not observed at 3 dpf when Purkinje cell birth begins, but emerged over the next 24 hours. The *aldoca* signal was first observed at 4 dpf (Figure 3.2A, 3.3A). Expression of *scn8aa* (Figure 3.2A, B) and *kcnc3a* (Figure 3.3A, B) was first observed at 4 dpf as well, suggesting expression emerges within the same time frame as the *aldoca* gene. Co-expression of the *aldoca* gene with *scn8aa* (Figure 3.2A, B) or *kcnc3a* (Figure 3.3A, B) was assessed by co-localization of the fluorescent signals, which appeared yellow. Co-expression was

observed at 4 dpf, 5 dpf, and 6 dpf. It appeared that the fluorescence attributed to co-localization increased in intensity through 6 dpf, although it was not quantified and unclear whether this increase in intensity originated from the *aldoca* gene or the *scn8aa* (Figure 3.2A) and *kcnc3a* (Figure 3.3A) genes. No fluorescence was observed in experiments using the sense probes (Figure 3.2C; Figure 3.3C).

Discussion

Emergence of *scn8aa* and *kncnc3a* expression in Purkinje cells parallels the emergence of excitability

The emergence of excitability was recently investigated in zebrafish Purkinje cells, and the pattern of excitability in mammals and zebrafish is highly conserved, along with Purkinje cell morphology and cerebellar circuitry (Bae et al., 2009; Tanabe et al., 2010; Hsieh et al., 2014). Spontaneous tonic firing emerges at 4 dpf and significantly increases in frequency and regularity before rapidly stabilizing over the following 48 hours. Resurgent Na^+ currents, primarily mediated by Nav1.6, and rapidly activating and deactivating K^+ currents, primarily mediated by Kv3.3 and Kv3.4, have been shown to regulate spontaneous tonic firing in mammalian Purkinje cells (Akemann & Knopfel, 2006). We performed whole mount double fluorescent *in situ* hybridization and determined that expression of both Nav1.6 and Kv3.3 is conserved in zebrafish Purkinje cells, suggesting the channels are functionally relevant.

Expression of the *scn8aa* (Figure 3.2A, B) and *kcnc3a* (Figure 3.3A, B) genes, which encode Nav1.6 and Kv3.3, respectively, first emerged in zebrafish Purkinje cells at 4 dpf and persisted through 6 dpf, with an apparent increase in fluorescence intensity. This could indicate

an increase in the density of Purkinje cells, as they are born between 3 dpf and 4 dpf, or may indicate an increase in channel expression. The emergence of expression occurs at a parallel time point to the emergence of zebrafish Purkinje cell excitability. The earliest that excitability typically emerges in these cells is 3.75 dpf, and the expression of these channels emerges after 3dpf, but before 4 dpf. As tonic firing frequency and regularity increases, and complex spiking emerges, it appears the expression of these channels either remains stable or increases. This supports the hypothesis that Nav1.6 and Kv3.3 mediate the pattern of excitability in zebrafish Purkinje cells. Conservation between the mechanisms that regulate mammalian and zebrafish Purkinje cell spontaneous tonic firing, plus conservation of circuitry and Purkinje cell morphology confirms that zebrafish are a strong model for studying the cerebellum and cerebellar dysfunction and disease.

Kv3.3 channels in zebrafish

The function of Kv3.3 channels is conserved in zebrafish. The zebrafish homolog of the Kv3.3 channel was previously identified and its biophysical properties were assessed in *Xenopus* oocytes. Two forms of Kv3.3 are expressed in zebrafish, Kv3.3a and Kv3.3b, encoded by *kcnc3a* and *kcnc3b*, respectively. It is worth noting that these genes are highly conserved, and the probe designed against *kcnc3a* for the *in situ* hybridization experiments likely recognized both genes. Zebrafish Kv3.3 (zKv3.3) is rapidly activating and deactivating, with a depolarized voltage range for activation, similar to that of human Kv3.3 (hKv3.3). N-terminal inactivation was observed, albeit faster than that in hKv3.3 because of a shorter N-terminal extension into the cytoplasm.

Zebrafish Kv3.3 subunits and hKv3.3 subunits can co-assemble, providing further evidence that a striking similarity exists between these homologs (Mock et al., 2010).

Strength of zebrafish as a model for SCA13 due to expression of Kv3.3 in Purkinje cells

Mutant and WT *KCNC3* alleles are expressed in SCA13 patients, therefore, both mutant and WT Kv3.3 subunits are translated (Waters et al., 2006). In *Xenopus* oocytes, it was determined that adult onset R420H mutant subunits cannot form functional channels and that infant onset R423H mutant subunits form functional channels inefficiently. This observation was likely not physiologically relevant, as it required 16X the amount of injected R423H RNA compared to WT RNA to record small currents (Minassian, Lin & Papazian, 2012). Transient transgenic zebrafish were developed through use of microinjections and Tol2 transposition, in which we expressed SCA13 adult or infant onset mutant *kcnc3a* specifically in zebrafish Purkinje cells. We confirmed expression of endogenous *kcnc3a* in zebrafish Purkinje cells, a requirement to observe the effects on Purkinje cell development and survival of either adult onset or infant onset mutant Kv3.3 channels, as the functional effects of these mutations can only be observed if they incorporate into channels with endogenous WT subunits. Co-assembly of WT and mutant subunits provides physiological relevance to what is observed in SCA13 patients.

A

T7 Promoter Sequence: TAATACGACTCACTATAGGG
SP6 Promoter Sequence: ATTTAGGTGACACTATAGAA

aldoca

5' - GGGAAGTACACGGTTTGTGGTGACAGCAGTGGAGCTACTGGTCTTTCCCATTATCTTTCCAGCTACG CATATTGAATTTGCCCCTGATTTCCATACTCCAACATTAGCTGAAAC
ATAGCAGATG TCACTGCCACTTG CATATAAAACTCATAAAGCATGTAAATGTTGATATGATACAGCACATGATGGT GTTCTCTAGGTGGTGGC GTCCTTTGCTTGTCTTAAAAAC
AAGCATAAATGTCTGTTGCTAATTAT ACTGACAAGATTATTAATAAAT GTACAGTTTGCTGTGTAATATCGATCCTTACTACTTACTGTACT TGACCCTTTAACTGTCACCCCACATT
C ATGCTTGAAAATTATAGATGATATATGCATGTTACATATA TAGTTAGTCAAGATAATTTCAGATTTAGACA TACATTTTTTTATTACATGTTCTGAAAAATGTCCAACATGTGGGGT
AAGGGGTTTCTTGAGTCTTAAGGA TTTGTGCTATACGCTTCTGCAATCAAACTTC ATCATC TAAAGCTTTAATAAAGCCTGTGCTTCGGTGACG AATAACAGCTTGGATTACAAG
TTTATC ACAGTATCTGGTATGGTATTTCTGTATGTTAGGCTTCATTATGG ACAACAGTGAAACTATTGACAG TCTGAATACAAACTGAAAGTGCTGCAATAAAACTGTGAGATG
TG - 3'

scn8aa

5' - GACAGTAAGGGCAAAAAGGGCAAAAACCAAAAAGATGTCAAGGAATCCAAGTTTTAGGAACGAT GGACACTGTCTAGTTGAGACTTAAACTATCTATTCCAACAAAATGT
ATAGAAGAAA ATTTGCAACAAAA AACACTGATATCTTTGAGCAAAACAGTTGTTTACATACAACAAATGCACCGGTGCAACAGGAAAGCAG CTTGGTTTTTACAAGATTCA
ATGATGACCAAACCAACTTATGAGCTTACTGTCTT ACATTTTGTGCTAAG TGACCAAGATTTTACTGTTCCAACTGCGGCCAAAAGGCACTTACAAGGACAAACTAAATAACAA
TCCA TGGCAGAAATCTTTGATAGGGACCACCTGCCAATGGACAAACTAGTA CAAAGCAAGCTCATAAGATGG CTTCCTTTGCACTCACATGTGTGTGGAGTTCAGCATTCCTCC
GC TACGGACATCCCGTTCAAACACTAC ACTGCCGAAATCCGACGGAAACCTCCCACTCATCCCAGG AGGATTCTGGGACTTTGTATTTTAACCATA GGAGAACCAATAATAATG
ATGTTAACTCAATCATGT GGAGTGTCTGCCGAAAAAAACAAACAAAAAAA ACAGAACATTATGCAAGGGTTTTCAGTTGTTG TGATGAATATTTCACCTTATTTGATCCACAG
AAAGTAG GGGAAAACGTTCAGCCCATT - 3'

kcnc3a

5'-ATGCTCAGTTCGGTGTGTGTCTCCTCTTTCAAAGGGCGCAAGGGTGGGAACAAGTGTCCAACAAAGCATGTTACAGCGCAGACATGACTTGTCCGTCAGACAGCGAGAAAA
TAGTGATAAACTGCGGGGGGGATTCGGCACGAGACGTACCGCAGCACACTGAAGA CGCTGCCCGGGACCCGCTTGTCCTGGCTGACGGAGCCAGATGCGTTCAGTAACTTTGAC
T ATGACCCCAAATCCGACGAGTTTTTC TTTGACCGTCACCCCAACACCTTTGCGTTCATCCTCAACTATTACCGCACAGGGAAGTTGCATTGTCCCAGTGATGTCTGCGGTCCT
CTGTTTGAGGAGGAGCTCGCCTTCTGGGGTATCGACGAGACGGACGTGGAGGCTTGCTGCTGGATGAACTACCGACAGCATCGGG ACGCCGAGGAAGCGCTGGACAGCTTCG
AGACGCCCGAGCCGGACCCACCAGAGGACGACCCGGCGCTAACTGGAGGAGCGGACGGTGACTTGAAGAGGTTGTGTCTAC AGGAGGATGGGCGAAACCCCAGCCGGTGG
AGTACCTGGCAACCCTGGGTCTGGGCGCT G TTTGAGGACCCCTACTCCTCGAAATACGCCAGGTATGTGGCGTTCGGCTCGCTCCTGTTCATCCTCATCTCCATCTCAACATTTTG
CTTGGAGACACACGAGGCCTTCAACACCATCTACAATAAGACAGAGAACGTGACGGTGGGGAACGTCACGCGGGAAGAGGTTG TG TTTGAGGTAGTGACTGACAACTGGCTG
ACCTACGTGGAGGGCGTTTGCGTGGTCTGGTTCACCATCGAGGTGTTCACCCGTGT CAT CTTTTGCCCGGACAAGGCTGAGTTCTTCAAGAGCTCGCTGAACATCATCGACT
TTGTAGCCATCCTGCCCTTTTACCTAGAGAT GGCGCTGAGCGGCCTCTCCTCTAAAGCAGCCAAAGATGTGCTGGGCTTTTTGCGTGTGGTGCGATTTGTCAGAATTCTGCGAAT
CT TC AAGCTCACGCGCCACTTTGTGGGGCTGAGGGTGCTGGGCCACACACTCCGTGCCAGTACCAATGAGTTCTTACTCCTCATC ATCTT CCTTGCTCTTGGGGTGCTCATCT
TCGCCACTATGATCTACTACGCCGAGCGCATCGGCGCCGACCCGGATGACCCTACAGCC AG TGC CCACACCGCCTTCAAAAACATCCCCATCGGCTTCTGGTGGGCGGTGGTC
ACCATGACGACTCTAGGCTATGGTGACATGT ATCCCG AGACATGGTCGGGCATGTTGGTGGGCGCCCTGTGTGCCCTGGCAGGCGTGCTGACCATCGCCATGCCTG TGCCCGTC
ATTGT-3'

B

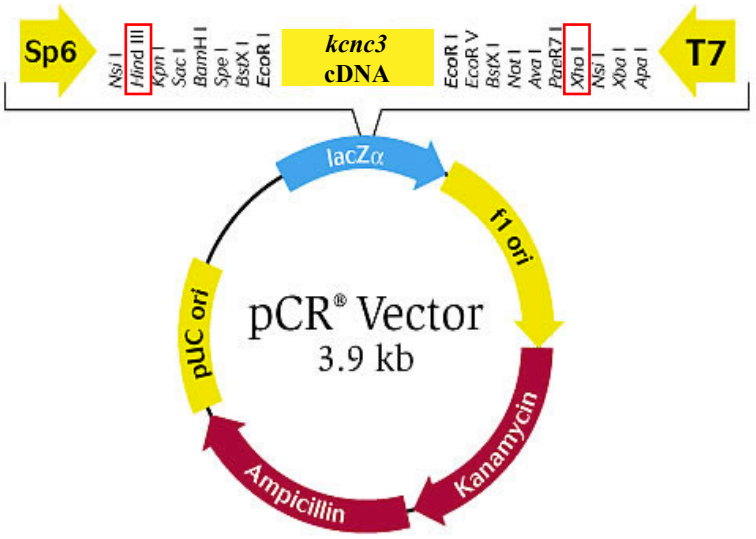

Figure 3.1 *In situ* hybridization probe design for *aldoca*, *scn8aa*, and *kcnc3a*.
(A) The template sequences for the *aldoca*, *scn8aa*, and *kcnc3a* antisense and sense probes are shown. Sequences from the last coding exon are in blue, and from the 3' untranslated region are in red for the *aldoca* and *scn8aa* templates. The SP6 promoter was added to the forward primer for transcription of the sense probe, and the T7 promoter was added to the reverse primer for transcription of the antisense probe. The *kcnc3a* template was designed using the first 1361 bp of the cDNA sequence. (B) The *kcnc3a* cDNA probe template was placed in the pCRII Vector (ThermoFisher), which was cut with HindIII or XhoI (red boxes) to transcribe the antisense probe with T7 polymerase or the sense probe with SP6 polymerase, respectively.

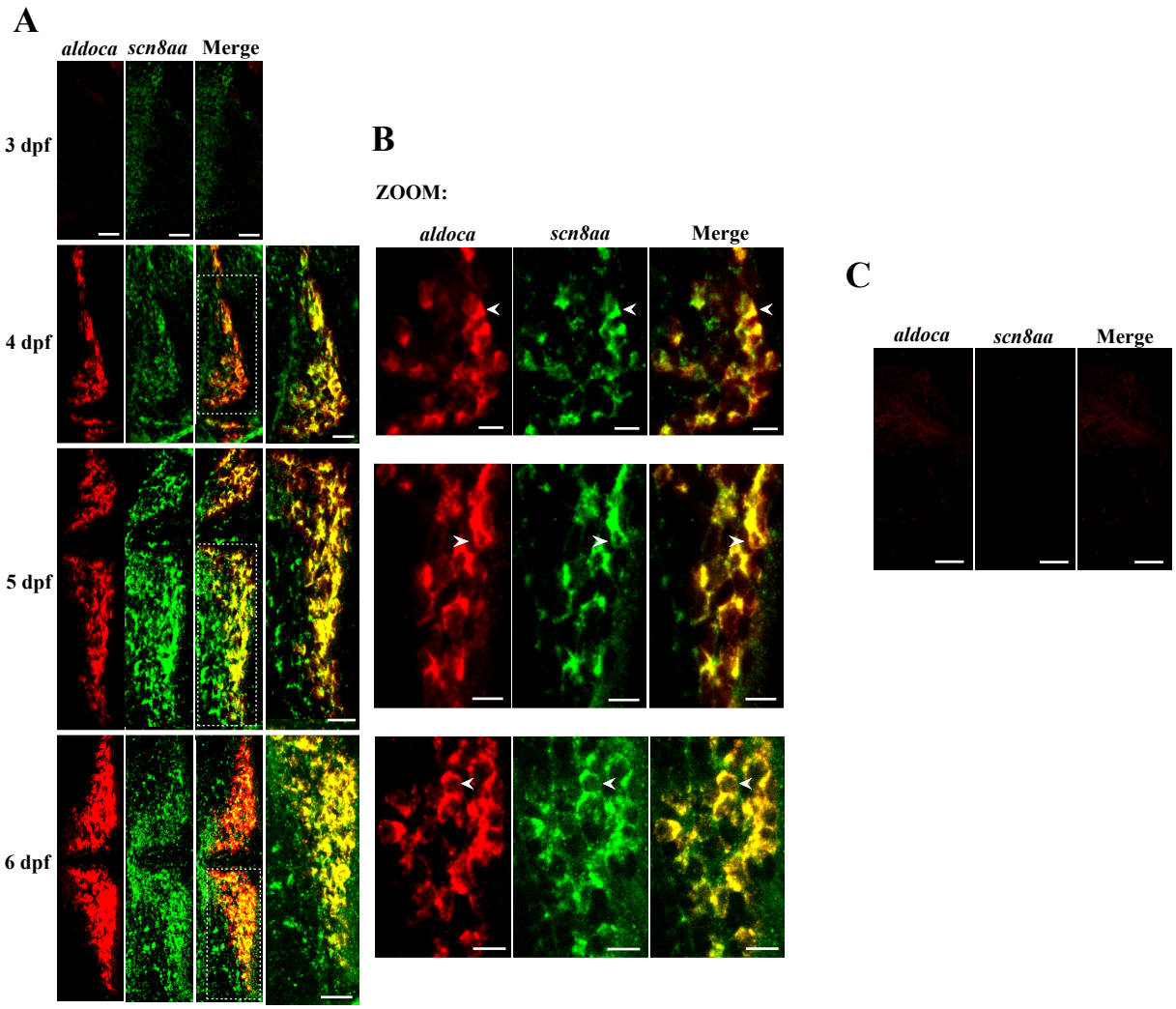

Figure 3.2 Expression of the *scn8aa* gene, encoding Nav1.6, in zebrafish Purkinje cells
(A) Whole mount double fluorescent *in situ* hybridization was performed on TLN zebrafish at 3 dpf, 4 dpf, 5 dpf, and 6 dpf using a digoxigenin-labeled antisense probe (red) for the *aldoca* gene, expressed specifically in zebrafish Purkinje cells, and a fluorescein-labeled antisense probe (green) for the *scn8aa* gene, which encodes Nav1.6. The merged panels indicate co-localization of the signals (yellow). Confocal image stacks are shown with 1 µm slices, with a dorsal view and anterior to the left. Scale bars are 40 µm. (B) Dashed white boxes indicate cerebellar hemispheres, single confocal slices of which are enlarged (zoom). White arrowheads indicate Purkinje cell bodies. Scale bars are 10 µm. (C) The experiment was repeated at 5 dpf with a digoxigenin-labeled sense probe (red) for the *aldoca* gene and a fluorescein-labeled sense probe (green) for the *scn8aa* gene. Confocal image stacks are shown with 1 µm slices, in the same orientation as (A). Scale bars are 40 µm.

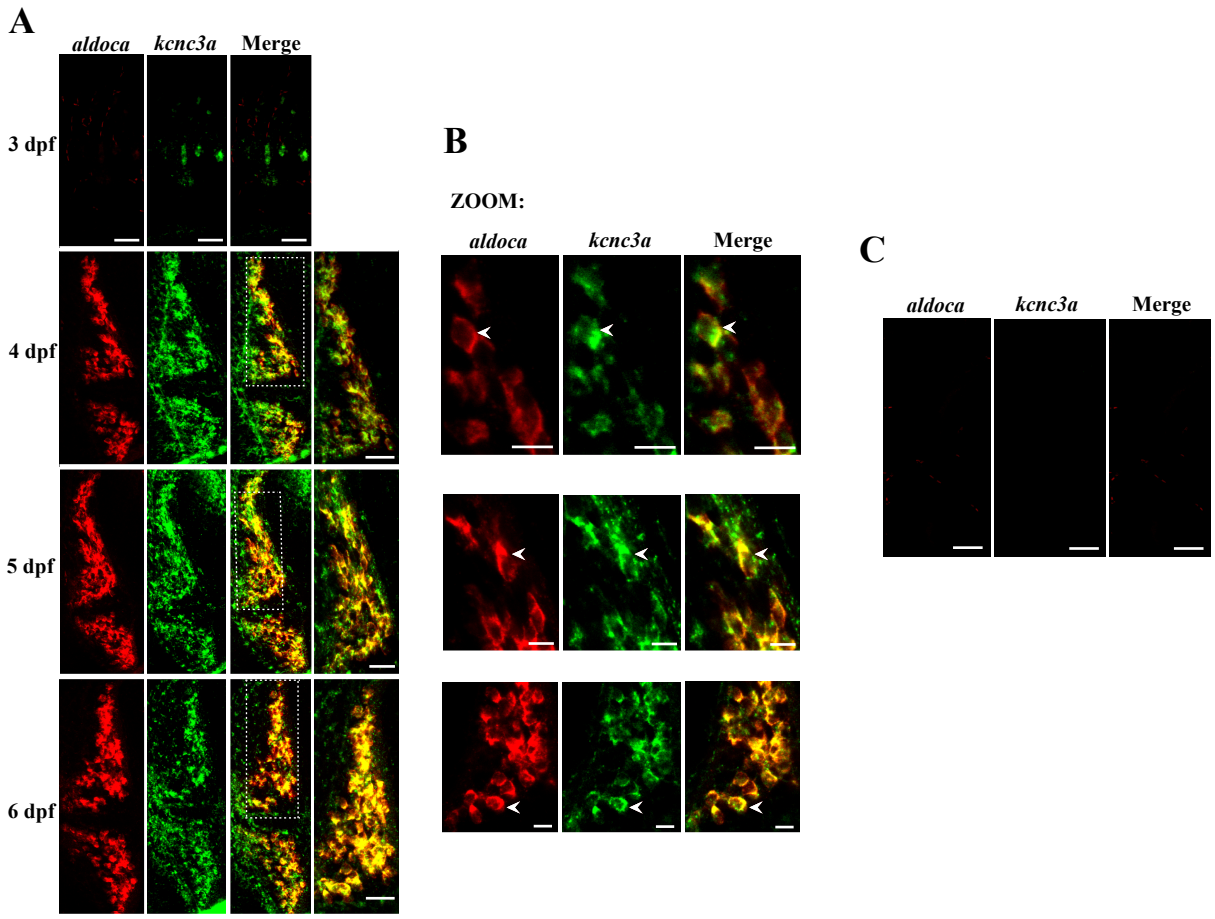

Figure 3.3 Expression of the *kcnc3a* gene, encoding Kv3.3, in zebrafish Purkinje cells
(A) Whole mount double fluorescent *in situ* hybridization was performed on TLN zebrafish at 3 dpf, 4 dpf, 5 dpf, and 6 dpf using a digoxigenin-labeled antisense probe (red) for the *aldoca* gene, expressed specifically in zebrafish Purkinje cells, and a fluorescein-labeled antisense probe (green) for the *kcnc3a* gene, which encodes Kv3.3. The merged panels indicate co-localization of the signals (yellow). Confocal image stacks are shown with 1 µm slices, with a dorsal view and anterior to the left. Scale bars are 40 µm. (B) Dashed white boxes indicate cerebellar hemispheres, single confocal slices of which are enlarged (zoom). White arrowheads indicate Purkinje cell bodies. Scale bars are 10 µm. (C) The experiment was repeated at 5 dpf with a digoxigenin-labeled sense probe (red) for the *aldoca* gene and a fluorescein-labeled sense probe (green) for the *kcnc3a* gene. Confocal image stacks are shown with 1 µm slices, in the same orientation as (A). Scale bars are 40 µm.

Chapter 4

SCA13 infant onset R4H mutation leads to rapid degeneration of Purkinje cells

Introduction

Spinocerebellar ataxia type 13 (SCA13) mutations occur in the *KCNC3* gene, which encodes the voltage-gated K^+ channel 3.3 (Kv3.3) (Figure 1.2) (Waters et al., 2006; Figueroa et al., 2010). Kv3 channels have unique biophysical properties, including rapid activation at a depolarized membrane potential and rapid deactivation. K^+ currents from these channels are apparent at potentials more positive than -10 mV. The probability of opening increases with voltage, and upon repolarization, deactivation occurs 10X faster than that in other voltage-gated K^+ channels. Kv3.3 is subject to N-type inactivation, confirmed by the absence of inactivation when the cytosolic N-terminal extension is removed (Rudy et al., 1999). The SCA13 adult onset R420H mutation and infant onset R423H mutation occur in the third and fourth positively charged arginine residues in the S4 transmembrane segment, an integral part of the voltage sensor (Figure 1.2) (Waters et al., 2006; Figueroa et al., 2010). These arginine residues are highly conserved and interact with the electric field across the membrane. When the membrane potential is hyperpolarized, the voltage sensor domain is drawn towards the intracellular side of the membrane. Upon depolarization, the voltage sensor moves towards the extracellular side of the membrane. This voltage-dependent conformational change is driven by the positively charged arginine residues in the S4 segment. Outward movement of the voltage sensor domain increases the probability of pore opening. This conformational change is stabilized by the formation of salt bridges and electrostatic interactions with the surrounding transmembrane segments and membrane lipids (Papazian et al., 1995; Seoh et al., 1996; Tiwari-Woodruff et al., 1997; Tiwari-Woodruff et al., 2000; Laine et al., 2003; Silverman et al., 2003; Brojesson & Elinder, 2008; Jensen et al., 2012).

Despite the proximity of the adult and infant onset mutant residues in the primary sequence, their functional similarities, and the fact that the are both arginine-to-histidine mutations, the adult onset R420H mutation and infant onset R423H mutation have differential effects on channel function. SCA13 patients express both a mutant *KCNC3* allele and a WT allele, which are both translated into subunits that co-assemble (Waters et al., 2006). Kv3.3 exists as a tetramer, either a homotetramer with other Kv3.3 subunits or a heterotetramer with other Kv3 family subunits (Mackinnon, 1991). Both the adult onset and infant onset mutations exert dose-dependent dominant negative suppression of current amplitude, however, distinct changes were observed as well (Waters et al., 2006; Figueroa et al., 2010). Subunits containing the adult onset R420H mutation cannot form functional channels on their own. At ratios of 1:0.25 to 1:4 (WT:R423H), the residual current amplitudes in *Xenopus* oocytes agreed with the prediction that one mutant subunit could incorporate into a functional channel, however, the remaining amplitudes were less than those expected if more than one mutant subunit could incorporate into a functional channel, assuming that the amount of protein translated is correlated to the amount of RNA injected (Lin, Minassian & Papazian, 2012). Subunits containing the infant onset R423H mutation were able to form functional channels on their own, albeit inefficiently. It took 16X as much R423H RNA compared to WT RNA to record small currents, therefore, this observation is likely not physiologically relevant. Current amplitudes in *Xenopus* oocytes at higher doses matched well with more than one mutant subunit incorporating into functional channels. Whereas the adult onset mutation does not change channel gating, incorporation of the infant onset mutation leads to modest changes in channel gating. These changes include a moderately hyperpolarized shift of the half-maximal activation voltage ($V_{1/2}$), slowed activation between

+10 and +50 mV, and slowed deactivation (Minassian, Lin & Papazian, 2012). Notably, the slowed deactivation is minor in physiologically relevant solutions.

Kv3 channels impart unique firing properties onto the neurons in which they are expressed, specifically spontaneous tonic firing such as that observed in Purkinje cells. Blocking Kv3 channels in fast spiking neocortical interneurons reduced the steady state firing rate and produced near complete elimination of the afterhyperpolarization, which plays an essential role in repolarization. Reduction of firing frequency became most apparent during the spike train and decreased the depolarization slope of each action potential after the first spike (Erisir et al., 1999). In Purkinje cells, blocking Kv3 channels decreased the number of Na^+ spikes in Na-Ca spike bursts, slowed the rate of Na^+ spike repolarization, and attentuated the afterhyperpolarization, much like the effect observed in neocortical interneurons (McKay & Turner, 2004). Taken together, it is clear that Kv3 channels are necessary in maintaining sustained firing by rapidly repolarizing Na^+ spikes for the next action potential by limiting the accumulation of inactivated Na^+ channels (Erisir et al., 1999; McKay & Turner, 2004). Kv3.3 and Kv3.4 are expressed in Purkinje cells. Kv3.3 channels are highly expressed in the soma and proximal dendrites of Purkinje cells and are likely activated by somatic action potentials, suggesting it is particularly important in the regulation of Purkinje cell firing (Martina, Yao & Bean, 2003).

We hypothesized that the differential effects of the adult onset R420H mutation and infant onset R423H mutation on channel function lead to differential changes in Purkinje cell excitability. This was investigated in the zebrafish cerebellum, using the zebrafish homolog of Kv3.3 (zKv3.3) and the corresponding mutations: R335H (adult onset, R3H) and R338H (infant

onset, R4H). Each mutation was expressed specifically in zebrafish Purkinje cells using the *aldoca* gene promoter. Loose patch recordings revealed that expression of the adult onset mutation leads to latent hypoexcitability in Purkinje cells (Figure 1.5). During spontaneous tonic firing, hypoexcitability is not apparent, but when cells are driven to fire at high frequencies through exposure to sudden darkness, significant hypoexcitability is observed (Hsieh & Papazian, unpublished). In contrast, expression of the infant onset mutation leads to rapid emergence of hyperexcitability in spontaneously firing Purkinje cells. Interestingly, a bursting phenotype is observed at frequencies of up to 50 Hz [compared to the spontaneous tonic firing frequency of ~9 Hz in control cells (Hsieh et al., 2014)] (Figure 1.6). Cells were typically silent by 5 dpf (Hsieh & Papazian, unpublished).

Considering the differential effects on Kv3.3 channel function and Purkinje cell excitability, we hypothesized that expression of the adult onset R3H mutation and infant onset R4H mutation would have differential effects on Purkinje cell development and survival. Previously, developmental phenotypes were investigated in zebrafish primary motor neurons expressing the adult onset R3H mutation, and a different infant onset mutation (FL) that has a similar effect on Kv3.3 channel gating to that of R4H, but does not exert a dominant negative effect (Issa et al., 2012). CaP motor neurons have a characteristic axonal loop around the ventral muscle of the zebrafish tail and consistent branching, along with rapid development within 48 hours, making them a strong starting point for preliminary studies. The adult onset mutation leads to excessive axonal branching at the distal end. The infant onset FL mutation leads to axonal pathfinding errors in CaP motor neurons with long collaterals that extend into peripheral

muscle (Issa et al., 2012). This provided evidence of a differential developmental phenotype depending on the expressed SCA13 mutation.

Although the evidence in zebrafish primary motor neurons was in line with our hypothesis, the main pathology of SCA13 in patients is within the cerebellum. In order to infer phyisological relevance, it is necessary for us to focus our investigations on the zebrafish cerebellum. To investigate the differential effects of the adult onset R3H mutation and infant onset R4H mutation, we expressed mutant *kcnc3a* specifically in zebrafish Purkinje cells. Expression of the infant onset mutation leads to rapid degeneration of Purkinje cells over developmental time, with the majority of cells disappearing by 6 dpf. Expression of the adult onset mutation did not significantly alter Purkinje cell morphology when compared to the EGFP and WT controls. The deterioration of Purkinje cells expressing the infant onset R4H mutation has negative implications on cerebellar function and interestingly, the pattern of degeneration paralleled the emergence of hyperexcitability previously recorded in these cells, suggesting a possible connection.

Results

Exogenous expression of WT and mutant zKv3.3 specifically in zebrafish Purkinje cells

To test the hypothesis that the adult and infant onset SCA13 mutations lead to differential changes in Purkinje cell development and survival, the *kcnc3* gene with the adult onset R3H mutation or infant onset R4H mutation was exogenously expressed in zebrafish Purkinje cells through the Purkinje cell-specific promoter of the *aldoca* gene (Tanabe et al., 2010). DNA was inserted into the zebrafish genome using the pminiTol2 plasmid backbone, which contains the

minimal sequences for Tol2 transposition, when injected into zebrafish embryos at the 1-2 cell stage of development (Balciunas et al., 2006). Exogenous wild-type (WT) or mutant *kcnc3* were co-expressed with membrane-bound EGFP (mEGFP) using the P2A sequence, which produces individual proteins from the same mRNA (Figure 4.1B). As a control, mEGFP was expressed (Figure 4.1A).

Zebrafish were screened for expression of mEGFP between 3 dpf and 3.75 dpf, as Purkinje cells may be born at any point within that time frame. Confocal imaging began at 3.25 dpf or 3.75 dpf, depending on when the cell was first observed, and followed 12 hours after first observation and every successive 24 hour interval until 8 dpf, or until the cell was no longer visible. Development of zebrafish Purkinje cells begins at birth, typically ~3 dpf, with the extension of small neurites. Within 24 hours, a primary dendrite forms and over the next several days the dendritic tree becomes more complex and spines develop (Tanabe et al., 2010).

Purkinje cells expressing mEGFP alone exhibit stereotypical development and characteristics

Purkinje cells expressing mEGFP alone exhibited the stereotypical pattern of Purkinje cell development. Purkinje cells were typically born between 3 dpf and 3.75 dpf with an obvious primary dendrite developing 12 -24 hours later (Figure 4.2A). Total process length increased over the next 4 days from an average of 224 μm to 573 μm, with a difference of 349 μm (Figure 4.6A). Process complexity, as determined by the number of branches, increased over the same developmental time period, from an average of ~28 branches to ~64 branches, with a difference of 36 branches (Figure 4.6B). Axons can be distinguished from dendrites based on the presence

of dendritic spines, which became apparent ~36 hours after first observation, typically at ~5 dpf (Figure 4.2B).

Expression of the infant onset R4H mutation leads to rapid degeneration and disappearance of Purkinje cells

Purkinje cells expressing the infant onset R4H mutation rapidly degenerated and out of 12 cells, all but two disappeared 48-72 hours after they were first observed. Cells were born between 3 dpf and 3.75 dpf, but did not develop an obvious primary dendrite (Figure 4.3). Total process length was significantly shorter than that in mEGFP controls at 0.5, 1, and 2 days after first observation, decreasing over developmental time from an average of 162 μm to 117 μm (compared to 244 μm and 423 μm in controls), with a difference of 44 μm after 48 hours (Figure 4.6A). Processes in infant onset mutant cells exhibited reduced complexity, with significantly fewer branches than the mEGFP control at 0.5, 1, and 2 days after first observation. Purkinje cells expressing the infant onset mutation were first observed with ~15 branches, versus ~28 branches in controls, and had ~13 branches 48 hours later compared to ~64 branches in controls (Figure 4.6B). Dendritic spines were not observed. Process retraction and reduced complexity, along with Purkinje cell disappearance, suggest that this infant onset mutation not only leads to structural defects and deterioration, but decreases cell survival. Statistical comparisons could only be made up to 48 hours after Purkinje cells were first observed because at later time points, too few cells remained.

Expression of the adult onset R3H mutation does not significantly alter Purkinje cell development or survival

Purkinje cells expressing the adult onset R3H mutation were born and developed within the same time frame as the mEGFP controls, neither total process length or the number of branches significantly differed, and a similar number of spines developed (Figure 4.4A). An interesting trend was observed in mutant Purkinje cells that did not reach a level of statistical significance compared to the mEGFP control at any time point. Rather than increasing, total process length remained stable over developmental time, from an average of 356 μm to 351 μm. The difference was 5 μm after 4 days compared to 349 μm in controls (Figure 4.6A). Similar stability was observed in the number of branches over the same time frame, from an average of ~37 branches to ~36 branches. The difference was ~1 branch compared to ~36 branches in controls (Figure 4.6B). A similar number of dendritic spines compared to mEGFP controls developed ~36 hours after cells were first observed (Figure 4.4B). Purkinje cells expressing the adult onset mutation did not disappear suggesting there is no effect on cell survival. This contrasts with Purkinje cells expressing the infant onset mutation, which typically disappeared within 48 hours. Total process length was significantly shorter and significantly fewer branches were observed in cells expressing the infant onset mutation at 0.5, 1 and 2 days after first observation compared to those expressing the adult onset mutation (Figure 4.6).

Overexpression of the zKv3.3 channel has no effect on stereotypical development in Purkinje cells or their characteristics

Purkinje cells expressing exogenous WT zKv3.3 were born and developed within the same time frame and in the same pattern as mEGFP control cells (Figure 4.5A). Total process length increased over developmental time from an average of 278 μm to 524 μm, with a difference of 246 μm after 4 days (Figure 4.6A). The number of branches increased over the same time frame, from an average of ~35 branches to ~62 branches with a difference of ~27 branches (Figure 4.6B). Total process length and the number of branches did not significantly differ in Purkinje cells expressing exogenous WT Kv3.3 compared to mEGFP control cells or cells expressing the adult onset mutation at any time point (Figure 4.6). A similar number of dendritic spines began to develop ~36 hours after cells were first observed as well (Figure 4.5B). In contrast, infant onset Purkinje cells had a significantly shorter total process length and significantly fewer branches at 0.5, 1, and 2 days after first observation than cells expressing exogenous WT Kv3.3 (Figure 4.6).

Discussion

The adult onset R3H mutation and infant onset R4H mutation had differential effects on Purkinje cell development and survival

The SCA13 adult onset R3H mutation and infant onset R4H mutation lead to differential effects on Purkinje cell development and survival. Expression of the infant onset mutation in zebrafish Purkinje cells leads to rapid degeneration (Figure 4.3). Over 48 hours, total process length decreased and was significantly shorter compared to mEGFP or WT control cells and cells

expressing the adult onset mutation at 0.5, 1, and 2 days after first observation (Figure 4.6A). Complexity of the dendritic arbor, measured as the number of branches, was significantly reduced compared to mEGFP or WT control cells and cells expressing the adult onset mutation at the same time points (Figure 4.6B). Dendritic spines were not observed in mutant cells. The majority of Purkinje cells disappeared within 48 hours of first observation, at ~6 dpf. In contrast, expression of the adult onset mutation resulted in no significant changes in total process length or dendritic complexity when compared to controls (Figure 4.4A). Whereas in mEGFP control cells, and those expressing exogenous WT zKv3.3, total process length and number of branches increased over developmental time, in the cells expressing the adult onset mutation, the measurements remained stable (Figure 4.6).

Negative implications of Purkinje cell degeneration and loss on cerebellar circuitry and function

The degeneration and loss of Purkinje cells have negative implications for cerebellar circuitry and function. Purkinje cells receive several inputs from other neurons within the cerebellum and from neurons in other brain regions. Mossy fibers from pre-cerebellar nuclei synapse onto granule cell bodies, which send parallel fibers to Purkinje cell dendrites (Bae et al., 2009; Hashimoto & Hibi, 2012). Mossy fibers can send inputs to ~500 granule cells and Purkinje cells may receive inputs from ~100,000 parallel fibers (Ito, 1984; Napper & Harvey, 1988; Ito, 2006). Climbing fibers originate in the inferior olive (IO) and synapse on the Purkinje cell body and dendrites. Mossy fiber inputs are known to modulate simple spiking, whereas activity at climbing fiber synapses induces complex spiking (D'Angelo et al., 2011).

The dendritic arbor of Purkinje cells expressing the infant onset R4H mutation degenerates, has reduced complexity, and dendritic spines, which are essential for contacts with parallel and climbing fibers, are not observed. Assuming that these observations are physiologically relevant to infant onset SCA13 patients, along with the possible loss of density due to cell disappearance, these changes likely lead to decreased input from other cerebellar neurons and regions of the brain. Long term depression (LTD) and long term potentiation (LTP) are required for motor learning, and both occur at parallel fiber-Purkinje cell synapses. LTD originates from coincident parallel fiber and climbing fiber input, and the resultant Ca^{2+} response triggered by climbing fiber depolarization (Ito, 1982; Ito, 1989; Krupa & Thompson, 1997). LTP can occur both pre- and post-synaptically at the parallel fiber-Purkinje cell synapse. Pre-synaptic LTP originates from brief parallel fiber stimulation at 4-8 Hz. This leads to Ca^{2+} influx within the parallel fiber terminal and triggers a cascade that increases glutamate release (Salin et al., 1996; Chen & Regehr, 1997; Storm et al., 1998; Jacoby, Sims & Hartell, 2001; Kaeser et al., 2008). Post-synaptic LTP originates from low frequency parallel fiber input at ~1 Hz and triggers α-amino-3-hydroxy-5-methyl-4-isoxazolepropionic acid (AMPA) receptor insertion in the Purkinje cell spine membrane (Anggono & Huganir, 2012). These essential events between synapses would be interrupted and diminished as dendritic degeneration progresses and Purkinje cells disappear.

Strength of experimental design and how results may reflect SCA13 age of onset

An earlier study used mouse cerebellar culture to investigate the effect of the infant onset R423H mutation on Purkinje cell morphology. Notably, Purkinje cells decreased in density

between DIV7 and DIV11 and dendritic development was impaired (Irie et al., 2014). While these results are important for our understanding of the infant onset mutation, without receiving inputs from parallel and climbing fibers and interneurons under physiological conditions, the results do not provide us with the pattern of degeneration or disappearance over relevant developmental time and cannot necessarily be applied to clinical events. We expressed the mutation in zebrafish Purkinje cells and imaged them *in vivo* with intact circuitry, in animals that were able to freely swim and that were not anesthetized at any time point. Rapid degeneration and cell death early in development correlates well with the early age of onset of clinical phenotypes in infant onset SCA13 patients, if these changes lead to an inability to receive, integrate, or send information to and from other regions of the brain. In adult onset SCA13, patients do not experience clinical phenotypes until much later in life, suggesting that the mutation has a delayed effect on the cerebellum. The stabilization of total process length and number of branches that we observed may indicate that although no significant effects on zebrafish Purkinje cell development or survival were observed early, that the phenotype is delayed or may only appear once zebrafish reach maturity.

Pattern of degeneration suggests a connection to hyperexcitability in Purkinje cells expressing infant onset R4H mutation

The pattern of degeneration in zebrafish Purkinje cells expressing the infant onset R4H mutation parallels the emergence of hyperexcitability (Hsieh & Papazian, unpublished). Degeneration begins rapidly, and no obvious primary dendrite forms (Figure 4.3). The formation of the primary dendrite typically occurs at ~4 dpf, which is when hyperexcitability was first

observed in loose patch recordings. The majority of cells disappeared between 5 dpf and 6 dpf, at the same time point when the majority of cells were silent. Although it remains unclear, it is reasonable to speculate that this silence reflects the deterioration and/or impending death of Purkinje cells, as firing is spontaneous and action potentials are not dependent on input. The observed parallel between structural deterioration of Purkinje cells and the emergence of hyperexcitability suggests that a relationship exists between alterations in spontaneous tonic firing and degeneration. The disappearance of Purkinje cells expressing the infant onset R4H mutation likely reflects cell death. We believe that reducing hyperexcitability in these cells will rescue the degenerative phenotype, and therefore the observed decrease in cell survival.

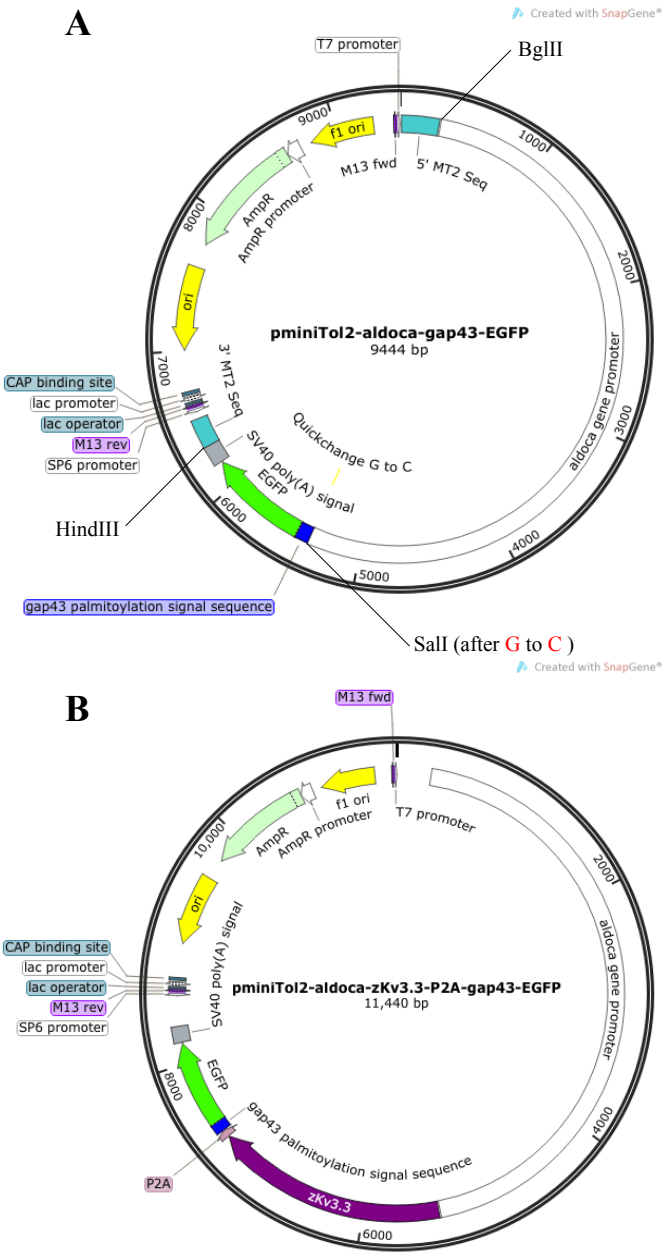

pminiTol2 digested with BglII and HindIII

aldoca:
F: 5'- taatttaaatagatcacgcgagttattcaatgagccc -3'
R: 5'- tggtccacaacctgaggacagtacagatgaggccct -3'

gap43:
F: 5'- tcatctgtactgtcctcaggttgtggaccatgctgtg -3'
R: 5'- gcccttgctcaccatggtggatccgatgggatcct -3'

EGFP:
F': 5'- cccatcggatccaccatggtgagcaagggcgaggg -3'
R: 5'- tggatcatcatcgatttacttgtacagctcgtccatgcc -3'

Quickchange G to C between aldoca and gap43:
F: 5'- gtactgtcctcaggttgtggaccatgctgtgctgc -3'
R: 5'- gcagcacacatggtccacaacctgaggacagtac -3'

pminiTol2-aldoca-gap43-aldoca cut with SalI

zKv3.3-P2A:
F: 5'- tcctcaggttgtcgaatgctcagttcggtgtgtgt -3'
R: 5'- gcacagcatggtcgaaggtccagggttctcctcca -3'

Figure 4.1 Clone design for morphological experiments in zebrafish Purkinje cells.
(A) Control clone pminiTol2-aldoca-gap43-EGFP. The pminiTol2 plasmid backbone was used for Tol2 transposition. The plasmid was digested with BglII and HindIII to clone the zebrafish Purkinje cell-specific *aldoca* gene promoter, *gap43* palmitoylation signal sequence, and EGFP between the miniTol2 sequences. Primers were designed for In Fusion cloning. The sequence between the *aldoca* promotor and *gap43* palmitoylation signal sequence was mutated using QuickChange XL mutagenesis to create a SalI restriction site.
(B) Experimental clone pminiTol2-aldoca-zKv3.3-P2A-gap43-EGFP. The control clone was digested with SalI to clone WT and mutant zKv3.3 and the viral P2A sequence, which creates separate proteins from the same mRNA. Primers were designed for In Fusion cloning.

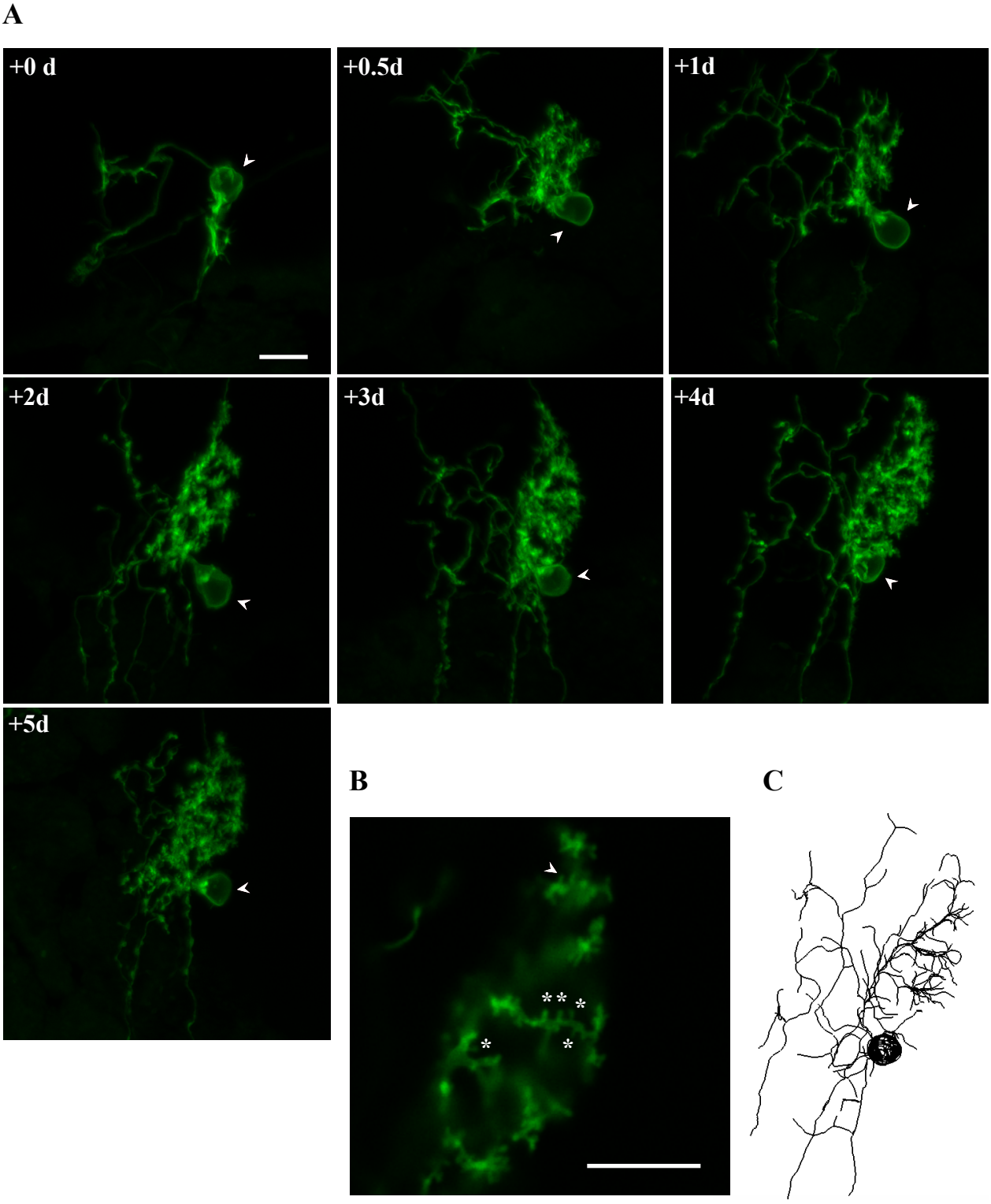

Figure 4.2 Purkinje cells expressing mEGFP alone exhibit stereotypical development and characteristics.

(A) Development of a zebrafish Purkinje cell specifically expressing mEGFP over time. Zebrafish embryos were injected with pminiTol2-aldoca-gap43-EGFP at the 1-2 cell stage of development. The Purkinje cell shown was first observed at 3.25 dpf and followed for 5 days.

Arrowheads indicate the Purkinje cell soma. Within 12 hours (+0.5d), the primary dendrite developed. The dendritic arbor increased in size and complexity, and dendritic spines developed over time. Confocal image stacks are shown with 1 μm slices. Scale bar is 10 μm. (B) A portion of the dendritic arbor at +4d was enlarged. Asterisks indicate dendritic spines. A single, 1 μm confocal slice is shown. Scale bar is 10 μm. (C) Representative trace (Imaris v8.0) of the Purkinje cell at +4d time point. Traces were made at every time point in order to quantify total process length and the number of branches.

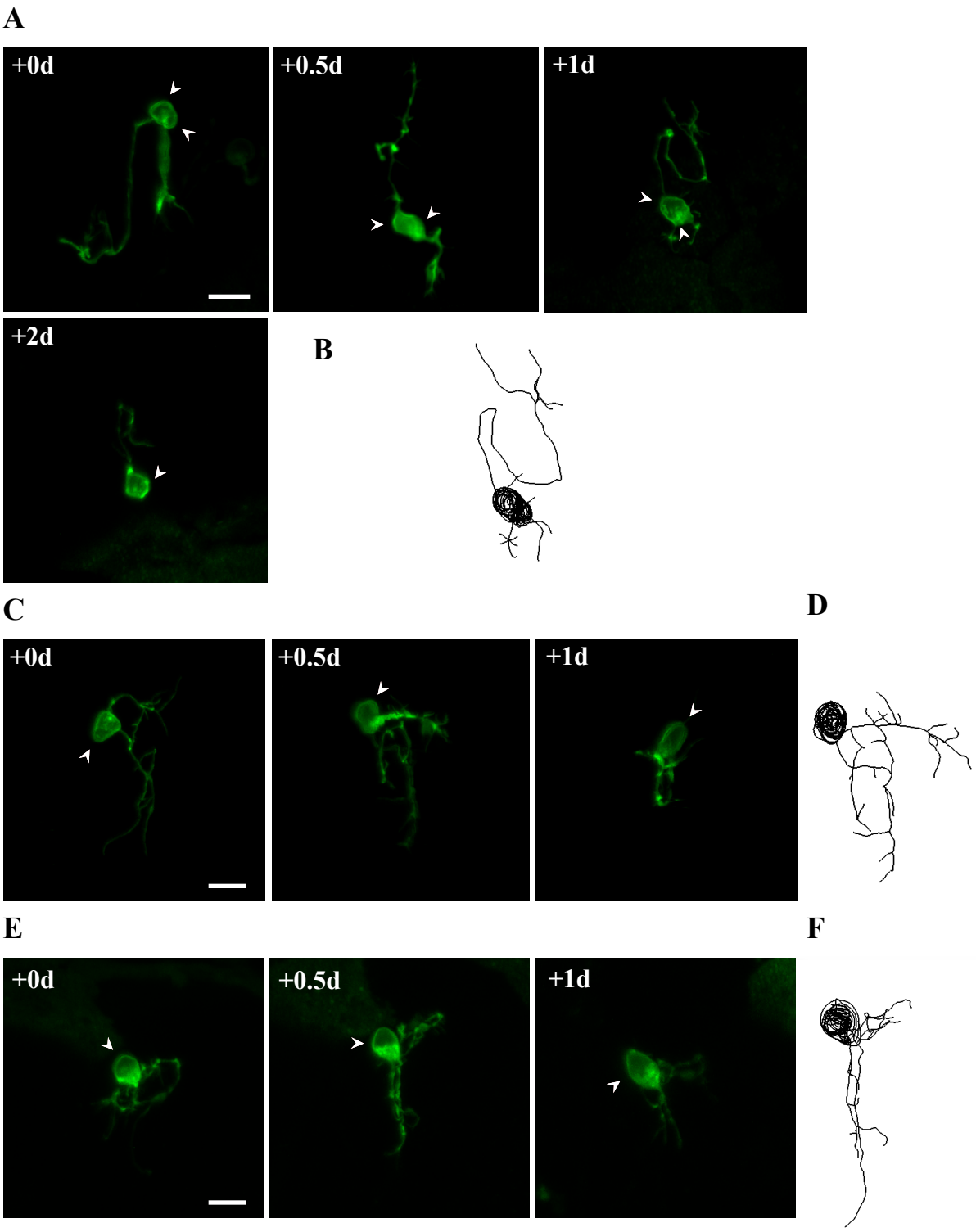

Figure 4.3 Purkinje cells expressing the infant onset R4H mutation rapidly degenerate and disappear.

Development of zebrafish Purkinje cells specifically expressing the infant onset R4H mutation in zKv3.3 and mEGFP. Embryos were injected with pminiTol2-aldoca-zKv3.3(R4H)-P2A-gap43-EGFP at the 1-2 cell stage of development. Examples

shown are confocal image stacks with 1 μm slices. Scale bars are 10 μm. (A) Two Purkinje cells were first observed at 3.5 dpf and followed for 2 days. Only one of two cells reamained visible at +2d, one of these cells disappeared after 1 day. The second cell disappeared after 2 days. (B) Representative trace (Imaris v8.0) of cells in (A) at +1d. (C) A Purkinje cell was first observed at 3.25 dpf and followed for 1 day, after which point the cell disapeared. (D) Represetative trace of cell in (C) at +0.5d. (E) A Purkinje cell was first observed at 3.25 dpf and followed for 1 day, after which point the cell disappeared. Arrowheads indicate Purkinje cell soma. An obvious primary dendrite did not develop, nor did dendritic spines. (F) Representative trace of cell (E) at +0.5d. Traces were made at every time point to quantify total process length and number of branches.

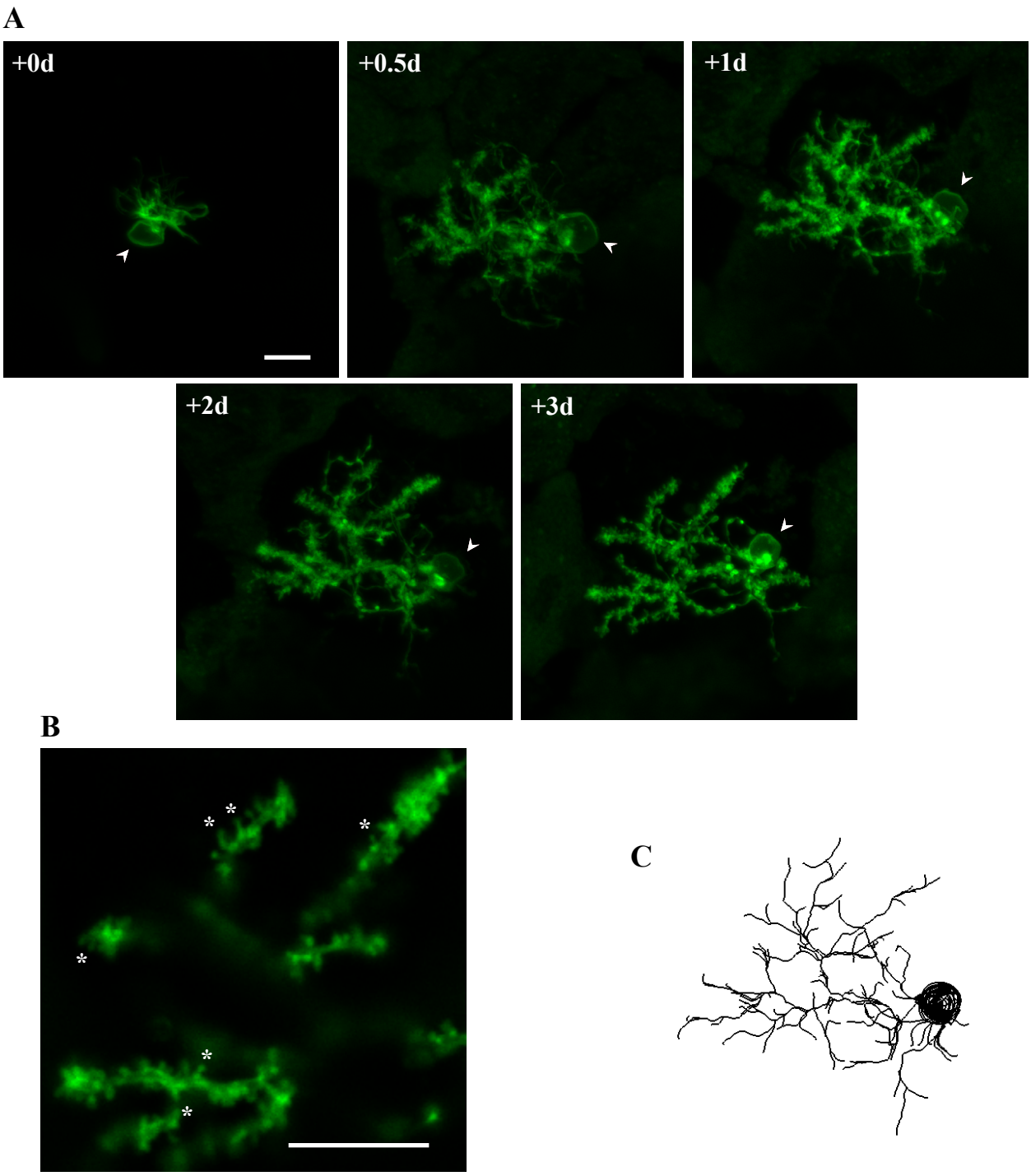

Figure 4.4 Purkinje cells expressing adult onset R3H mutation display no significant changes in development or cell survival.

(A) Development of zebrafish a Purkinje cell specifically expressing the adult onset R3H mutation over time. Zebrafish embryos were injected with pminiTol2-aldoca- zKv3.3(R3H)-P2A-gap43-EGFP at the 1-2 cell stage of development. The Purkinje cell shown was first observed at 3.75 dpf and followed for 3 days. Arrowheads indicate the Purkinje cell soma. Within 12 hours (+0.5d), the primary dendrite developed. The dendritic arbor increased in

in size and complexity over time, and dendritic spines developed. Confocal image stacks are shown with 1 μm slices. Scale bar is 10 μm. (B) A portion of the dendritic arbor at +3d was enlarged. Asterisks indicate dendritic spines. A single, 1 μm confocal slice is shown. Scale bar is 10 μm. (C) Representative trace (Imaris v8.0) of the Purkinje cell at +3d. Traces were made at every time point in order to quantify total process length and the number of branches.

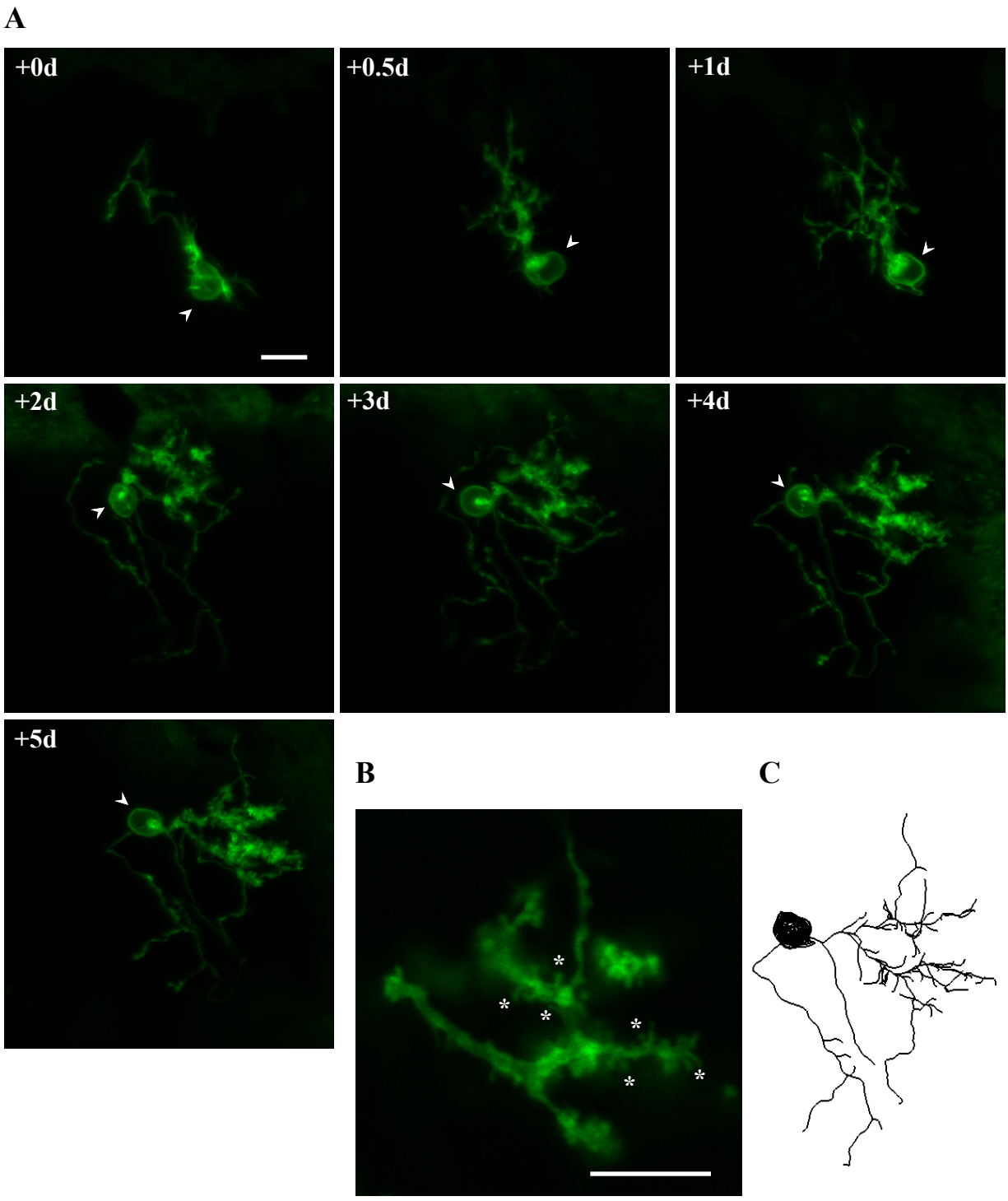

Figure 4.5 Overexpression of WT zKv3.3 in Purkinje cells does not have an effect on development or cell survival.
(A) Development of zebrafish a Purkinje cell specifically expressing the adult onset R3H mutation over time. Zebrafish embryos were injected with pminiTol2-aldoca-zKv3.3(WT)-P2A-gap43-EGFP at the 1-2 cell stage of development. The Purkinje cell shown was first observed at 3.25 dpf and followed for 5 days. Arrowheads indicate the Purkinje cell soma.

Within 12 hours (+0.5d), the primary dendrite developed. The dendritic arbor increased in size and complexity over time, and dendritic spines became apparent. Confocal image stacks are shown with 1 μm slices. Scale bar is 10 μm. (B) A portion of the dendritic arbor at +5d was enlarged. Asterisks indicate dendritic spines. A single, 1 μm confocal slice is shown. Scale bar is 10 μm. (C) Representative trace (Imaris v8.0) of the Purkinje cell at +5d. Traces were made at every time point in order to quantify total process length and the number of branches.

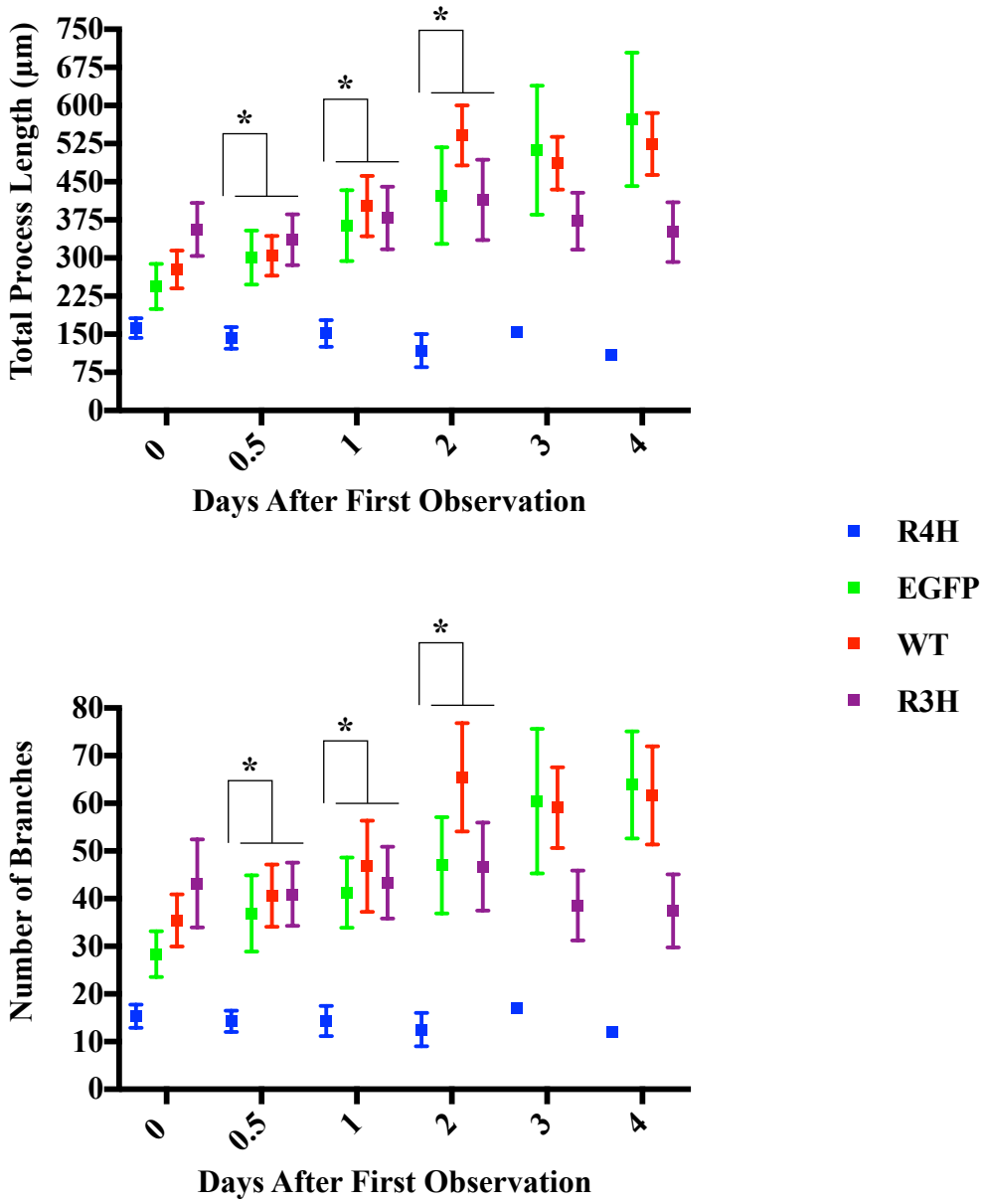

Figure 4.6 Quantitative analysis of total process length and number of branches in Purkinje cells expressing adult onset R3H and infant onset R4H mutations.
Traces were made at all time points for Purkinje cells expressing mEGFP alone (green), WT zKv3.3 (red), the adult onset R3H mutation (purple), or the infant onset R4H mutation (blue), using Imaris v8.0 (Bitplane). Measurements of (A) total process length and (B) number of branches were taken and compared between each expression condition. Both significantly shorter total process length and significantly fewer branches were observed in Purkinje cells expressing the infant onset mutation compared to those expressing mEGFP

alone, WT zKv3.3, and the adult onset mutation at +0.5d, +1d, and +2d. No other significant differences were observed. Statistical analyses were performed with SPSS (IBM). Samples sizes were as follows: for mEGFP n=11 cells, for WT zKv3.3 n=11 cells, for R4H n=12 cells, and for R3H n=11 cells. Linear Mixed Model was performed on $\log_{10}$-transformed data with Bonferroni post-hoc test, $p < 0.05$ (*).

Chapter 5

An SK2 channel agonist increases the frequency of Purkinje cells expressing the infant onset R4H mutation

Introduction

Expression of the SCA13 infant onset R4H mutation has an obvious and dramatic effect on Purkinje cell excitability. Spontaneous tonic firing emerges in a similar manner to control cells, first observed in loose patch recordings at ~3.75 dpf with a frequency of 1-2 Hz. Rapidly, within 6 hours, hyperexcitability becomes apparent with a bursting phenotype at frequencies of up to 50 Hz, compared to a normal spontaneous tonic firing frequency of ~9 Hz (Figure 1.6). Purkinje cell excitability in mutant cells was followed over developmental time. The majority of cells were silent by 5 dpf (Hsieh & Papazian, unpublished).

The emergence of hyperexcitability in Purkinje cells expressing the infant onset R4H mutation parallels the pattern of observed degeneration. Mutant cells were born within the same time frame as controls, between 3 dpf and 3.75 dpf. Within 12 hours, degeneration began. An obvious primary dendrite and spines were not observed, and dendritic complexity was significantly reduced (Figure 4.3; Figure 4.6). Hyperexcitability emerged at ~4 dpf (Figure 1.6A), which correlates well with the developmental time at which the primary dendrite failed to develop. The majority of Purkinje cells expressing the infant onset mutation disappear between 5 dpf and 6 dpf, the same time at which the majority of cells fall silent. It remains unclear as to whether or not the deteriorating condition of the cells and/ or impending cell death are reflected by this recorded silence.

The disappearance of Purkinje cells likely reflects cell death induced by the infant onset R4H mutation. There are two main mechanisms of cell death, apoptosis and necrosis. Apoptosis is programmed cell death and involves the activation of initiator and executioner caspases. The apoptotic cascade is often activated during development or in response to cellular dysfunction

and stress (Penazola et al., 2006; Youle & Strasser, 2008). If caspases are inhibited, necrosis occurs in response to cellular distress rather than apoptosis. A certain type of necrosis may be associated with autophagy, but the main purpose of autophagy is to rid the cell of harmful organelles and protein aggregates through the formation of autophagasomes that feed into the lysosome (Mizushima, Yamamoto & Matsui, 2004; Pattingre et al., 2005; Pattingre et al., 2008; Wei et al., 2008; Jung et al., 2009). We decided to focus on apoptotic cell death as the source of Purkinje cell disappearance, as it is implicated in several neurodegenerative diseases (reviewed in Friedlander, 2003) and can easily be assessed in zebrafish through vital dyes such as acridine orange and Hoescht 33342, TUNEL staining, and immunostaining with antibodies against activated caspases (Eimon & Ashkenazi, 2009). We used acridine orange to preliminarily asses apoptosis, as it can be used *in vivo* during development.

Altered Purkinje cell development and survival, as well as altered excitability are implicated in several neurodegenerative diseases, most notably in the polyQ expansion diseases spinocerebellar ataxia type 2 and 3 (SCA2 and 3). In SCA2 mouse models, loss of molecular layer (ML) thickness is observed along with the eventual loss of Purkinje cells (Kasumu et al., 2012; Hansen et al., 2012). The loss of ML thickness is indicative of dendritic atrophy. There have been conflicting results from investigations in these models, but dysfunction of Purkinje cell spontaneous tonic firing was apparent in all cases. Kasumu et al. reported a bursting phenotype, both persistent and transient, with intermittent periods of tonic firing or silence (Kasumu et al., 2014). This bursting phenotype was observed in another investigation, however, rarely and at levels that did not reach statistical significance. The most notable change in this study was a progressive shift towards slower firing frequencies over time (Hansen et al., 2012).

In SCA3 mouse models, a loss of ML thickness was observed, suggesting Purkinje cell dendritic atrophy occurs in a similar manner to that observed in SCA2 models. Less than half of Purkinje cells exhibited spontaneous tonic firing due to depolarization block (Shakkottai et al., 2011).

In another polyQ expansion disease, Huntington's Disease (HD), loss of Purkinje cells and altered excitability are observed in mouse models as well. GABAergic cell markers were decreased in the cerebellum, and immunohistochemistry confirmed this loss was specific to Purkinje cells (Dougherty et al., 2012). A significant reduction in spike frequency was observed prior to the onset of symptoms, which were assessed using the rotarod (Dougherty et al., 2012; Dougherty et al., 2013). Interestingly, in SCA3 mice, the dysfunction in Purkinje cell excitability preceded motor phenotypes as well (Shakkottai et al., 2011). Although the changes in Purkinje cell excitability differ between SCA2, SCA3, and HD, Purkinje cell loss and dysfunction are common observations. Altered excitability was recorded before the onset of behavioral phenotypes, however, it remains unclear in these examples and in other examples of neuronal dysfunction related to neurodegeneration, whether changes in firing frequency lead to the manifestation of degeneration and clinical phenotypes, or if the observed effects are a product of changes in protein or ion channel expression and function, or structural changes in the neuronal population.

Small conductance Ca^{2+}-activated K^{+} (SK) channels are involved in the regulation of Purkinje cell firing. SK2 channels are highly expressed in mammalian Purkinje cells, and treating cells with the SK2 channel blocker apamin increased the maximum firing rate and altered the shape of the afterhyperpolarization after each action potential, increasing its immediate amplitude during burst firing, but decreasing its amplitude during subsequent

depolarizations (Womack & Khodakhah, 2003). SK2 channel agonists are a strong target for reducing excitability in Purkinje cells. In both SCA2 and SCA3 models, treatment with small conductance Ca^{2+}-activated K^+ (SK) channel agonists led to an improvement in beamwalk performance, and in the case of SCA2, an SK2 channel agonist rescued the degenerative phenotype observed in the ML (Shakkottai et al., 2011; Kasumu et al., 2012).

We hypothesized that reducing hyperexcitability in Purkinje cells expressing the infant onset R4H mutation would rescue degeneration and cell disappearance. The SK2 channel agonist NS13001 was developed specifically to regulate Purkinje cell firing in SCA2 mouse models through oral delivery (Kasumu et al., 2012). We have previously confirmed that acute treatment of zebrafish with NS13001 during loose patch recordings yielded a decrease in firing rate in Purkinje cells and the response was dose dependent and reversible. We chose to chronically treat animals expressing the infant onset mutation in Purkinje cells with NS13001. Although a reduction in hyperexcitability could not be recorded electrophysiologically in these animals, we observed slowed swimming behavior. Chronic treatment with NS13001 increased the frequency of Purkinje cells expressing the infant onset mutation. It did not rescue degeneration and apoptotic cell death, which was confirmed when acridine orange stained condensed and fragmented chromatin within mutant Purkinje cells. It was determined that this was not a proliferative effect. Although the relationship between degeneration and hyperexcitability induced by the infant onset mutation remains unclear, it appears it may play a role in Purkinje cell viability and/or development.

Results

The infant onset R4H mutation induces apoptotic cell death in Purkinje cells

Purkinje cells expressing the infant onset R4H mutation typically disappeared between 5 and 6 dpf, when cells were first observed between 3.25 dpf and 3.75 dpf. Out of 12 Purkinje cells, 25% disappeared by 5 dpf, and ~83% disappeared by 6 dpf. Only ~8% of cells survived to 8 dpf, equivalent to 1 out of 12 (Figure 5.1A). In control cells and those expressing the adult onset R3H mutation, 100% of cells remained visible through 8 dpf (Figure 5.1B, C, D). The disappearance of Purkinje cells expressing the infant onset R4H mutation suggests that the mutation reduces cell viability. To investigate whether cells die by apoptosis, zebrafish were stained with 1 ug/mL acridine orange. Acridine orange is a fluorescent dye that stains nucleic acids in healthy and early apoptotic cells. In healthy cells, it stains the whole intact nucleus, whereas in apoptotic cells it exhibits intense green fluorescence with the appearance of condensed and fragmented chromatin (Atale et al., 2014). This stain can be used *in vivo* in developing zebrafish to stain neuronal populations.

We expressed the infant onset mutation as described previously, however, because acridine orange fluoresces green we replaced mEGFP with mtdTomato for these experiments. Zebrafish were screened for mtdTomato fluorescence beginning between 3 dpf and 3.75 dpf, and Purkinje cells were monitored intermittently to determine when degeneration became severe. This occured at ~5 dpf in the majority of cells, which is the time point at which the majority of cells began to disappear. When zebrafish were stained with acridine orange, intense and fragmented green fluorescence was observed within mutant Purkinje cells. Co-localization of acridine orange fluorescence and mtdTomato fluorescence appeared yellow, and confirmed that

staining was within the target cell (Figure 5.2). This staining pattern was not observed in mtdTomato controls. Faint green nuclear fluorescence was observed surrounding mutant and control Purkinje cells, in a morphological pattern consistent with that of the cerebellum. This was interpreted as healthy nuclear staining in non-expressing Purkinje cells.

Treatment with SK2 channel agonist NS13001 increased the frequency of Purkinje cells expressing the infant onset R4H mutation

To investigate the relationship between hyperexcitability and degeneration, we treated zebrafish expressing the infant onset R4H mutation in Purkinje cells with the SK2 channel agonist NS13001. This drug has been shown to decrease Purkinje cell excitability when orally delivered to mice (Kasumu et al., 2012), and through direct application to the brain during loose patch recordings (Hsieh & Papazian, unpublished). The infant onset mutation was expressed with mEGFP as previously described. Zebrafish were chronically treated with a concentration of 20 μM NS13001 in the water, which was replaced once daily to avoid precipitation and because we were unsure of its stability at 28°C.

Zebrafish were treated beginning at 3.25 dpf and animals were screened for mEGFP fluorescence and imaged beginning at 4 dpf and in 24 hours increments through 7 dpf, or until cells disappeared. The expression frequency, defined as the number of fluorescent Purkinje cells per animal, was significantly increased in the NS13001-treated animals at 4 dpf, 5 dpf, and 6 dpf when compared to DMSO controls (Figure 5.3; Figure 5.5A). At 4 dpf, an average of ~7 Purkinje cells expressing the infant onset mutation were observed in NS13001-treated animals versus ~2 cells in DMSO-treated animals (Figure 5.5A). Obvious primary dendrites did not develop,

dendritic complexity was reduced, and spines were not observed in mutant Purkinje cells (Figure 5.3). The frequency of expression did not differ in NS13001-treated animals versus DMSO controls at 7 dpf, suggesting that NS13001 treatment did not rescue degeneration or cell death induced by the infant onset mutation (Figure 5.5A). Control Purkinje cells expressing mEGFP alone developed normally when animals were treated with NS13001 or DMSO (Figure 5.4) and the expression frequency did not significantly differ in either treatment at any developmental time point (Figure 5.5B), suggesting that the increase observed in animals expressing the infant onset mutation was not due to increased proliferation.

Discussion

Disappearance reflects apoptotic cell death inPurkinje cells expressing the infant onset R4H mutation

Acridine orange stained condensed, fragmented chromatin in Purkinje cells expressing the infant onset R4H mutation, which was clear by its intense green fluorescence overlapping with mtdTomato fluorescence (Figure 5.2). This strongly suggests that Purkinje cell disappearance reflects apoptotic cell death. Autophagy may be occurring in some Purkinje cells expressing the infant onset mutation as well. We would not be able to detect the staining of autophagic vesicles, as acridine orange fluoresces red in this case and would overlap with mtdTomato fluorescence.

One of the weaknesses of using acridine orange is high background staining. High background staining is observed and can make it difficult to quantify processes and capture cells as their fluorescence weakens during apoptosis. Acridine orange extensively bleaches when

exposed to ambient light or high laser intensity during imaging. To minimize bleaching, we performed staining experiments with minimal ambient light and imaged within 15 minutes of staining. Intense staining could be an artifact that appears in some healthy cells, however, this was controlled for in Purkinje cells expressing mtdTomato alone. It would be worthwhile to explore the expression of active caspases in Purkinje cells expressing the infant onset mutation through immunohistochemistry at ~5dpf, when we observed severe degeneration. There are several caspases, including initiator caspases (caspase-2,-8,-9,-10), executioner caspases (caspase-3,-6,-7), and inflammatory caspases (caspase-1,-4,-5). The apoptotic cascade can be initiated by a wide variety of cellular stresses, and which specific caspases are activated can give us information on the causative factor (Cohen, 1997; Elmore, 2007).

Treatment with NS13001 reveals an unclear mechanistic role for hyperexcitability

Treatment of zebrafish expressing the infant onset R4H mutation in Purkinje cells significantly increased the frequency of mutant Purkinje cells at 4 dpf, 5 dpf, and 6 dpf compared to controls treated with DMSO (Figure 5.5A). However, it did not rescue the degenerative phenotype (Figure 5.3). NS13001-treated mutant Purkinje cells did not develop a primary dendrite, they lacked dendritic complexity, and spines were not observed (Figure 5.3). The majority of Purkinje cells expressing the infant onset mutation disappeared between 5 dpf and 6 dpf, as observed previously, and only at 7 dpf did the expression frequency no longer differ from controls, suggesting that Purkinje cell death was not prevented (Figure 5.5A). Expression frequency in zebrafish expressing mEGFP alone in Purkinje cells did not differ significantly between treatments, ruling out the possibility that NS13001 acts by increasing the proliferation

of Purkinje cells (Figure 5.5B). The observed increase in expression frequency suggests that hyperexcitability due to the infant onset R4H mutation may contribute to reduced viability of Purkinje cells.

The infant onset R4H mutation leads to both developmental and degenerative phenotypes

The infant onset R4H mutation does not only lead to a degenerative phenotype with rapid apoptotic cell death, but a phenotype affecting the ability of Purkinje cells to develop normal structural characteristics. Alterations in the firing properties of Purkinje cells may explain the lack of an obvious primary dendrite and reduced dendritic complexity. Kv3.3 channels with infant onset mutant subunits may act as "super" Kv3.3 channels, meaning that they are better at repolarizing Purkinje cells for the next action potential, thus shortening the interspike interval and increasing the firing frequency. Although the half-maximal activation voltage ($V_{1/2}$) is hyperpolarized in channels containing both WT and mutant subunits, this change is modest and activation remains depolarized compared to other K^+ channels. Activation is only significantly slowed within a small range of membrane potentials. Deactivation is slowed as well, however, in physiological bath conditions, the decrease in deactivation rate was minor (Minassian, Lin & Papazian, 2012). Considering these alterations in channel gating, Kv3.3 channels with infant onset mutant subunits may open earlier during the action potential due to their hyperpolarized open probability, but still not at resting potentials, and may, to a small degree, remain open longer. If the changes in channel gating, including hyperpolarized $V_{1/2}$ and slowed activation and deactivation, were more dramatic, the properties of the mutant Kv3.3 channel would be more similar to that of other K^+ channels. Since the incorporation of an infant onset mutant subunit

leads to small alterations, mutant Kv3.3 channels remain unique, but are able to conduct a K^+ current that results in faster repolarization.

Previous experiments in zebrafish Purkinje cells expressing the infant onset R4H mutation revealed an increased Ca^{2+} response to stimulation using the genetically encoded Ca^{2+} indicator GCaMP-HS (Issa & Papazian, unpublished), thought to be a direct outcome of hyperexcitability induced by the ability of mutant Kv3.3 channels that facilitate faster repolarization. Increased Ca^{2+} has been shown to alter the cytoskeleton in projection neurons. Calcineurin is Ca^{2+}-dependent, and its activation leads to the dephosphorylation of cofilin by slingshot phosphatase. Dephosphorylated cofilin binds and catalyzes the depolymerization of actin. Another mechanism, observed in Huntington's Disease (HD), by which Ca^{2+} can lead to this effect is through the activation of transglutaminase 2, mediating covalent linkage between cofilin and actin (Munsie & Truant, 2012). The depolymerization of actin can lead to reduced cytoskeletal support and process retraction, which is reflected well in Purkinje cells expressing the infant onset mutation by the degenerative phenotypes, including the decrease in total process length over time and the reduced number of branches.

Increased Ca^{2+} in Purkinje cells expressing the infant onset R4H mutation was observed in the soma, and the distribution of this Ca^{2+} response has not been studied in detail. Dendritic Kv3.3 channels in Purkinje cells are thought to dampen Ca^{2+} spiking in distal dendrites. Kv3.3 KO mice displayed a robust Ca^{2+} response, measured using the Ca^{2+} indicating dye bis-fura2, in both the proximal and distal dendrites compared to WT mice, in which large transients were observed mainly in the proximal dendrites (Zagha et al., 2010). If Kv3.3 channels with infant onset mutant subunits are better at their function, this may indicate that the Ca^{2+} response tapers

to a higher degree within the dendritic tree. Increased Ca^{2+} is observed in fillopodia of dendrites and axons, and is required for dendritic outgrowth and synapse formation (Rajan & Cline, 1998; Gomez et al., 2001; Wong & Ghosh, 2001; Lohmann, Myhr & Wong, 2002; Lohmann, Finski & Bonhoeffer, 2005). If Ca^{2+} tapers to a higher degree in mutant cells, this may cut off the Ca^{2+} supply required for development and may explain why an obvious primary dendrite does not develop and why spines are not observed in Purkinje cells expressing the infant onset mutation.

Decreased viability in Purkinje cells expressing the infant onset R4H mutation may be explained by early and rapid cell death. NS13001 treatment began at 3.25 dpf and mutant Purkinje cells were not screened or followed until 18 hours later, at 4 dpf. During previous electrophysiological experiments, cell death induced by the infant onset mutation occurred regularly between screening and recording. This time frame was often less than one hour, therefore, it is reasonable to assume that cell death may occur rapidly, soon after cells are born. NS13001 treatment may have prevented cell death that occurred during the DMSO treatment over the first 18 hours, suggesting that it led to prolonged early survival of mutant Purkinje cells. Since we did not start screening until 4 dpf and the majority of cells in animals treated with NS13001 disappeared during the same developmental time period as previously observed, between 5 and 6 dpf, we would not have observed this phenomenon. Originally, we were investigating the effect of NS13001 on the degenerative phenotype, therefore, we assigned zebrafish to treatment groups randomly, without screening. It would be worthwhile to revisit this experiment, count mutant Purkinje cells before treatment begins, and monitor them over the first 18 hours after treatment. If NS13001 prolongs early survival, we would expect to see a similar frequency of Purkinje cells expressing the infant onset mutation in zebrafish before either

treatment, followed by the frequency decreasing to a higher degree in DMSO-treated animals than the frequency in NS13001-treated animals.

Unfortunately, electrophysiological recordings cannot be taken from Purkinje cells in zebrafish chronically treated with NS13001. The treatment would become acute once the skull is removed, and if the drug is removed before dissection, the effect would be reversed. We do not know the efficacy of the decrease in hyperexcitability because we are unaware of drug permeability through the skin and skull of the zebrafish and the length of effectiveness at 28°C. Therefore, it is plausible that hyperexcitability was not reduced to a level at which we would observe a rescue of the degenerative phenotype caused by the infant onset R4H mutation.

Reduced Purkinje cell viability and developmental defects of the dendritic tree in zebrafish expressing the infant onset R4H mutation are consistent with the presence of clinical phenotypes as early as the first year of life in infant onset SCA13 patients with the R423H mutation. Cerebellar atrophy in patients may be reflected by the degenerative phenotype, including the decrease in total process length, presence of fewer branches, and eventual apoptotic cell death. Although it remains unclear as to what cerebellar neurons contribute to the clinical phenotypes and cerebellar atrophy, there are several factors that could contribute to the pathogenesis of infant onset SCA13, including decreased cell viability, reduced dendritic complexity, degeneration, and cell death which have the potential to effect the ability of the cerebellum to receive, send, and integrate motor, and possibly cognitive, information.

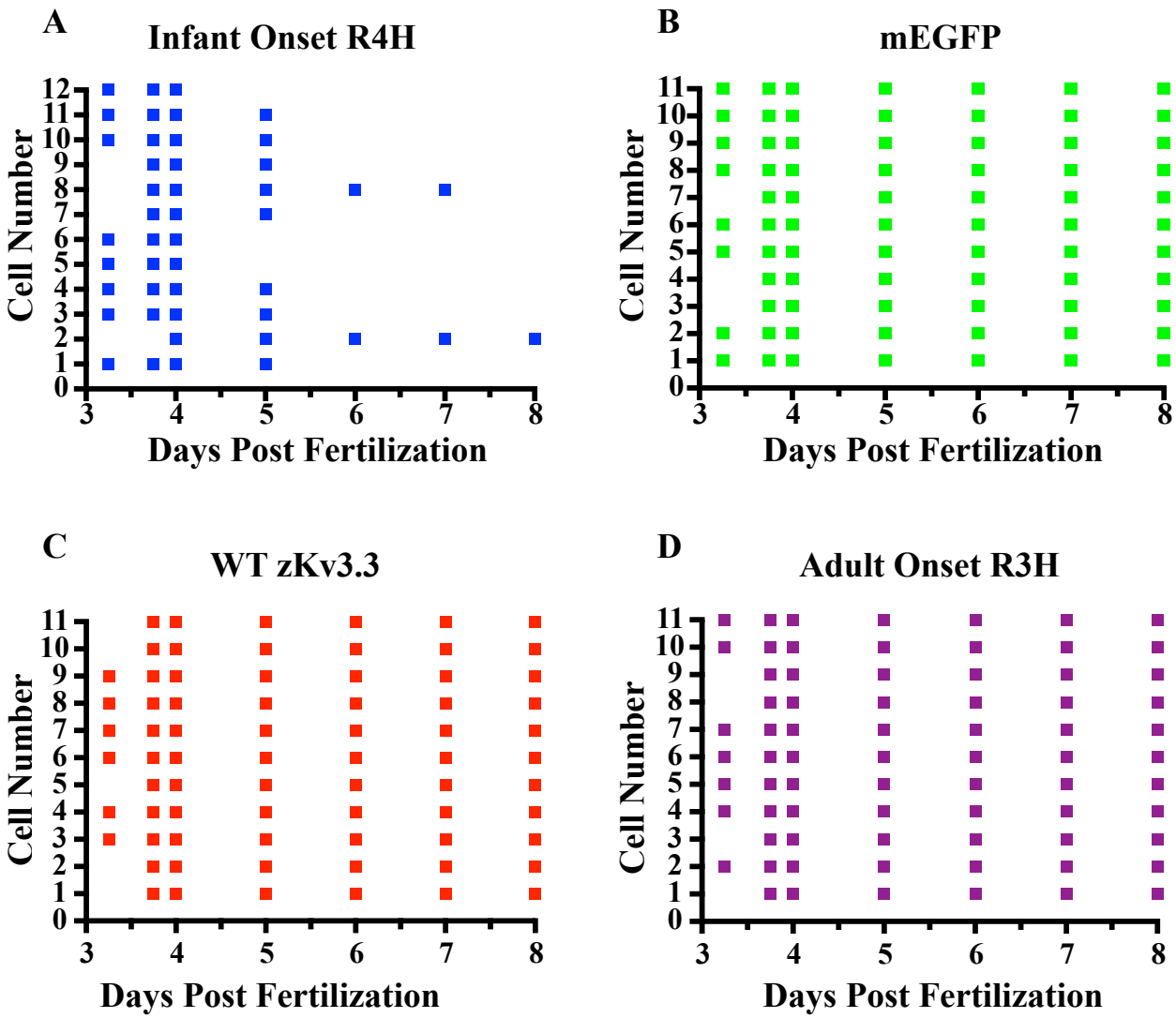

Figure 5.1 Purkinje cells expressing the infant onset R4H mutation rapidly disappear over developmental time.
Scatter plots of each Purkinje cell expressing the (A) infant onset R4H mutation, (B) mEGFP alone, (C) exogenous WT zKv3.3, and (D) the adult onset R3H mutation over developmental time. Whereas all Purkinje cells were visible through 8 dpf when expressing mEGFP, exogenous WT zKv3.3, and the adult onset mutation, cells expressing the infant onset mutation began disappearing after 4 dpf, with the majority of cells disappearing between 5 dpf and 6 dpf. Out of 12 Purkinje cells, 25% disappeared by 5 dpf and ~83% by 6 dpf. Only 1 cell (~8%) was visible through 8 dpf. The disappearance of cells was thought to reflect cell death.

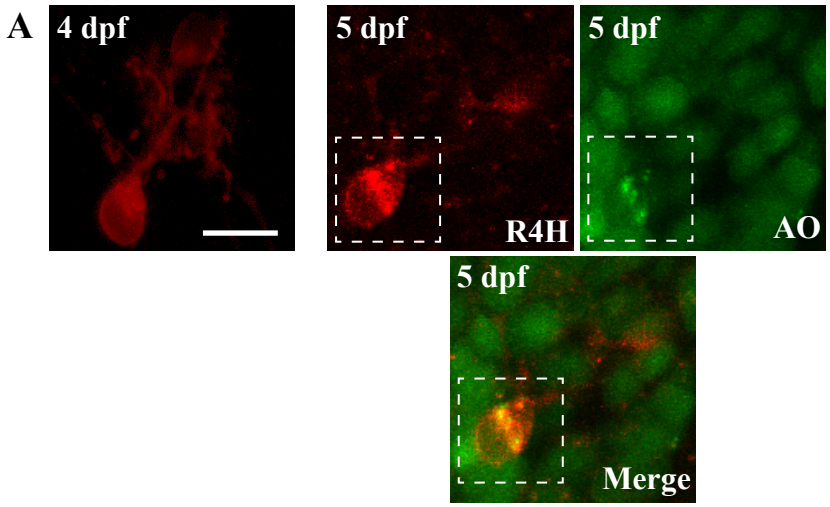
A
4 dpf
5 dpf
R4H
5 dpf
AO
5 dpf
Merge

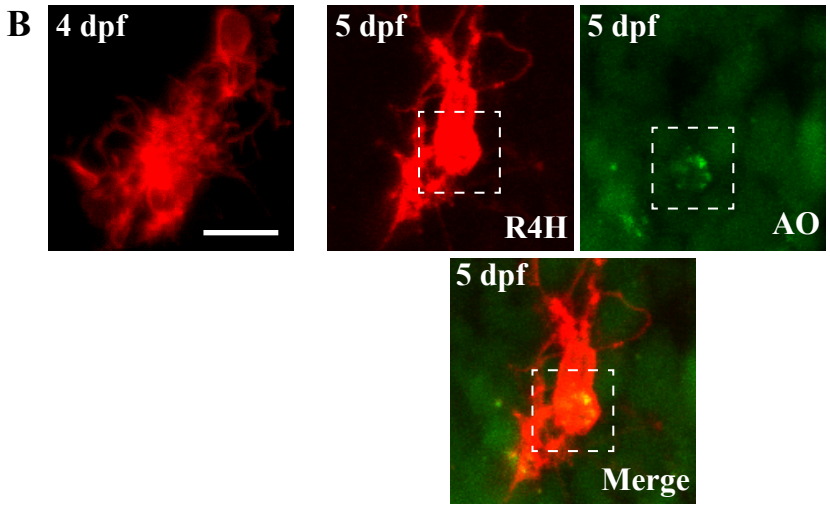
B
4 dpf
5 dpf
R4H
5 dpf
AO
5 dpf
Merge

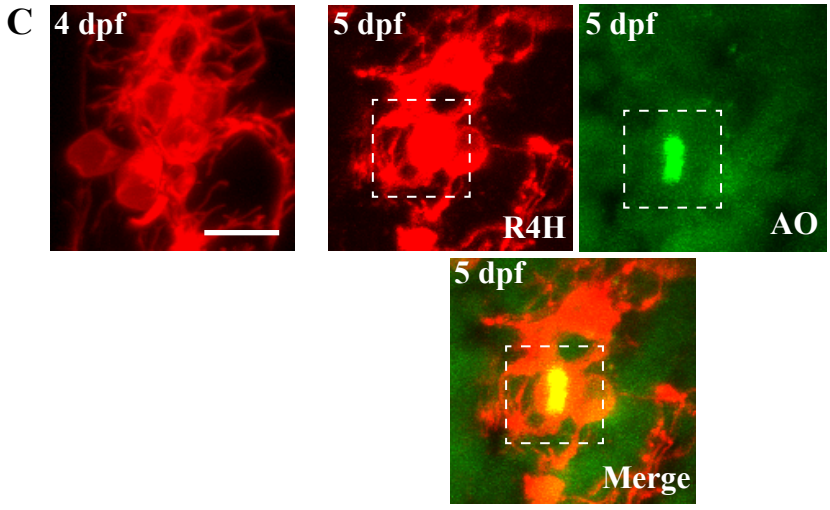
C
4 dpf
5 dpf
R4H
5 dpf
AO
5 dpf
Merge

Figure 5.2 Acridine orange staining reveals that Purkinje cells expressing the infant onset R4H mutation undergo apoptotic cell death.
(A), (B), (C) Three examples of positive acridine orange staining in Purkinje cells expressing the infant onset R4H mutation. Cells were imaged at 4 dpf and again once severe degeneration became apparent, typically at 5 dpf. At this time point, zebrafish were stained with 1 ug/mL acridine orange. Dashed boxes indicate cells in which intense green fluorescence was observed, indicating early apoptotic cell death. Co-localization of acridine orange and mtdTomato fluorescence appeared yellow, as shown in the merged images. Less intense green staining surrounding mutant Purkinje cells likely represents healthy cell and background staining. Confocal image stacks are shown with 1 μm slices. Scale bars are 10 μm.

A

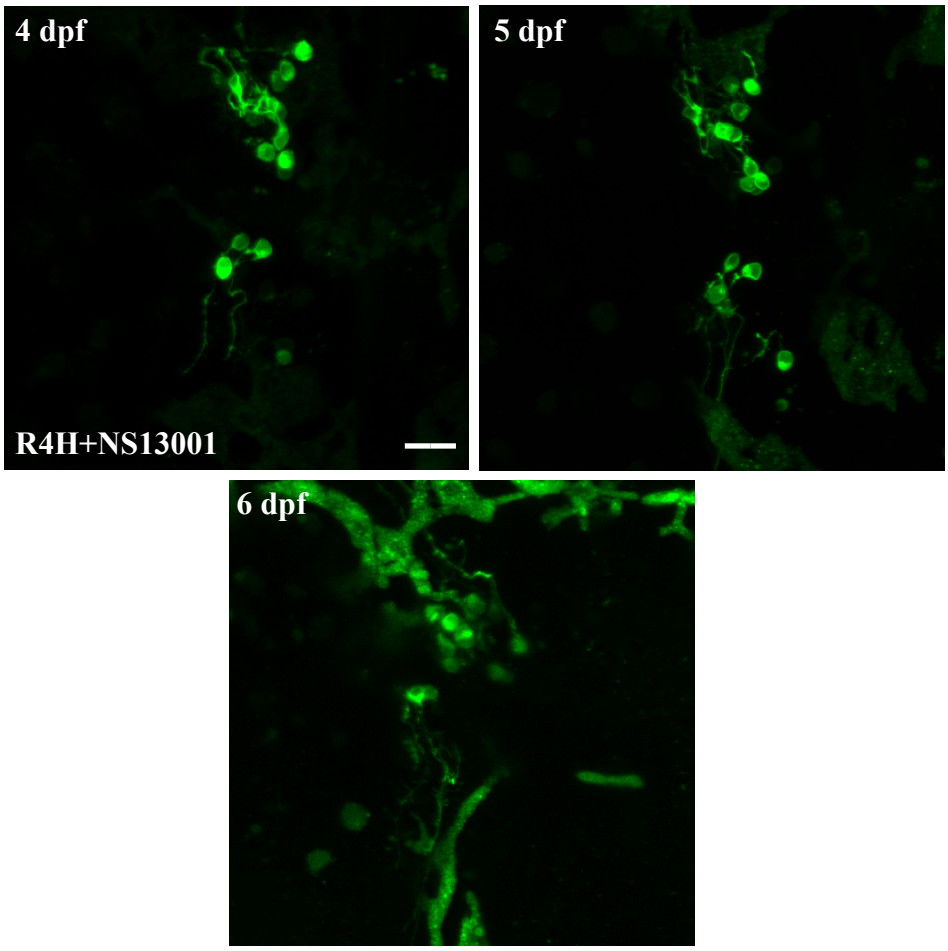

B

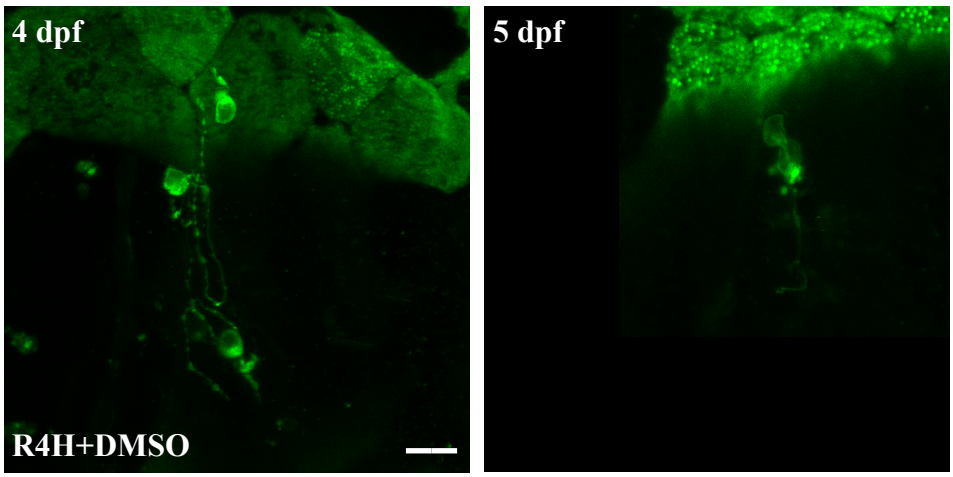

Figure 5.3 Chronic treatment with positive SK channel modulator NS13001 leads to increased expression frequency of infant onset R4H mutation in Purkinje cells.
(A) Chronic treatment of zebrafish expressing the infant onset R4H mutation in Purkinje cells with NS13001. Zebrafish were injected with pminiTol2-aldoca-zKv3.3(R4H)-P2A-gap43-EGFP at the 1-2 cell stage of development. NS13001 was added to fish water at a concentration of 20 μM, and replaced every 24 hours. Treatment began at 3.25 dpf, Purkinje cells were screened and imaged beginning at 4 dpf, and imaging continued until Purkinje cells disappeared. NS13001 treatment increased the expression frequency of the infant onset mutation in Purkinje cells, however, cells did not develop a primary dendrite, lacked dendritic complexity, and disappeared rapidly - in this case after 6 dpf. Confocal image stacks are shown with 1 μm slices. Scale bar is 10 μm. (B) DMSO control treatment of zebrafish expressing the infant onset mutation in Purkinje cells. The same concentration of DMSO was added to fish water as NS13001 and replaced every 24 hours. Treatments began and ended at the same time points as NS13001 treatment. DMSO controls did not exhibit an increase in expression frequency, and the developmental and degenerative phenotypes were still observed. Purkinje cells disappeared after 5 dpf. Confocal image stacks are shown with 1 μm slices. Scale bar is 10 μm.

A

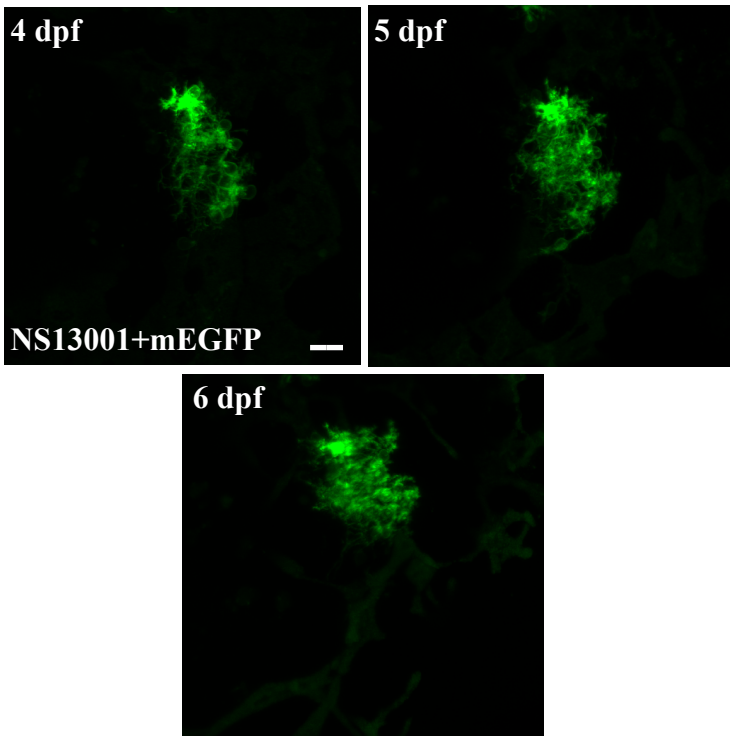

B

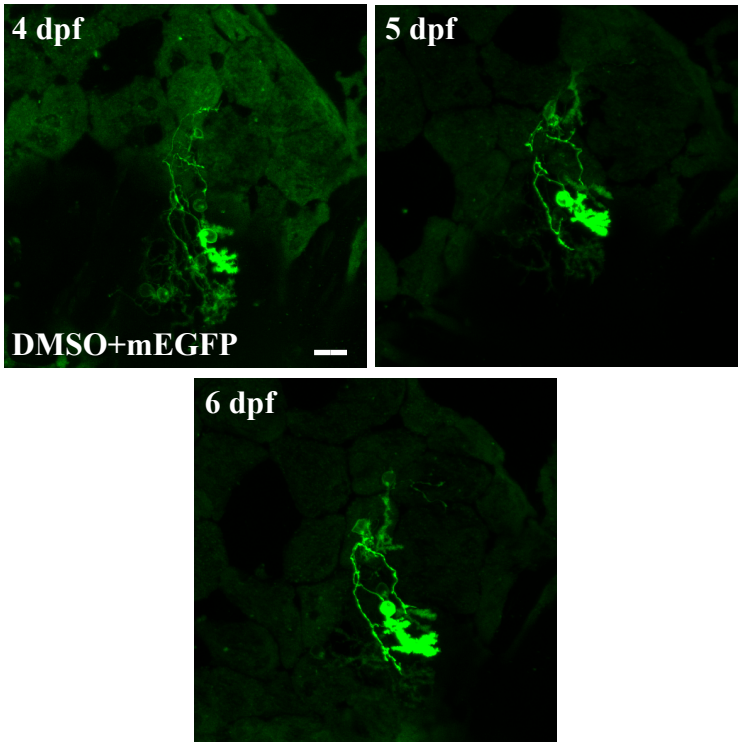

Figure 5.4 Purkinje cells expressing mEGFP alone did not exhibit an increase in frequency after treatment with NS13001, ruling out proliferative effect.
(A) Chronic treatment of zebrafish expressing mEGFP alone in Purkinje cells with NS13001. Zebrafish were injected with pminiTol2-aldoca -gap43-EGFP at the 1-2 cell stage of development. NS13001 was added to fish water at a concentration of 20 μM, and replaced every 24 hours. Treatment began at 3.25 dpf, Purkinje cells were screened and imaged beginning at 4 dpf, and imaging continued through 6 dpf. NS13001 did not increase the expression frequency of mEGFP in Purkinje cells. The dendritic arbor developed normally. Confocal image stacks are shown with 1 μm slices. Scale bar is 10 μm. (B) DMSO control treatment of zebrafish expressing mEGFP in Purkinje cells. The same concentration of DMSO was added to fish water as NS13001 and replaced every 24 hours. Treatments began and ended at the same time points as NS13001 treatment. Confocal image stacks are shown with 1 μm slices. Scale bar is 10 μm.

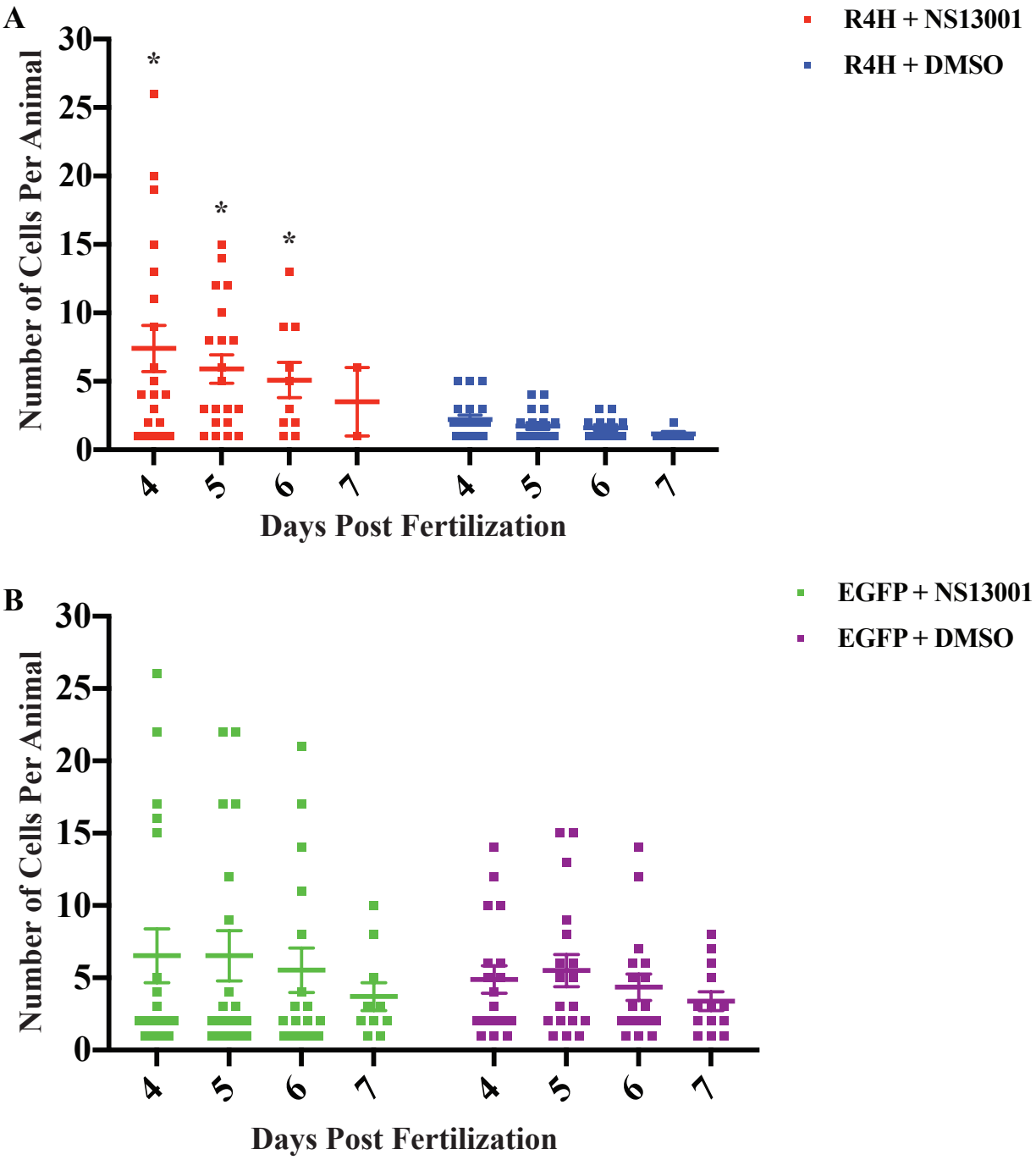

Figure 5.5 Quantitative analysis reveals that NS13001 treatment significantly increases the number of Purkinje cells expressng the infant onset R4H mutation.
The number of cells per animal was counted manually through each slice using ImageJ (NIH) for (A) Purkinje cells expressing the infant onset R4H mutation and (B) Purkinje cells expressing mEGFP alone. Expression frequency was compared between NS13001 treatment and DMSO control treatment. NS13001 treatment significantly increased the number of Purkinje cells expressing the infant onset mutation at 4 dpf, 5 dpf, and 6 dpf compared to the DMSO control. The frequency did not differ at 7 dpf. This increase was not observed between treatments for Purkinje cells expressing mEGFP alone. Statistical analyses were

performed with SPSS (IBM). Sample sizes were as follows: R4H+NS13001 n=20 animals, R4H+DMSO n=19 animals, mEGFP+NS13001 n=19 animals, and mEGFP+DMSO n=18 animals. Linear Mixed Model was performed on $\log_{10}$-transformed data with Bonferroni post-hoc test, $p < 0.05$ (*).

Chapter 6

Conclusion

Conservation of the mechanism controlling Purkinje cell excitability

Resurgent Na^+ currents, primarily mediated by voltage-gated Na^+ channel 1.6 (Nav1.6), and rapidly activating and deactivating K^+ currents, primarily mediated by voltage-gated K^+ channel 3.3 (Kv3.3) have been found to control spontaneous tonic firing in mammalian Purkinje cells (Akemann & Knopfel, 2006). In zebrafish Purkinje cells, Nav1.6 and Kv3.3 expression emerges between 3 dpf and 4 dpf, and persists through 6 dpf, at which point we ended our *in situ* hybridization experiments. A possible increase in the level of expression is observed based on the qualitative increase in fluorescence intensity of co-localization with the *aldoca* probe. Interestingly, Purkinje cell excitability emerges at approximately the same time point at which the expression of Nav1.6 and Kv3.3 emerges. The parallel emergence of excitability and channel expression suggests that the regulation of tonic firing is conserved in zebrafish Purkinje cells. It is necessary to look at several intermediate time points between 3 dpf and 4 dpf to pinpoint, with the most accuracy, the time at which expression of Nav1.6 and Kv3.3 first emerges. The earliest time at which excitability is recorded in zebrafish Purkinje cells is at ~3.75 dpf, therefore, we would expect the expression of these channels would be first observed prior to that time point.

Whole mount *in situ* hybridization is a useful tool in zebrafish, however, it can only give us information on whether or not genes are transcribed and on the level of mRNA expression. This highlights the need for better antibodies specifically against zebrafish proteins for immunohistochemistry. Oftentimes, we must utilize antibodies developed against proteins from different species, such as mice, rabbits, and humans and attempt to take advantage of cross-reactivity with the zebrafish homolog. Zebrafish proteins typically have different sequence and structural characteristics, and several isoforms. An antibody against Kv3.3 was developed

previously in the laboratory, however, its affinity and specificity were not strong. Immunohistochemistry would confirm that protein is translated and expressed from the mRNA message and would allow us to determine if the pattern of expression is conserved in zebrafish Purkinje cells. Kv3.3 has been shown to be unequally distributed in mammalian Purkinje cells, with the highest level of expression in the soma and proximal dendrites (Martina, Yao & Bean, 2003). This pattern of expression suggests its functional importance for Purkinje cell tonic firing, as somatic action potentials would activate channels in these locations.

Methods exist to ensure that antibodies recognize zebrafish proteins with specificity, either through better screening for cross-reactivity or creating antibodies against the proteins themselves. In both cases zebrafish epitopes are chosen and recombinantly expressed in *Escherichia coli*, followed by purification using 6X-His tags. To screen antibodies created against epitopes from other species, Western blot can be employed. This is useful in order to determine the level of recognition, as several isoforms of zebrafish epitopes can be screened with several antibodies at once (Zepeda et al., 2017). To obtain specific antibodies, which would be the strongest for protein identification, mice can be immunized with the purified zebrafish epitopes. Antibodies can then be collected and purified for use in wholemount fixed tissue (Crosnier Staudt & Wright, 2015). This method has been used for zebrafish neural receptors, however, leaves open the possibility that the same can be done for other zebrafish proteins, such as Nav1.6 and Kv3.3.

It would be worthwhile to explore what effect the loss of Nav1.6 or Kv3.3 would have on zebrafish Purkinje cell excitability. This has been extensively studied in mammalian Purkinje cells, and determined that these channels are the primary regulators of spontaneous tonic firing.

A useful tool for knocking down expression in zebrafish is shRNA, and hairpins can be specifically designed and targeted to the gene sequences (De Rienzo, Gutzman & Sive, 2012). The shRNA sequence is inserted into an miR plasmid backbone with Tol2 transposition sequences, in frame with a fluorescent protein. The clone would then be injected into zebrafish embryos as previously described. The shRNAs can be specifically expressed in Purkinje cells using the *aldoca* promotor, and fluorescence allows for screening of cells in which they are expressed. Because shRNA result in the degradation of targeted mRNAs, i*n situ* hybridization can be used to confirm knockdown of gene expression. Once knockdown is confirmed, loose patch recordings would be taken from Purkinje cells expressing shRNAs against either Nav1.6 or Kv3.3. If changes in Purkinje cell excitability are observed, and match those reported in mammalian Purkinje cells, the evidence would strongly suggest that these channels regulate zebrafish Purkinje cell excitability.

Rapid degeneration of Purkinje cells caused by SCA13 infant onset R4H mutation

A differential effect on Purkinje cell development and survival was observed between the SCA13 adult and infant onset mutations, R3H and R4H, respectively. While the adult onset R3H mutation had a trend toward more stability in quantitative measurements of total process length and number of branches over developmental time compared to the obvious increases observed in controls, it had no significant effect on Purkinje cell development or survival. The infant onset R4H mutation, however, had an obvious and dramatic effect, leading to rapid degeneration and the disappearance of cells by ~6 dpf, only 72 hours after Purkinje cell birth typically begins. Total process length decreased over developmental time, and was significantly shorter compared

to controls, and to cells expressing the adult onset mutation. Significantly fewer branches were observed as well. An obvious primary dendrite did not develop and dendritic spines were not observed. Acridine orange experiments confirmed that Purkinje cell disappearance reflects apoptotic cell death.

While lower Purkinje cell density and dendritic maldevelopment have been observed previously in mouse cerebellar cultures expressing the infant onset R4H mutation through viral induction (Irie et al., 2014), this is the first study that has followed the morphological effects of this mutation *in vivo* over developmental time, specifically in Purkinje cells. This allowed us to better understand the characteristics and progression of the developmental and degenerative phenotypes and eventual cell death through apoptosis, while development occurred in physiological conditions, presumably with all connections intact. Using this model, we were able perform loose patch recordings of Purkinje cells under the same conditions as the developmental images, allowing for us to establish a direct relationship between the functional and structural defects caused by the infant onset mutation. In the experiments using mouse cerebellar culture, the high degree of overexpression caused the dominant negative effect of the infant onset mutation to mask the gating abnormalities and hyperexcitability over time. Physiologically relevant results with a developmental time frame allow us to relate our observations back to the age of onset in infant onset SCA13 patients. The maldevelopment, rapid degeneration, and disappearance of zebrafish Purkinje cells appears consistent with clinical phenotypes in patients manifesting within the first year of life and cerebellar atrophy (Herman-Bert, 2000).

There are some caveats to our experimentation, including our inability to control the expression level of mutant zKv3.3. Using Tol2 transposition, we cannot determine the level of

protein expression in Purkinje cells. Subunits containing the adult onset R3H mutation and infant onset R4H mutation can assemble with other mutant subunits, and with endogenous WT subunits in zebrafish Purkinje cells. Adult onset mutant subunits cannot form functional channels on their own, and infant onset mutant subunits form functional channels on their own so inefficiently that it is unlikely to be a physiological phenomenon. Experiments in *Xenopus* oocytes determined that the effects on channel function when mutant subunits co-assemble with WT subunits are dose dependent (Waters et al., 2006), and working within our model, this suggests that the effects on Purkinje cell excitability, development, and cell survival may be dose dependent as well.

Previous studies have determined that Kv3.3 is not only expressed in mammalian and teleost Purkinje cells within the cerebellum. Kv3.3 immunostaining was observed in the granule cell layer (GCL), Purkinje cell layer (PCL), and molecular layer (ML) in mice, specifically in granule cells and deep-cerebellar nuclei (DCN). In the cerebellum of the brown ghost knife fish, a teleost, immunostaining revealed Kv3.3 expression in granule cells, golgi cells, stellate cells, and eurydendroid cells. In both cases, Purkinje cell expression was observed as well. Expression of the infant onset R4H mutation in other cerebellar neurons may change their pattern of excitability, or may lead to developmental or degenerative phenotypes distinct from those observed in Purkinje cells and it has not yet been determined which neuronal populations within the cerebellum are affected in SCA13. Granule cells receive inputs from mossy fibers that originate in pre-cerebellar nuclei and send parallel fibers to Purkinje cell dendrites (Bae et al., 2009; Hashimoto & Hibi, 2012). Parallel fibers modulate spontaneous tonic firing (D'Angelo et al., 2011), and are necessary for LTP through coincident input with climbing fibers (Ito, 1982; Ito, 1989; Krupa & Thompson, 1997), and for pre- and post-synaptic LTD through input of

differential firing frequencies (Salin et al., 1996; Chen & Regehr, 1997; Storm et al., 1998; Jacoby, Sims & Hartell, 2001; Kaeser et al., 2008; Anggono & Huganir, 2012). Purkinje cells are the sole output neurons of the cerebellum, therefore, changing their firing pattern and plasticity would not only affect how the cerebellar circuitry functions to integrate information on movement and cognition, but how the cerebellum sends integrated information to other regions of the brain. The α6 subunit of the $GABA_A$ receptor is specifically expressed in the adult mouse cerebellum, which one study confirmed using *in situ* hybridization. Emulsion autoradiogram revealed that the subunit was more specifically expressed in the granule cell layer. The promotor of the gene encoding this subunit may be a useful tool to identify zebrafish granule cells for expression experiments and to use molecular techniques to specifically express mutant Kv3.3 and fluorescent proteins (Kato et al., 1990). As this subunit is only expressed in the adult mouse cerebellum, it is worth exploring other genes differentially expressed in granule cells, as their transcriptome is distinct from Purkinje cells and other neurons of the cerebellum (Takeuchi et al., 2017).

Complex mechanistic role of hyperexcitability induced by the infant onset R4H mutation

Results obtained by treating zebrafish expressing the infant onset R4H mutation in Purkinje cells with the SK2 channel agonist NS13001 were not clear, but they did provide some insight into the complexity of the infant onset mutation. Although degeneration and cell death were not rescued through chronic NS13001 treatment, a significant increase in the frequency of Purkinje cells expressing the infant onset mutation was observed compared to that in DMSO-treated controls. Since this phenomenon was not observed in animals expressing mEGFP alone

specifically in Purkinje cells treated with NS13001 or DMSO, it suggests the increase in frequency was not due to increased cell proliferation. The results from the NS13001 experiments provided further evidence that the infant onset mutation does not only cause a degenerative phenotype, but a developmental phenotype as well, and that altered excitability may play a role in Purkinje cell viability and development.

Since we cannot electrophysiologically record Purkinje cells in animals chronically treated with NS13001 to confirm the reduction of hyperexcitability, we cannot rule out hyperexcitability as a contributor to the degenerative phenotypes. To address this issue, we attempted to reduce hyperexcitability using molecular techniques, by co-expressing inward rectifying K^+ channel 2.1 (Kir2.1) and soluble tdTomato with the infant onset R4H mutation and mEGFP specifically in Purkinje cells. The preliminary results revealed the same effect as that observed with chronic NS13001 treatment, with an increase in the frequency of cells expressing both the infant onset mutation and Kir2.1 compared to that of cells expressing the infant onset mutation alone. The degenerative phenotype and reduced cell survival were still observed. It would be worthwhile to record from cells co-expressing Kir2.1 and the infant onset mutation, to determine the level to which the hyperexcitability was reduced and determine if further depression is necessary to achieve a pattern of excitability similar to that in normal Purkinje cells.

Possible mechanisms downstream of hyperexcitability implicated in neuronal degeneration

Several factors should be considered while investigating the mechanism of the infant onset R4H mutation behind the degenerative phenotype. Strong evidence exists implicating an

increase in intracellular Ca^{2+} concentration. Previous experiments in zebrafish Purkinje cells expressing the infant onset mutation revealed an increased Ca^{2+} response to stimulation using the genetically-encoded Ca^{2+} indicator GCaMP-HS (Issa & Papazian, unpublished). Another investigation in cultured mouse cerebellum expressing the infant onset mutation revealed increased basal intracellular Ca^{2+} in Purkinje cells using the Ca^{2+}-indicating fluorescent dye Fura-2 (Irie et al., 2014). Increased intracellular Ca^{2+} load can lead to mitochondrial dysfunction which can activate the apoptotic cascade, and models have suggested it may lead to endoplasmic reticulum (ER) stress as well.

Mitochondrial Ca^{2+} is highly regulated, and changes in the carefully balanced concentration of Ca^{2+} can alter mitochondrial function. Increased Ca^{2+} in the mitochondria can increase the production of reactive oxygen species (ROS), which can cause damage by oxidation of cellular components such as lipids, amino acids, and DNA. Mitochondrial dysfunction and/or loss of mitochondrial integrity together with increased Ca^{2+} concentration can lead to the release of pro-apoptotic factors, such as cytochrome c, from the mitochondria. The transfer of Ca^{2+} from the ER to the mitochondria through their associated membrane can initiate this cascade (reviewed in Smaili et al., 2013). The ER is responsible for protein folding and acts as a Ca^{2+} reservoir for the cell. Increased Ca^{2+} leads to Ca^{2+}-induced Ca^{2+} release (CICR) from 1,4,5-inositol triphosphate receptors (IP3R) responding to 1,4,5-inositol triphosphate (IP3), which is produced when Ca^{2+} is elevated, and through ryanadine receptors (RyR). These receptors are located in the ER membrane, and it has been proposed that this release of Ca^{2+}, if excessive, can trigger the unfolded protein response (UPR), which includes an increase in expression of Ca^{2+} chaperones, inhibition of translation, an increase in ER volume, and degradation of unfolded

proteins. The splicing of XBP1 to modulate transcription factors and activation of JNK are associated with apoptosis and activation of autophagy (reviewed in Bravo et al., 2013).

Increased Ca^{2+} leading to mitochondrial dysfunction is implicated in a wide variety of neurodegenerative diseases, oftentimes with associated ER stress, including in other spinocerebellar ataxias. In amyotrophic lateral sclerosis (ALS), motor neuron Ca^{2+} levels are elevated, through susceptibility to glutamate excitotoxicity, which increases Ca^{2+} permeability. This leads to transfer of Ca^{2+} from the ER to the mitochondria, triggering the UPR and mitochondrial Ca^{2+} overload (Prell, Lautenschlager & Grosskreutz, 2013). When spliced XBP1 was knocked-down in cultured SOD1 mutant motor neurons, increased motor neuron survival was observed, and when action potentials were reduced with the use of tetrodotoxin (TTX), the ER stress response was reduced. Interestingly, reducing the ER stress response using the drug salubrinal decreased hyperexcitability as well (Kiskinis et al., 2014). This highlights the interdependence between altered excitability and the ER stress response in motor neurons containing ALS mutations. In Alzheimer's Disease (AD), Ca^{2+} is increased in the dendrites of cortical pyramidal neurons, particularly in those close to amyloid-β (Aβ) plaques. IP3R and RyR receptors in the ER are activated, and increased ROS are observed in the mitochondria (Berridge et al., 2014). Aβ plaques in AD and α-synuclein plaques in Purkinson's Disease (PD) possibly lead to increased Ca^{2+} through similar mechanisms, by forming Ca^{2+} permeable channels in the membrane or other mechanisms that remain unclear (Arispe, Rojas & Pollard, 1993; Volles et al., 2001). Mitochondrial involvement in PD has been widely studied and debated, but several neurotoxins inhibiting the electron transport chain lead to PD-like symptoms and are used to create PD models. A mutation in the kinase involved in mitochondrial fission and quality control

(PINK-1) causes PD in patients, and a relationship appears to exist between the formation of α-synuclein deposits in the PD brain and reduced activity of complexes in the electron transport chain, along with further mitochondrial dysfunction within the mitochondria-associated ER membrane (Zaltieri et al., 2015).

Interestingly, in the same polyQ diseases that exhibit Purkinje cell dysfunction, including spinocerebellar ataxia type 2 and 3 (SCA2 and 3), increased Ca^{2+} and ER stress are implicated as well. In Huntington's Disease (HD), HTT^{exp} binds to the C-terminal end of IP3R and increases the sensitivity to IP3, leading to an increased Ca^{2+} release from these receptors. The Ca^{2+} signal is further destabilized due to the activation of other channels, including voltage-gated Ca^{2+} channels (Tang et al., 2003; Swayne et al., 2005; Kaltenbach et al., 2007). Similarly, in both spinocerebellar ataxia type 2 and 3 (SCA2 and 3) mutant ataxin 2 and 3, respectively, bind and activate IP3R which leads to excess Ca^{2+} release from the ER (Chen et al., 2008; Liu et al., 2009). In an SCA3 mouse model, when mice were fed RyR inhibitors, to decrease CICR from the ER, and dantrolene, a Ca^{2+} stabilizer, motor defects were alleviated and neuronal loss was prevented in the cerebellum (Chen et al., 2008).

Zebrafish are a strong model to investigate the role of increased neuronal Ca^{2+}, ER stress, and mitochondrial dysfunction in infant onset SCA13. Ca^{2+} imaging can be performed *in vivo*, preferably with sensitive indicators that can capture the spontaneous Ca^{2+} response in Purkinje cells, including GCaMP6 and YC3.6, the latter of which has successfully been used in spontaneously firing pyramidal neurons (Kuchibhotla et al., 2008). Chronic treatment with Ca^{2+} stabilizers, such as dantrolene, or co-expression of parvalbumin with the infant onset R4H mutation in Purkinje cells, either independently or in concert with chronic NS13001 treatment,

may rescue the degenerative phenotype more successfully than reducing hyperexcitability alone. Markers for ER stress exist, such as the chaperone GRP78/BiP or spliced XBP1, and can be detected in zebrafish Purkinje cells through *in situ* hybridization and/or immunohistochemistry. Chronic treatment with salubrinal, which reduces ER stress, has been used pharmacologically in mouse models of ALS to decrease ER stress (Kiskinis et al., 2014) and has been investigated in zebrafish. Thapsigargin induces ER stress, and has been used to cause degeneration of zebrafish Purkinje cells in *Tg(aldoca:gap43-Venus),* in which cells are labeled with mVenus yellow fluorescence, through chronic treatment. When salubrinal was added to the treatment, the degeneration was rescued, suggesting that salubrinal is permeable and effective. Zebrafish expressing the infant onset mutation in Purkinje cells can be chronically treated with salubrinal, to determine if reducing ER stress can rescue the degenerative phenotype. Molecular techniques can be used to investigate mitochondrial number and morphology by co-expressing Mito-DsRed in Purkinje cells with the infant onset mutation. These experimental tools can be used to investigate whether the common observations of increase Ca^{2+} and cellular stress responses in other neurodegenerative diseases are observed in Purkinje cells expressing the infant onset R4H mutation.

Neuronal excitability is altered in several neurodegenerative diseases, although it remains unclear as to whether these alterations are a product of the causative mutation themselves or related to changes ion channel expression, protein aggregation, or alterations in the neuronal population. Furthermore, excitability may contribute to pathogenesis or may represent an epiphenomenon. Another common link between neurodegenerative diseases is increased Ca^{2+} levels, leading to mitochondrial dysfunction and/or ER stress that induce apoptotic cell death.

Reducing these harmful processes has been shown to alleviate neuronal degeneration and even motor disturbances in mouse models. We have determined that differential alterations in Purkinje cell excitability are caused by the SCA13 adult onset R3H mutation and infant onset R4H mutation, and that differential changes in development and cell survival are observed as well. The infant onset mutation leads to rapid degeneration and apoptotic cell death, and treating the intact animal with an SK2 channel agonist was not sufficient to rescue this phenotype. It has become increasingly clear that this mutation leads to a wide array of defects. Preliminary evidence suggests that hyperexcitability induces an increase in intracellular Ca^{2+} concentration, revealing another commonality observed in other neurodegenerative diseases, that may set into motion all of the subsequent changes observed in diseased neurons. As we advance our knowledge of SCA13 and progress towards treatments, we advance our knowledge of other neurodegenerative diseases. Using zebrafish as our model will allow us to perform experiments *in vivo* and follow them over developmental time, which will reveal candidate pathogenic mechanisms that may underlie to the disease in patients. An apparent relationship exists between neurodegenerative diseases that range from mild to rapidly deleterious and fatal, and exceedingly rare to common, confirming the importance of carrying on with our investigation into the mechanisms of action of SCA13 mutations.

References

Akemann, W. & Knopfel, T. (2006) Interaction of Kv3 potassium channels and resurgent sodium current influences the rate of spontaneous firing of Purkinje neurons. *J. Neurosci*. **26(17)**: 4602-4612.

Angonno, V. & Huganir, R. (2012) Regulation of AMPA receptor trafficking and synaptic plasticity. *Current Opinion in Neurobiology.* **22(3)**: 461-469.

Ariano, M., Cepeda, C., Calvert, C., Flores-Hernández, J., Hernández-Echeagaray, E., Klapstein, G., Chandler, S., Aronin, N., DiFiglia, M. & Levine, M. (2005) Striatal potassium channel dysfunction in Huntington's Disease transgenic mice. *J. Neurophysiol*. **93(5)**: 2565-2574.

Arispe, N., Rojas, E. & Pollard, H. (1993) Alzheimer disease amyloid beta protein forms calcium channels in bilayer membranes: blockade by tromethamine and aluminum. *PNAS*. **90(2)**: 567-571.

Armengol, J-A. & Sotelo, C. (1991) Early dendritic development of Purkinje cells in the rat cerebellum. A light and electron microscopic study using axonal tracing in ‘in vitro’ slices. *Developmental Brain Research.* **64(1-2)**: 95-114.

Atale, N., Gupta, S., Yadav, U. & Rani, V. (2014) Cell-death assessment by fluorescent and nonfluorescent cytosolic and nuclear staining techniques. *J. Microscopy*. **255(1)**: 7-19.

Bae, J., Simon, N., Menon, P., Vucic, S. & Kiernan, M. (2013) The puzzling case of hyperexcitability in amyotrophic lateral sclerosis. *J. Clin. Neurol.* **9(2)**: 65-74.

Bae, Y-K., Kani, S., Shimizu, T., Tanabe, K., Nojima, H., Kimura, Y., Higashijima, S. & Hibi, M. (2009) Anatomy of zebrafish cerebellum and screen for mutations affecting its development. *Developmental Biology*. **330(2)**: 406-426.

Balciunas, D., Wangensteen, K., Wilber, A., Bell, J., Geurts, A., Sivasubbu, S., Wang, X., Hackett, P., Largaespada, D., McIvor, R. & Ekker, S. (2006) Harnessing a high cargo-capacity transposon for genetic applications in vertebrates. *PLOS One*. **DOI**: 10.1371/journal.pgen.0020169.

Bell, C. (2002) Evolution of cerebellum-like structures. *Bran, Behavior and Evolution*. **59**: 312-326.

Bell, C., Han, V. & Sawtell, N. (2008) Cerebellum-like structures and their implications for cerebellar function. *Ann. Rev. Neurosci.* **31**: 1-24.

Berridge, M. J. (2013). Dysregulation of neural calcium signaling in Alzheimer disease, bipolar disorder and schizophrenia. *Prion.* **7**: 2–13.

Borjesson, S. & Elinder, F. (2008) Structure, function, and modification of the voltage sensor in voltage-gated ion channels. *Cell Biochem. Biophys.* **52**: 149-174.

Bradley, P. & Berry, M. (1976) The effects of reduced climbing and parallel fibre input on Purkinje cell dendritic growth. *Brain Research*. **109(1)**: 133-151.

Bravo, R., Parra, V., Gatica, D., Rodriguez, A., Torrealba, N., Paredes, F., Wang, Z., Zorzano, A., Hill, J., Jaimovich, E., Quest, A. & Lavandero, S. (2013) Endoplasmic reticulum and the unfolded protein response: dynamics and metabolic integration. *Int. Rev. Cell. Mol. Biol.* **301**: 215-290.

Brend, T. & Holley, S. (2009) Zebrafish whole mount high-resolution double fluorescent *in situ* hybridization. *JoVE*. **DOI**: 10.3791/1229.

Cepeda, C., Hurst, R., Calvert, C., Hernández-Echeagaray, E., Nguyen, O., Jocoy, E., Christian, L., Ariano, M. & Levine, M. (2003) Transient and progressive electrophysiological alterations in the corticostriatal pathway in a mouse model of Huntington's Disease. *J. Neurosci.* **23(3)**: 961-969.

Chen, C. & Regehr, W. (1997) The mechanism of cAMP-mediated enhancement at a cerebellar synapse. *J. Neurosci*. **17(22)**: 8687-8694.

Chen, X., Tang, T-S., Tu, H., Nelson, O., Pook, M., Hammer, R., Nukina, N. & Bezprozvanny, I. (2008) Deranged calcium signaling and neurodegeneration in spinocerebellar ataxia type 3. *J. Neurosci.* **28(48)**: 12713-12724.

Chopra, R. & Shakkottai, V. (2014) The role for alterations in neuronal activity in the pathogenesis of polyglutamine repeat disorders. *Neurotherapeutics*. **11(4)**: 751-763.

Cohen G. (1997) Caspases: the executioners of apoptosis. *Biochemical Journal*. **326(1)**: 1-16.

Crosnier, C., Staudt, N. & Wright, G. (2015) A rapid and scalable method for selecting recombinant mouse monoclonal antibodies. *BMC Biology*. **DOI**: 10.1186/1741-7007-8-76.

Cummings, D., Andre, V., Uzgil, B., Gee, S., Fisher, Y., Cepeda, C. & Levine, M. (2009) Alterations in cortical excitation and inhibition in genetic mouse models of Huntington's Disease. *J. Neurosci*. **29(33)**: 1037-10386.

D'Angelo, E., Mazzarello, P., Prestori, F., Mapelli, J., Solinas, S., Lombardo, P., Cesana, E., Gandolfi, D. & Congi, L. *Brain Research Reviews*. **66(1-2)**: 5-15.

Davie, J., Clark, B. & Hausser, M. (2008) The origin of the complex spike in cerebellar Purkinje neurons. *J. Neurosci*. **28(30)**: 7599-7609.

de Felipe, P., Luke, G., Hughes, L., Gani, D., Halpin, C. & Martin, D. (2006) E unum pluribus: multiple proteins from a self-processing polyprotein. *Trends in Biotechnology*. **24(2)**: 68-75.

De Rienzo, G., Gutzmann, J. & Sive, H. (2012) Efficient shRNA-mediated inhibition of gene expression in zebrafish. *Zebrafish*. **9(3)**: 97-107.

Dougherty, S., Reeves, J., Lucas, E., Gamble, K., Lesort, M. & Cowell, R. (2012) Disruption of Purkinje cell function prior to huntingtin accumulation and cell loss in an animal model of Huntington Disease. *Experimental Neurology*. **236(1)**: 171-178.

Dougherty, S., Reeves, J., Lesort, M., Detloff, P. & Cowell, R. (2013) Purkinje cell dysfunction and loss in a knock-in mouse model of Huntington Disease. *Experimental Neurology.* **240**: 96-102.

Eimon, P. & Ashkenazi, A. (2009) The zebrafish as a model organism for the study of apoptosis. *Apoptosis*. **15(3)**: 331-349.

Eisen, A., Kim, S. & Pant, B. (1992) Amyotrophic lateral sclerosis (ALS): a phylogenetic disease of the corticomotoneuron? *Muscle & Nerve*. **15(2)**: 219-224.

Elmore, S. (2007) Apoptosis: a review of programmed cell death. *Toxicologic Pathology*. **35(4)**: 495-516.

Erisir, A., Lau, D., Rudy, B. & Leonard, C. (1999) Function of specific K+ channels in sustained frequency of firing of fast-spiking neocortical interneurons. *J. Neurophys*. **82(5)**: 2476-2489.

Figueroa, K., Minassian, N., Stevanin, G., Waters, M., Garibyan, V., Forlani, S., Strzelczyk, A., Burk, K., Brice, A., Durr, A., Papazian, D., Pulst, S. (2010) KCNC3: phenotypes, mutations, channel biophysics - a study of 260 familial ataxia patients. *Human Mutation.* **31(2)**: 191-196.

Figueroa, K., Waters, M., Garibyan, V., Bird, T., Gomez, C., Ranum, L., Minassian, N., Papazian, D. & Pulst, S. (2011) Frequency of KCNC3 DNA variants as causes of spinocerebellar ataxia 13 (SCA13). *PLOS One.* **DOI**: 10.1371/journal.pone.0017811.

Friedlander, R. Apoptosis and caspases in neurodegenerative diseases. *The New England Journal of Medicine.* **348**: 1365-1375.

Gomez, T., Robles, E., Poo, M. & Spitzer, N. (2001) Filopodial calcium transients promote substrate-dependent growth cone turning. *Science*. **291(5510)**: 1983-1987.

Hall, A., Throesch, B., Buckingham, S., Marwardt, S., Peng, Y., Wang, Q., Hoffman, D. & Roberson, E. (2015) Tau-Dependent Kv4.2 Depletion and Dendritic Hyperexcitability in a Mouse Model of Alzheimer's Disease. *Neurobiology of Disease*. **35(15):** 6221-6230.

Hansen, S., Meera, P., Otis, T. & Pulst, S. (2012) Changes in Purkinje cell firing and gene expression precede behavioral pathology in a mouse model of SCA2. *Human Molecular Genetics.* **22(2)**: 271-283.

Hashimoto, M. & Hibi, M. (2012) Development and evolution of cerebellar neural circuits. *Development, Growth & Differentiation.* **54(3)**: 373-389.

Hausser, M. & Clark, B. (1997) Tonic synaptic inhibition modulates neuronal output pattern and spatiotemporal synaptic integration. *Neuron*. **19(3)**: 665-678.

Hendelmen, W. & Aggerwal, A. (1980) The Purkinje neuron: I. A Golgi study of its development in the mouse and in culture. *J. Comp. Neurol.* **193(4)**: 1063-1079.

Herman-Bert, A., Stevanin, G., Netter, J-C., Rascol, O., Brassat, D., Calvais, P., Camuzat, A., Yuan, Q., Schalling, M. & Durr, A. (2000) Mapping of spinocerebellar ataxia 13 to

chromosome 19q13.3-q13.4 in a family with autosomal dominant cerebellar ataxia and mental retardation. *AJHG*. **67(1)**: 229-235.

Hibi, M. & Shimizu, T. (2011) Development of the cerebellum and cerebellar neural circuits. *Developmental Neurobiology.* **72(3)**: 282-301.

Hsieh, J-Y., Ulrich, B., Issa, F., Wan, J. & Papazian, D. (2014) Rapid development of Purkinje cell excitability, functional cerebellar circuit, and afferent sensory input to cerebellum in zebrafish. *Front. Neural Circuits*. **8**: 147.

Irie, T., Matsuzaki, Y., Sekino, Y. & Hirai, H. (2014) Kv3.3 channels harbouring a mutation of spinocerebellar ataxia type 13 alter excitability and induce cell death in cultured cerebellar Purkinje cells. *J. Physiol*. **592(1)**: 229-247.

Issa, F., Mock, A., Sagasti, A. & Papazian, D. (2012) Spinocerebellar ataxia type 13 mutation that is associated with disease onset in infancy disrupts axonal pathfinding during neuronal development. *Disease Models & Mechanics*. **DOI**: 10.1242/dmm.010157.

Ito, M. (1982) Cerebellar control of the vestibulo-ocular reflex around the flocculus hypoethesis. *Ann. Rev. Neurosci*. **5**: 275-296.

Ito, M. (1984) The modifiable neuronal network of the cerebellum. *The Japanese J. Physiol.* **34(5)**: 781-792.

Ito, M. (1989) Long-term depression. *Ann. Rev. Neurosci*. **12**: 85-102.

Ito, M. (2002) Historical review of the significance of the cerebellum and the role of Purkinje cells in motor learning. *Ann. NY Acad. Sci.* **978**: 273-288.

Ito, M. (2006) Cerebellar circuitry as a neuronal machine. *Progress in Neurobiology.* **78(3-5)**: 272-303.

Ito, M. (2008) Control of mental activities by internal models in the cerebellum. *Nature Reviews*. **9**: 304-313.

Jacoby, S., Sims, R. & Hartell, N. (2001) Nitric oxide is required for the induction and heterosynaptic spread of long-term potentiation in rat cerebellar slices. *J. Physiol*. **535(3)**: 825-839.

Jensen, M., Jogini, V., Borhani, D., Leffler, A., Dror, R. & Shaw, D. (2012) Mechanism of voltage gating in potassium channels. *Science*. **336(6078)**: 229-233.

Jung, C., Jun, C., Ro, S-H., Kim, Y-M., Otto, N., Cao, J., Kundu, M. & Kim, D-H. ULK-Atg13-FIP200 complexes mediate mTOR signaling to the autophagy machinery. *Molecular Biology of the Cell.* **20(7):** 1992-2003.

Kaeser, P., Kwon, H-B., Blundell, J., Chevaleyre, V., Morishita, W., Malenka, R., Powell, C., Castillo, P. & Sudhof, T. (2008) RIM1α phosphorylation at serine-413 by protein kinase A is not required for presynaptic long-term plasticity or learning. *PNAS*. **105(38)**: 14680-14685.

Kaltenbach, L., Romero, E., Becklin, R., Chettier, R., Bell, R., Phansalkar, A., Strand, A., Torcassi, C., Savage, J., Hurlburt, A., Cha, G-H., Ukani, L., Chepanoske, C., Zhen, Y., Sahasrabudhe, S., Olson, J., Kurschner, C., Ellerby, L., Peltier, J., Botas, J. & Hughes, R. (2007) Huntingtin interacting proteins are genetic modifiers of neurodegeneration. *PLOS One*. **DOI**: 10.1371/journal.pgen.0030082.

Kapfhammer, J. (2004) Cellular and molecular control of dendritic growth and development of cerebellar Purkinje cells. *Progress in Histochemistry and Cytochemistry*. **39(3)**: 131-182.

Kasumu, A., Hougaard, C., Rode, F., Jacobsen, T., Sabatier, J., Eriksen, B., Strobaek, D., Liang, X., Egorova, P., Vorontsova, D., Christophersen, P., Ronn, L. & Bezprozvanny, I. (2012) Selective positive modulator of calcium-activated potassium channels exerts beneficial

effects in a mouse model of spinocerebellar ataxia type 2. *Cell Chemistry & Biology.* **19(10)**: 1340-1353.

Kim, J., Lee, S-R., Li, L-H., Park, H-J., Park, J-H., Lee, K., Kim, M-K., Shin, B. & Choi, S-Y. (2011) High cleavage efficiency of a 2A peptide derived from porcine Teschovirus-1 in human cell lines, sebrafish and mice. *PLOS One*. **DOI**: 10.1371/journal.pone.0018556.

Kiskinis, A., Sandoe, J., Williams, L., Boulting, G., Moccia, R., Wainger, B., Han, S., Peng, T. & Thams, S. (2014) Pathways disrupted in human ALS motor neurons identified through genetic correction of mutant SOD1. *Cell Stem Cell*. **14(6)**: 781-795.

Khaliq, Z., Gouwens, N. & Raman, I. (2003) The contribution of resurgent sodium current to high-frequency firing in Purkinje neurons: an experimental and modeling study. *J. Neurosci*. **23(12)**: 4899-4912.

Klapstein, G., Fisher, R., Zanjiani, H., Cepeda, C., Jokel, E., Chesselet, M-F. & Levine, M. (2001) Electrophysiological and morphological changes in striatal spiny neurons in R6/2 Huntington's Disease transgenic mice. *J. Neurophysiol*. **86(6)**: 2667-2677.

Krupa, D. & Thompson, R. (1997) Reversible inactivation of the cerebellar interpositus nucleus completely prevents acquisition of the classically conditioned eye-blink response. *Learning and Memory*. **3**: 545-556.

Kuchibhotla, K., Goldman, S., Lattarulo, C., Wu, H-Y., Hyman, B. & Bacskai, B. (2008) Aβ plaques lead to aberrant regulation of calcium homeostasis in vivo resulting in structural and functional disruption of neuronal networks. *Neuron*. **59(2)**: 214-225.

Laine, M., Lin, M-C., Bannister, J., Silverman, W., Mock, A., Roux, B. & Papazian, D. (2003) Atomic proximity between S4 segment and pore domain in shaker potassium channels. *Neuron*. **39(3)**: 467-481.

Liu, J., Tang, T-S., Tu, H., Nelson, O., Herndon, E., Huynh, D., Pulst, S. & Bezprozvanny, I. (2009) Deranged calcium signaling and neurodegeneration in spinocerebellar ataxia type 2. *J. Neurosci.* **29(29)**: 9148-9162.

Lohmann, C., Myhr, K. & Wong, R. (2002) Transmitter-evoked local calcium release stabilizes developing dendrites. *Nature*. **418**: 177-181.

Lohmann, C., Finski, A. & Bonhoeffer, T. (2005) Local calcium transients regulate the spontaneous motility of dendritic filopodia. *Nature Neuroscience*. **8**: 305-312.

MacKinnon, R. (1991) Determination of the subunit stoichiometry of a voltage-activated potassium channel. *Nature*. **350(6315)**: 232-235.

Martina, M., Yao, G. & Bean, B. (2003) Properties and functional role of voltage-dependent potassium channels in dendrites of rat cerebellar Purkinje neurons. *J. Neurosci*. **23(13)**: 5698-5707.

McKay, B. & Turner, R. (2004) Kv3 K+ channels enable burst output in rat cerebellar Purkinje cells. *European J. Neurosci*. **20(3)**: 729-739.

McKay, B. & Turner, R. (2005) Physiological and morphological development of the rat cerebellar Purkinje cell. *J. Physiol.* **567(3)**: 829-850.

Minassian, N., Lin, M-C. & Papazian, D. (2012) Altered Kv3.3 channel gating in early-onset spinocerebellar ataxia type 13. *J. Physiol*. **590(7)**: 1599-1614.

Mizushima, N., Yamamoto, A. & Matsui, M. (2003) In vivo analysis of autophagy in response to nutrient starvation using transgenic mice expressing a fluorescent autophagosome marker. *Molecular Biology of the Cell*. **15(3)**: 1101-1111.

Mock, A., Richardson, J., Hsieh, J-Y., Rinetti, G. & Papazian, D. (2010) Functional effects of spinocerebellar ataxia type 13 mutations are conserved in zebrafish Kv3.3 channels. *BMC Neuroscience*. **DOI**: 10.1186/1471-2202-11-99.

Munsie, L. & Truant, R. (2012) The role of the cofilin-actin rod stress response in neurodegenerative diseases uncovers potential new drug targets. *Bioarchitecture*. **6**: 204-208.

Napper, R. & Harvey, R. (1988) Number of parallel fiber synapses on an individual Purkinje cell in the cerebellum of the rat. *J. Comp. Neurol*. **274(2)**: 168-177.

Papazian, D., Shao, X., Seoh, S-A., Mock, A., Huang, Y. & Wainstock, D. (1995) Electrostatic interactions of S4 voltage sensor in shaker K+ channel. *Neuron*. **14(6)**: 1293-1301.

Pattingre, S., Tassa, A., Qu, X., Garuti, R., Liang, X., Mizushima, N., Packer, M., Schneider, M. & Levine, B. Bcl-2 antiapoptotic proteins inhibit Beclin 1-dependent autophagy. *Cell*. **122(6)**: 927-939.

Pattingre, A., Espert, L., Biard-Piechaczyck, M. & Codogno, P. (2008) Bcl-2 antiapoptotic proteins inhibit Beclin 1-Dependent autophagy. *Biochimie*. **90(2)**: 313-323.

Penazola, C., Lin, L., Lockshin, R. & Zakeri, Z. (2006) Cell death in development: shaping the embryo. *Histochemistry and Cell Biology*. **126**: 149-158.

Prell, T., Lautenschlager, J. & Grosskreutz, J. (2013) Calcium-dependent protein folding in amyotrophic lateral sclerosis. **54(2)**: 132-143.

Pulst, S. M. (2003) Inherited ataxias: an introduction in genetics of movement disorders. *Genetics of Movement Disorders*. 19-34.

Rajan, I. & Cline, H. (1998) Glutamate receptor activity is required for normal development of tectal cell dendrites in vivo. *J. Neurosci*. **18(19)**: 7836-7846.

Raman, I. & Bean, B. (1997) Resurgent sodium current and action potential formation in dissociated cerebellar Purkinje neurons. *J. Neurosci.* **17(12)**: 4517-4526.

Rodriguez, F., Duran, E., Gomez, A., Ocana, F., Alvarez, E., Jimenez-Moya, F., Broglio, C. & Salas, C. Cognitive and emotional functions of the teleost fish cerebellum. *Brain Res. Bull.* **66(4-6)**: 365-370.

Rudy, B., Chow, A., Lau, D., Amarillo, Y., Ozaita, A., Saganich, M., Moreno, H., Nadal, M. S., Hernandez-Pineda, R., Hernandez-Cruz, A., et al. (1999) Contributions of Kv3 channels to neuronal excitability. *Ann. N. Y. Acad. Sci*. **868**: 304–343.

Ryan, M. & Drew, J. (1991) Foot-and-mouth disease virus 2A oligopeptide mediated cleavage of an artificial polyprotein. *The EMBO Journal*. **13(4)**: 928-933.

Salin, P. & Prince, D. (1996) Spontaneous GABAA receptor-mediated inhibitory currents in adult rat somatosensory cortex. *J. Neurophysiol.* **75(4)**: 1573-1588.

Schöls, L. , Bauer, P. , Schmidt, T. , Schulte, T. & Riess, O. (2004) Autosomal dominant cerebellar ataxias: clinical features, genetics, and pathogenesis. *Lancet Neurol*. **3**: 291–304.

Seoh, S-A., Sigg, D., Papazian, D. & Bezanilla, F. (1996) Voltage-sensing residues in the S2 and S4 segments of the shaker K+ channel. *Neuron*. **16(6)**: 1159-1167.

Shakkottai, V., do Carmo Costa, M., Dell'Orco, J., Sankaranarayanan, A., Wulff, H. & Paulso, H. (2011) Early changes in cerebellar physiology accompany motor dysfunction in the polyglutamine disease spinocerebellar ataxia type 3. *J. Neurosci*. **31(36)**: 13002-13014.

Shin, S-L., Hoebeek, F., Schonewille, M., De Zeeuw, C., Aertsen, A. & De Schutter, E. (2007) Regular patterns in cerebellar Purkinje cell simple spike trains. *PLOS One*. **DOI**: 10.1371/journal.pone.0000485.

Silverman, W., Roux, B. & Papazian, D. (2003) Structural basis of two-stage voltage-dependent activation in K+ channels. *Proc. Natl. Acad. Sci. USA*. **100(5)**: 2935-2940.

Siskova, Z., Justus, D., Keneko, H., Friedrichs, D., Henneberg, N., Beutel, T., Pitsch, J., Schooch, S., Becker, A., Krammer, H. & Remy, S. (2014) Dendritic structural

degeneration is functionally linked to cellular hyperexcitability in a mouse model of Alzheimer's Disease. *Neuron*. **84(5)**: 1023-1033.

Smaili, S., Pereira, J., Cost, M., Rocha, K., Rodrigues, L., do Carmo, G., Hirata, H. & Hsu Y-T. (2013) The role of calcium stores in apoptosis and autophagy. *Current Molecular Medicine*. **13(2)**: 252-265.

Storm, D., Hansel, C., Hacker, B., Parent, A. & Linden, D. Impaired cerebellar long-term potentiation in Type I Adenylyl Cyclase mutant mice. *Neuron*. **20(6)**: 1199-1210.

Szymack, A. & Vignali, D. (2005) Development of 2A peptide-based strategies in the design of multicistronic vectors. *Expert Opinion on Biological Therapy*. **5**: 627-638.

Tanabe, K., Kani, S., Shimizu, T., Bae, Y-K., Abe, T. & Hibi, M. (2010) Atypical protein kinase c regulates primary dendrite specification of cerebellar Purkinje cells by localizing Golgi apparatus. *J. Neurosci.* **30(50)**: 16983-16992.

Tang, T-S., Tu, H., Chan, E., Maximov, A., Wang, Z., Wellington, C., Hayden, M. & Bezprozvanny, I. (2003) Huntingtin and Huntingtin-Associated Protein 1 influence neuronal calcium signaling mediated by Inositol-(1,4,5) Triphosphate Receptor Type 1. *Neuron*. **39(2)**: 227-239.

Takeuchi, M., Yamaguchi, S., Skakibara, Y., Hayashi, T., Matsuda, K., Hara, Y., Tanegashima, C., Shimizu, T., Kuraku, S. & Hibi, M. (2017) Gene expression profiling of granule cells and Purkinje cells in the zebrafish cerebellum. *J. Comp. Neurol.* **525(7)**: 1558-1585.

Thisse, C. & Thisse, B. High-resolution *in situ* hybridization to whole-mount zebrafish embryos. *Nature Protocols.* **3**: 59-69.

Tiwari-Woodruff, S., Schulteis, C., Mock, A. & Papazian, D. (1997) Electrostatic interactions between transmembrane segments mediate folding of Shaker K+ channel subunits. *Biophysical Journal.* **72(4)**: 1489-1500.

Tiwari-Woodruff, S., Lin, M-C., Schulteis, C. & Papazian, D. (2000) Voltage-dependent structural interactions in the shaker K+ channel. *J. Gen. Phys.* **115(2)**: 123-138.

Tsai, C-W., Tseng, J-J., Lin, S-C., Chang, C-Y., Wu, J-L., Horng, J-F. & Tsey, H-J (2001). Primary structure and developmental expression of zebrafish sodium channel Nav1.6 during neurogenesis. *DNA Cell Biol*. **20**: 249–255.

Swayne, L., Chen, L., Hameed, S., Barr, W., Charlesworth, E., Colicos, M., Zamponi, G. & Braun, J. (2005) Crosstalk between huntingtin and syntaxin 1A regulates N-type calcium channels. *Molecular and Cellular Neuroscience*. **30(3)**: 339-351.

Volles, M., Lee, S-J., Rochet, J-C., Shtilerman, M., Ding, T., Kessler, J. & Lansbury, P. (2001) Vesicle permeabilization by protofibrillar α-Synuclein: implications for the pathogenesis and treatment of Parkinson's Disease. *Biochemistry*. **40(26)**: 7812-7819.

Wainger, B., Kiskinis, E., Mellin, C., Wiskow, O., Han, S., Sandoe, J., Perez, N., Williams, L., Lee, S. & Boulting, G. (2014) Intrinsic membrane hyperexcitability of amyotrophic lateral sclerosis patient-derived motor neurons. *Cell Reports*. **7(1)**: 1-11.

Waters, M., Minassian, N., Stevanin, G., Figueroa, K., Bannister, J., Nolte, D., Mock, A., Evidente, V., Fee, D., Muller, U., Durr, A., Brice, A., Papazian, D. & Pulst, S. (2006) Mutations in voltage-gated potssium channel KCNC3 cause degenerative and developmental central nervous system phenotypes. *Nature Genetics*. **38**: 447-451.

Wei, Y., Pattingre, S., Sinha, S., Bassik, M. & Levine, B. JNK1-mediated phosphorylation of Bcl-2 regulates starvation-induced autophagy. *Molecular Cell*. **30(6)**: 678-688.

Womack, M. & Khodakhah, K. (2003) Somatic and dendritic small-conductance calcium-activated potassium channels regulate the output of cerebellar Purkinje neurons. *J. Neurosci*. **23(7)**: 2600-2607.

Wong, R. & Ghosh, A. (2001) Activity-dependent regulation of dendritic growth and patterning. *Nature Reviews*. **3**: 803-812.

Wulff, P., Schonewille, M., Renzi, M., Viltono, L., Sassoe-Pognetto, M., Badura, A., Gao, Z., Hoebeek, F., van Dorp, S., Wisden, W., Farrant, M. & De Zeeuw, C. (2009) Synaptic inhibition of Purkinje cells mediates consolidation of vestibulo-cerebellar motor learning. *Science*. **12**: 1042-1049.

Youle, R. & Strasser, A. (2008) The BCL-2 protein family: opposing activities that mediate cell death. *Nature Reviews*. **9**: 47-59.

Zagha, E., Manita, S., Ross, W. & Rudy, B. (2010) Dendritic Kv3.3 Potassium Channels in Cerebellar Purkinje Cells Regulate Generation and Spatial Dynamics of Dendritic Ca2+ Spikes. *J. Neurophysiol*. **103(6)**: 3516-3525.

Zaltieri, M., Longhena, F., Pizzi, M., Missale, C., Spano, P. & Bellucci, A. (2015) Mitochondrial dysfunction and α-Synuclein synaptic pathology in Parkinson's Disease: who's on first? *Parkinson's Disease*. **DOI**: 10.1155/2015/108029.

Zepeda, S., Villarreal, M., Biediger, N., Bonner, N., Miller, J., Ricard, B., Garcia, D. & Lewis, K. Determining zebrafish epitope reactivity to commercially available antibodies. *The FASEB Journal*. **31(1)**: 1-3.